Hox11-Expression Defines a Skeletal Mesenchymal Stem Cell that Contributes to Skeleton Development, Growth, and Repair

by

Kyriel Marie Pineault

A dissertation submitted in partial fulfillment
of the requirements for the degree of
Doctor of Philosophy
(Cell and Developmental Biology)
in The University of Michigan
2018

Dissertation Committee:
Associate Professor Jason R. Spence, Chair
Associate Professor Benjamin L. Allen
Professor Jiandie D. Lin
Assistant Professor Daniel Lucas
Professor Deneen M. Wellik

Kyriel M. Pineault

kyrielmp@umich.edu

ORCID iD: 0000-0001-9359-9718

Dedication

To my family, for the unconditional love and encouragement. To my mom, Louisa, for believing in the power of a quality education and fostering my love of learning. To my dad, Sylvain, for the constant support and complete faith in my ability to succeed. To my sister, Lydia, for all the laughs and all the adventures. To my best friends, Emily and Shelby, for always being there whenever I need support and believing in my dreams. Finally, to all the women who were told they were not good enough but succeeded anyway.

Acknowledgements

First, I thank Deneen Wellik for six years of mentorship and support. My time in the laboratory has been an adventure and more rewarding than I could have imagined. Thank you for believing in me and pushing me as hard as you did to begin to achieve my full potential. Your enthusiasm is contagious and made the work even more exciting. I am grateful that you were there to help me start my journey as a scientist.

To the members of the Wellik lab over the years, I am eternally grateful for your friendship and support. Bonding over happy hours will be one of my favorite memories from this experience. To Steve, I have loved having you as a desk neighbor to share in my successes, get me through the failures, and always make me laugh. To Leilani, you brightened each day with your lovely personality and delicious baked treats. To Danielle, for helping me get started on the *Hox11* project. To Jane, for all your hard work and being the best collaborator ever for this project. To Lauren, for your enthusiasm and happiness each day. To all of the undergraduate researchers, Kayla, Katarina, Andrew, Nick, Christina, Noah, and Ella, thank you for allowing me to be your mentor as you begin your scientific careers. I could not have asked for a better group of people to work with. I wish you all success.

To the members of my thesis committee, thank you for all the feedback and guidance throughout my Ph.D. training. To Daniel, thank you pushing me to always examine my work critically and demanding excellence. To Ben, thank you for acting as the devil's advocate and forcing me to articulate my ideas clearly. To Jason, thank you for your positive attitude and willingness to make time to discuss my research and brainstorm future experiments. To Jiandie, thank you for providing an outside perspective and reminding me to consider the broader implications of my body of research.

To Sherry Taylor, thank you for your continuous support throughout this whole process and your willingness to assist with any problem big or small. I loved all our crafting discussions, and I wish you all the best in your retirement.

I would not have succeeded in this process without the amazing support and friendship of my peers. To the Spence lab members, thank you for creating such an amazing work environment. It was a joy coming to work next to you every day. To the students of the CDB department, thank you for fostering a positive and collaborative research environment. To the members of the Developmental Genetics group meetings, thank you for all the constructive feedback over the years and making me a better scientific communicator.

To the Cell and Developmental Biology department faculty and staff, I do not think there is a better department I could have worked with. To Scott Barolo, Kristen Verhey, and Roman Giger, thank you for your feedback as Graduate Student Coordinators. Finally, to the administrative staff for being willing to help me with any problem big or small.

Thank you to the Michigan Core facilities and staff: the microscopy and imaging analysis core, the flow cytometry core, and the transgenic animal model core. This research would not have been possible without your facilities. To the staff members, thank you for the technical expertise and the training.

To my funding sources, thank you for providing the financial resources to support this research and fostering my professional growth. Thank you to the National Institutes of Health RO1 AR061402 awarded to Deneen Wellik. Thank you to the Tissue Engineering at Michigan (T32 DE007057) and the Organogenesis (T32 HD007505) training grants for the exceptional training programs. Thank you to the Rackham Graduate School for the Pre-Candidate Graduate Student Research Grant, Conference Travel Grant, and the Professional Development Grant. Thank you to Program in Biomedical Sciences (PIBS) for the Benard Maas/Dean's fellowship and to the Cell and Developmental Biology department for the Bradley M. Patten fellowship.

TABLE OF CONTENTS

LIST OF FIGURES

LIST OF APPENDICES

ABSTRACT

The skeleton is one of the most widely explored organs for defining mesenchymal stem/progenitor cell (MSC) populations, and there is significant interest in MSCs for their potential in novel and potentially curative therapies for a variety of musculoskeletal disorders. The skeleton is a highly dynamic tissue and MSCs function as a reservoir of new cellular material to support skeletal growth, turnover, and repair. Using a *Hoxa11eGFP* reporter allele, recent work demonstrated Hox11-expressing cells in the adult skeleton are identified as an MSC-enriched population in the bone marrow and on the cortical bone surfaces. In fact, at all stages examined Hoxa11eGFP-expression is excluded from all differentiated skeletal cell types. Developmentally, *Hox* genes are critically important patterning regulators and function regionally along the axes of the mammalian skeleton. The *Hox11* genes specifically function to pattern the lumbar spine and zeugopod region (radius/ulna and tibia/fibula) of the limb. In addition to classical functions for *Hox* genes during development, ongoing work has revealed continuing functions for Hox11 during skeletal growth and adult injury repair. Given the continuum of Hox11-expression in undifferentiated stromal cells and the genetic evidence for Hox11 function at all stages, I investigated the possibility that Hox11-expression may identify a skeletal progenitor population throughout the life of the animal. These studies aimed to understand the lineage-relationship of Hox11-expressing stromal cells from embryonic to adult stages and to test the skeletal progenitor potential of this population over time.

The first evidence to support the hypothesis that Hox11-expressing cells are skeletal progenitors at all stages, was flow cytometry data demonstrating that Hoxa11eGFP-expressing cells co-express adult MSC markers PDGFRα/CD51 and Leptin Receptor (LepR) throughout life, beginning from embryonic stages. To rigorously investigate the skeletal progenitor potential of this population *in vivo*, I generated a *Hoxa11-CreER*^{T2} allele by Cas9/CRISPR genetic engineering. I demonstrate that

Hoxa11-lineage marked cells are multi-potent *in vivo* and contribute to all mesenchymal cell types of the skeleton; cartilage, bone, and adipose. *Hoxa11*-lineage marked cells continue to contribute to new skeletal cells out to at least one year of age. In addition to giving rise to the skeleton, *Hoxa11*-lineage marked stromal cells persist within the bone marrow and on the bone surfaces throughout life, even from embryonic stages. Lineage-marked stromal cells co-express MSC markers PDGFRα/CD51 and LepR and continue to express Hoxa11eGFP at all time points. The expression of Hoxa11eGFP within *Hoxa11*-lineage marked MSCs throughout life, and the continuous contribution to new skeletal cells provides evidence that Hox11-expressing MSCs are self-renewing skeletal stem cells. These data reconcile conflicting reports in the field regarding when MSCs arise and provide definitive genetic evidence for an embryonic, perichondrial origin for life-long skeletal stem cells.

CHAPTER I

Introduction

Hox genes as patterning regulators of embryonic development

The *Hox* genes are a family of highly evolutionarily conserved homeodomain-containing transcription factors that pattern the developing embryo as first described in the fruit fly, *Drosophila melanogaster*. The first spontaneous homeotic mutations in the fly body plan, where one segment is transformed to acquire the identity of another, were described in the late nineteenth and early twentieth century [1, 2]. Seminal work by E.B. Lewis and T.C. Kaufman described a series of ordered homeodomain containing genes that had the capacity to regulate segment identity [Figure 1.1] [3-5]. They determined that the positional arrangement of the genes within the *Drosophila* homeotic complex (*HOM-C*) was directly correlated with their functional domain along the anterior to posterior (AP) axis, a concept termed colinearity [3-5]. *Hox* genes have been conserved throughout all bilaterians from flies to rodents to humans, and the clustered organization of these genes has been maintained throughout evolution [6]. Through multiple genomic duplication events, the number of *Hox* genes in all mammals, including mouse and human, has increased resulting in four chromosomal clusters, *HoxA, HoxB, HoxC,* and *HoxD* [Figure 1.1] [7]. Teleost fish represent a unique example of additional duplications and possess 7 or more *Hox* clusters [8-10].

The four mammalian clusters contain a total of 39 *Hox* genes [Figure 1.1] [11, 12]. Correlation of sequence similarity, position within the cluster, and expression domains has permitted further organization of these genes into 13 paralogous groups, *Hox1-Hox13*, positioned 3' to 5' along the chromosome, although no cluster contains the full complement of 13 *Hox* genes [13]. The highly conserved features of paralogous *Hox*

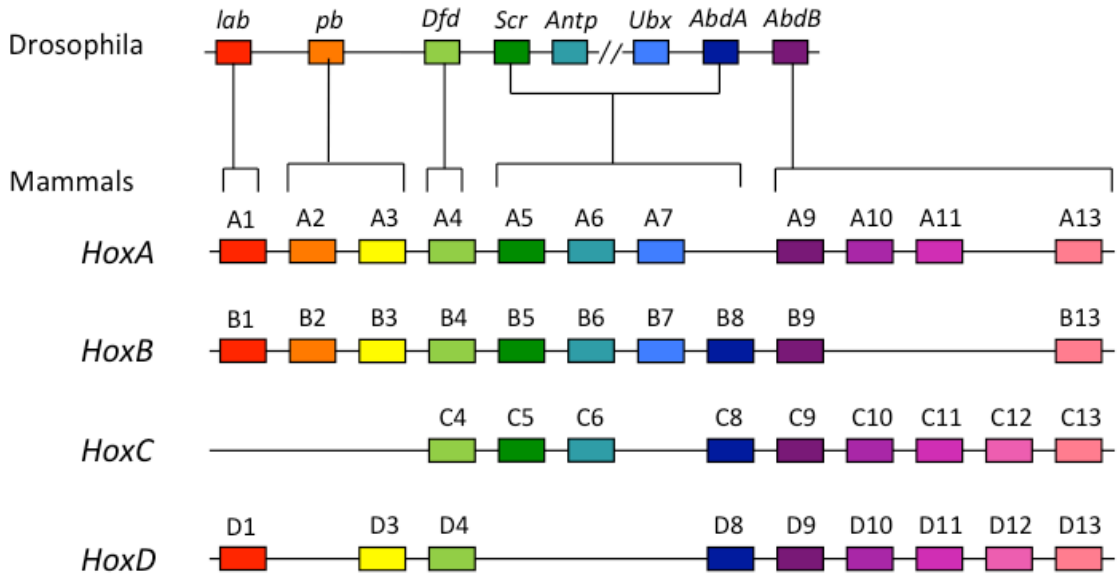

Figure 1.1: Schematic of *Drosophila* HOM-C complexes and mammalian *Hox* genes clusters. Colored boxes represent linear arrangement of genes 3' to 5' (left to right) along the chromosome. Color-coding depicts orthologous relationships between *Drosophila* and mammalian *Hox* genes, and paralogous relationships within the mammalian *Hox* clusters.

genes results in substantial functional redundancy between members. Loss-of-function mutations in a single *Hox* paralog generally results in a mild or no phenotype due to the redundant functions of the remaining paralogs [14-16]. In many cases, assessing *Hox* gene function has required combining loss-of-function mutations in multiple or all members within the paralogous groups [14-29].

Hox paralogs that are located at the most 3' end of the cluster (*Hox1* and *Hox2*) are expressed earliest in the anterior embryo with next most paralogous genes being expressed progressively later with more posterior domains [30-37]. Collinearity is a property of *Hox* genes that has been preserved throughout evolution of the cluster and is predicted to be one of the strongest drivers protecting the clustering of *Hox* genes within the genome [6, 7, 11]. It is perhaps impossible to determine whether *cis*-collinearity, clustering of *Hox* genes along the chromosome, drove the development of spatial and temporal collinearity in expression or *vice versa*, however it is clear that these two properties are intimately linked [7]. Interestingly, vertebrates appear to have the tightest organization of the *Hox* clusters suggesting evolutionary pressure to maintain and refine this configuration [7].

Collinear *Hox* gene expression correlates with changes in vertebral morphology along the AP axis of the body [38]. The result is overlapping paralog expression domains that are increasingly posteriorly restricted. This combinatorial code of *Hox* expression along the AP axis results in vertebrae morphology being determined by patterning information from multiple *Hox* genes, usually two paralogous groups [39-42]. With loss-of-function mutations in an entire paralogous group, the region that normally receives this input is patterned by the remaining *Hox* genes expressed in that region. Generally, the region most affected by paralogous loss-of-function mutations corresponds to the anterior limit of expression of the lost *Hox* genes [14-16]. In the majority of cases, this leads to anterior homeotic transformations in which the vertebrae assume a more anterior morphology [14-16, 26]. For example, the *Hox10* genes normally pattern the lumbar region of the spine, however with complete paralogous loss-of-function of *Hox10* genes, the lumbar vertebrae acquire a thoracic-like morphology with rib-like projections extending throughout the lumbosacral region of the spine [16]. Similar homeotic transformations are observed in complete *Hox11* mutants where the sacral spinal region is

transformed to a lumbar-like morphology [16]. The function of *Hox* genes in determining segment identity was also demonstrated in the gain-of-function scenario where ectopic expression of *Hox10* genes in the thoracic region of the spine suppressed normal rib formation [43]. Thus, *Hox* genes are essential regulators of axial patterning and skeletal morphology.

In addition to their functions in the axial skeleton, the posterior *Hox* paralogs (*Hox9-13*) have been co-opted to pattern the limb skeleton along the proximodistal (PD) axis. The vertebrate limb can be divided into three segments along this axis: the proximal stylopod (humerus/femur), the medial zeugopod (radius and ulna/tibia and fibula), and the distal autopod (carpals and metacarpals/tarsals and metatarsals). Each region of the limb is patterned by specific *Hox* paralogs; *Hox9* and *Hox10* genes pattern the stylopod, *Hox11* genes pattern the zeugopod, and *Hox13* genes pattern the autopod [16, 22, 23]. Additionally, the posterior *HoxA* and *HoxD* clusters are expressed in both the forelimb and the hindlimb, while the *HoxC* cluster is only expressed in the hindlimb [16, 21, 44]. *Hox* loss-of-function phenotypes in the limb cannot be described as classical homeotic transformations as observed in the axial skeleton. In the limb, there is little overlap of paralog expression and *Hox* mutants exhibit a complete, regional loss of patterning information within the segment in which they are expressed. For example, loss of *Hox10* paralogs results in severe mis-patterning of the stylopod while *Hox11* mutants have severe zeugopod mis-patterning [16, 21, 22]. *Hox13* mutants exhibit a complete loss of all autopod skeletal elements [23]. It is important to note that specification of the skeletal elements, with respect to position and number is normal and it is the subsequent elaboration of that pattern that is disrupted with loss of *Hox* function. In fact, with loss of the complete posterior *HoxA* and *HoxD* genes in the limb bud, early specification of the proximal skeletal elements still occurs [45]. These data establish the posterior *Hox* genes as critical regulators of organization of the limb skeletal structures. Despite substantial genetic evidence establishing the importance of *Hox* genes in skeletal patterning, remarkably little is understood regarding the molecular or cellular mechanisms of Hox function.

Development of the Musculoskeletal System

Origin of the musculoskeletal tissues

The limb musculoskeletal system is composed of mesodermal tissue that is derived from two distinct embryonic compartments [Figure 1.2]. The lateral plate mesoderm gives rise to the limb bud itself and all the cartilage and tendon precursors are derived from this compartment [46, 47]. In contrast, muscle precursors differentiate from the dermomyotomal compartment of the axial somites adjacent to the limb field and migrate into the limb bud to form the limb musculature [48-51]. Limb development involves highly coordinated differentiation and patterning of all three tissues.

In mouse, the forelimb bud emerges at embryonic day 9 (E9.0) from the lateral plate mesoderm on either side of the embryo with the hindlimb bud emerging approximately a half a day later. The skeletal pattern of the limb arises as *Sox9*-positive cartilage precursors condense centrally within the limb bud mesenchyme from proximal (stylopod, ~E10.0) to distal (autopod, ~E11.5) [52-55]. Concurrently, muscle precursor cells delaminate from the ventrolateral dermomyotome of the axially-located somites adjacent to the limb bud and migrate into the limb as dorsal and ventral masses, where they continue to proliferate, aggregate, and differentiate into muscle tissue [48, 56]. The tendon primordia and the other connective tissues of the limb arise from within the limb lateral plate mesoderm and align between the muscle masses and the skeletal elements [57-59]. The transcription factor *Scleraxis* (*Scx*) is the earliest known tendon marker and can be detected in the limb buds by E10.5, however an overt tendon pattern is not observed until E12.5 [58-60]. The dorsal and ventral muscle bundles segregate into individual anatomical groups as muscle connective tissue cells align along future sites of splitting and initiate cell death [57, 61, 62]. This process generally proceeds in a proximal to distal and dorsal to ventral fashion along the limb axes. Bone, tendon, and muscle precursors undergo concurrent differentiation and patterning in a highly coordinated fashion to allow for proper integration of the tissues into a functional musculoskeletal unit. The mechanisms governing these integration events are an area of active study.

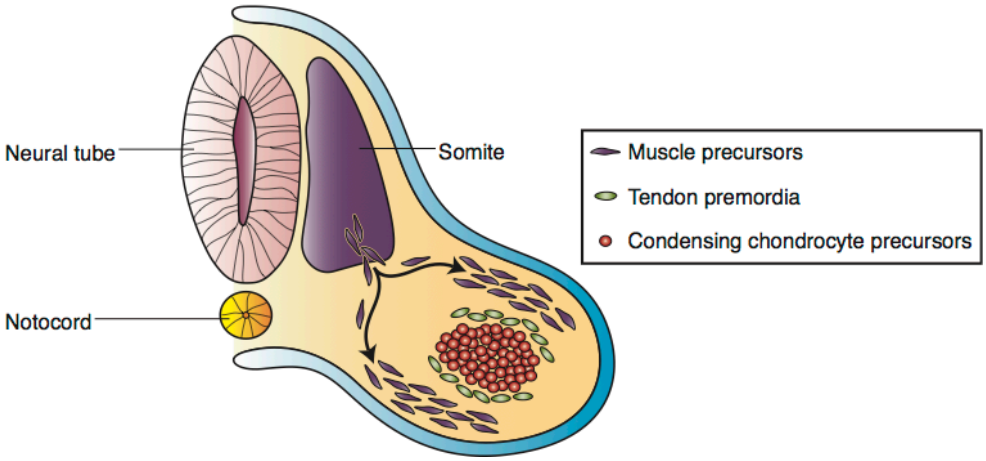

Figure 1.2: Limb musculoskeletal tissues are derived from two distinct mesodermal compartments. Tendon (green) and chondrocyte (red) precursors are derived from the lateral plate mesoderm within the limb bud, and tendon primordia arise adjacent to the centrally localized chondrocyte condensations. Muscle precursors (purple) delaminate from the ventral somite adjacent to the limb and migrate into the limb bud as dorsal and ventral muscle masses.

Integration of the Musculoskeletal Unit

Much is understood regarding the development of the three main tissues of the skeleton individually, but only recently has progress been made in understanding how these tissues are integrated into a functional musculoskeletal unit. For proper function, the appropriate muscles must be precisely connected to the bony elements, via tendon, to allow for locomotion. At the earliest stages of limb development, specification and patterning of cartilage, tendon, and muscle tissues appear to be tissue autonomous and each of these tissues can initially develop in the absence of the others [47, 48, 63]. As development proceeds, tissue-tissue interactions are required for the maintenance and continued maturation of each component.

Muscle precursors themselves have no intrinsic or pre-determined patterning information. Classical chick-quail graft experiments, where somites outside the normal limb region are grafted into the axial region adjacent to the limb, demonstrated that muscles from any somite are capable of migrating into the limb and forming normal limb musculature [48, 49]. Retroviral-labeling of myogenic progenitors migrating into the developing limb field showed that individual myoblasts are not biased towards contributing to any specific muscle bundle [64]. Additionally, if tendon primordia are surgically removed, muscle progenitors still migrate into the limb bud mesenchyme and are able to undergo maturation demonstrating that differentiation of muscle tissue is autonomous and does not require signals from the tendon [57]. However, following removal of tendon primordia, muscle patterning is entirely disrupted.

The entirety of the muscle patterning information is contained within the muscle connective tissue elements of the limb. Prior to muscle invasion, muscle connective tissue fibroblasts form a muscle pre-pattern that functions to sub-divide the dorsal and ventral muscle streams into individual muscle groups [65]. Muscle connective tissue fibroblasts are marked by the transcription factor *Tcf4* and can be observed as early as E12.5 in the developing limb bud [65, 66]. Tcf4-positive fibroblasts are intimately associated with the myofibers of the limb musculature during development and remain associated throughout life [66]. There is evidence that Tcf4-positive connective tissue fibroblasts function as an extrinsic source of signals to regulate muscle myofiber type and myofiber maturation

[66]. In addition to being a marker of the muscle connective tissue, Tcf4 appears to have a functional role in regulating muscle patterning. *Tcf4* loss-of-function disrupts several aspects of muscle patterning resulting in abnormal muscle splitting and truncation of several muscles, as well as mispatterning of the sites of muscle integration with the bone [65, 66]. Collectively, these data establish the importance of the connective tissue elements, including tendon, in patterning the individual muscle bundles and also regulating the fiber type composition of the individual muscles.

Initial tendon patterning events are tissue autonomous, however continued maintenance of tendon progenitors requires interactions with the muscle and the skeletal elements. Careful examination of muscle-less and skeletal-less limb models revealed that tendon requirements for tissue-tissue interactions differs along the proximal to distal axis of the limb. In the absence of muscle, proximal tendon progenitors are progressively lost while tendon differentiation occurs normally in the distal autopod region [57, 67, 68]. In contrast, if skeletal formation is inhibited through conditional loss of *Sox9* in the limb bud, the muscle and tendon of the proximal elements occurs normally while autopod tendons are completely absent [60]. Tendon progenitor induction and skeletal condensation are tightly linked as increases or decreases in the number of digits results in a corresponding increase or decrease in formation of the associated tendons [69]. These data suggest a requirement for muscle-tendon interactions in the proximal limb and cartilage-tendon interactions in the distal limb for tendon tissue maintenance. Interestingly, it is still unclear whether physical interactions or signaling between tissues is required for tendon maintenance.

The differences between proximal and distal tendon maturation led to a re-examination of how tendons develop, particularly tendons that span the zeugopod/autopod boundary. There are several long tendons that originate within the zeugopod but anchor to the skeleton within the autopod which appeared inconsistent with data indicating differing requirements for tendon within these two regions. Careful examination of tendon development during the transition from the muscle-independent phase to the muscle-dependent phase revealed a modular mechanism of tendon development [60]. Initially, short tendon progenitors integrate with the proximal and distal ends of the individual muscle groups. As limb outgrowth continues, the short

tendons integrate with the skeletal elements at the proximal end of the muscle and form connections with their counter parts, that arise within the autopod, at the distal end of the muscle, modularly forming a differentiated linear tendon [60]. Following the integration of zeugopod and autopod tendons at the wrist, muscle contractions appear to be necessary for further individuation of the autopod tendons.

Tendon Integration and Secondary Skeletal Structures

The most important outputs resulting from tendon-bone interactions are the formation of the secondary structures of the skeleton, eminences, and the sites of tendon-bone insertion, entheses. The enthesis, or tendon-bone interface, is a specialized fibrocartilage matrix that serves as a graded transition zone between the collagen-rich matrix of the tendon and the highly mineralized bone matrix [70]. These attachment sites form by the end stages of embryonic development but undergo maturation postnatally [71-73]. This maturation process additionally requires muscle loading for proper development. If muscle paralysis is induced at early postnatal stages, growth, maintenance, and mineralization of the fibrocartilage matrix are all severely compromised [72]. Additionally, the maturation process appears to be dependent, at least in part, on hedgehog signaling [74, 75]. Lineage tracing of Hedgehog-responsive cells by *Gli1*-CreER, demonstrated that enthesis fibrocartilage cells are derived from this population [74]. Cell ablation or inhibition of the Hedgehog signaling response within this population leads to defects in fibrocartilage development; however, the source of Hedgehog ligand for enthesis development remains unclear [74, 75].

A subset of tendons will integrate with the skeleton at specialized protrusions from the long bone surface termed eminences [76]. These specialized secondary structures of the skeleton are derived from a unique pool of Sox9 and Scx double-positive progenitors that are distinct from the main skeletal elements and function to dissipate mechanical stress from muscle contractions [77, 78]. Double-positive eminence progenitors undergo differentiation and assume either a tendon or cartilage cell fate to generate the tendon-bone interface and integrate the two tissues. Interestingly, if cartilage fate is inhibited through *Sox9* deletion in Scx-expressing cells, there is a complete loss of eminence formation. However, tendons still differentiate and attach to the skeleton [77].

Alternatively, if Scx is inhibited there is also a loss of eminence formation due to a loss of BMP expression resulting in the inhibition of normal cartilage differentiation [77, 79]. Following the initial patterning of eminence progenitors, subsequent maintenance and growth requires muscle loading. Inhibition of muscle contraction or complete loss of muscle will result in loss of the secondary structure by the end of embryonic development [79]. Therefore, eminence formation represents a unique situation requiring proper integration of all three skeletal tissues for normal development.

Establishment of Regional Patterning

A critical component in patterning the musculoskeletal system is the incorporation of regional differences in patterning along the anterior to posterior axis of the vertebrae and the proximal to distal axis of the limb. The same tissue components, muscle, tendon, and bone, are present throughout the limb, but substantial morphological differences and unique connections occur within these tissues along the axial and limb skeletal axes. How these tissues form precise connections, sometimes spanning two regions of the limb, and integrate into a functional unit is largely unknown. Critical examination of the *Hox11* mutant phenotype provides new data suggesting that regional pattering information is informed, at least in part, by the master developmental regulators, the *Hox* genes [80].

A *Hoxa11eGFP* knock-in mouse model was utilized to examine *Hox11* expression in detail within the developing limb [80, 81]. Characterization of Hoxa11eGFP expression in whole mount and in longitudinal limb sections shows broad expression throughout the distal limb bud mesenchyme early in development [80]. This expression is rapidly restricted to the presumptive zeugopod by E12.5 [Figure 1.3A]. Interestingly, Hoxa11eGFP-positive cells are excluded from the Sox9-expressing chondrogenic precursors and early Osterix (Osx) positive osteoblast progenitors at all stages of development [Figure 1.3B] [80]. Careful examination shows Hoxa11eGFP-positive cells in the outer perichondrial layer surrounding the zeugopod condensations immediately adjacent to the chondrocyte and osteoblast cells. Hoxa13GFP expression has also been reported to be expressed in the perichondrium and excluded from condensing cartilaginous elements [82] .Co-expression analyses also revealed Hoxa11eGFP is not expressed within developing muscle cells [80]. Rather Hoxa11eGFP expression is

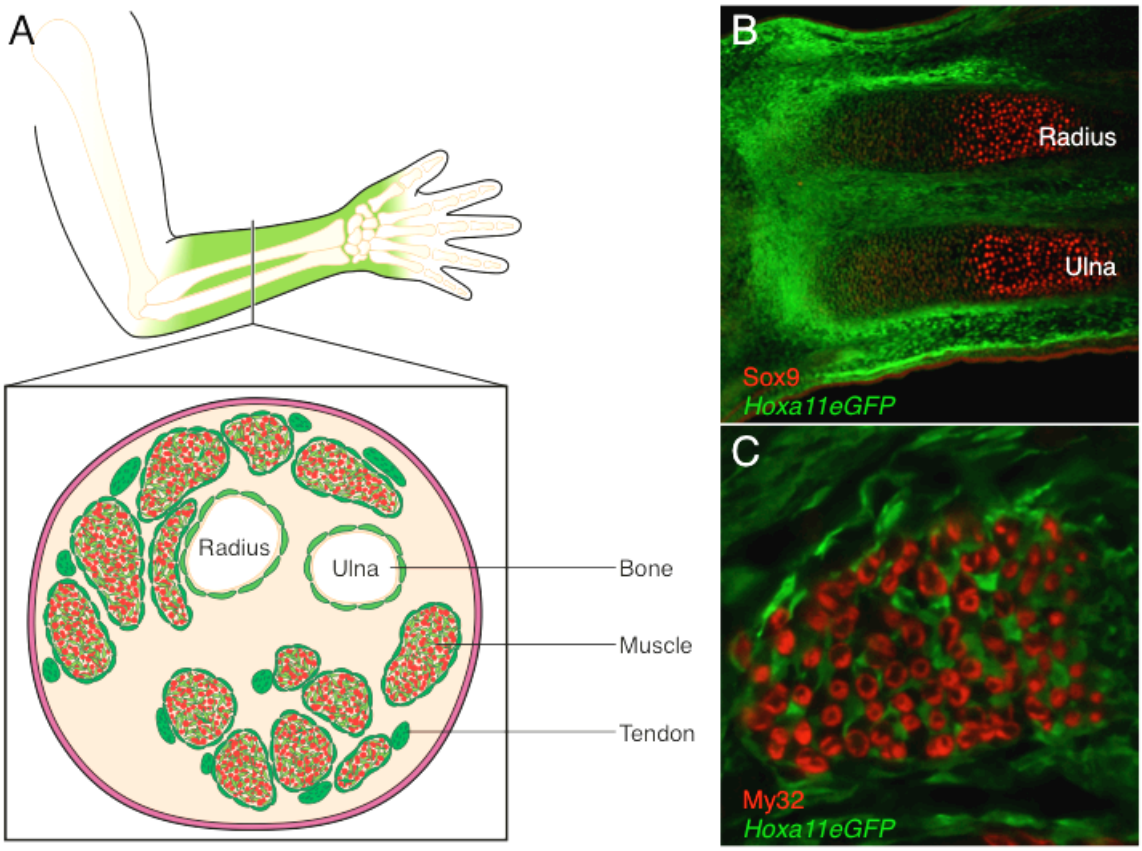

Figure 1.3: Hox11 is expressed in the connective tissue (stromal) compartment of the forelimb. (**A**) Hoxa11eGFP expression is restricted to the zeugopod and excluded from bone and muscle cells. Hox11 is expressed in the outer perichondrium surrounding the bones, in the muscle connective tissue, and in the tendons. (**B**) Longitudinal section of E14.5 forelimb showing expression of Hox11eGFP (green) surrounding the Sox9+ (red) skeletal elements. (**C**) Transverse view of an individual forelimb muscle bundle at E14.5 showing expression of *Hox11eGFP* (green) in the muscle connective tissue surrounding individual muscle (red) cells. My32, myosin 32.

observed within all muscle connective tissue cells and in the connecting tendons [Figure 1.3C] [80]. The collective data demonstrating the importance of the connective tissue elements of the limb in integrating the musculoskeletal unit suggested additional patterning roles for Hox beyond the skeleton.

As mentioned previously, the cartilage elements destined to become the zeugopod bones condense normally in *Hox* loss-of-function mutants, but the pattern is not elaborated to form morphologically appropriate bones [16, 21-23, 83]. In addition to the well-described regional skeletal phenotypes, severe mis-patterning of the zeugopod muscles and tendons is observed in *Hox11* loss-of-function mutants [80]. Early tendon progenitors are specified in *Hox11* mutants and appear similar to controls, suggesting that *Hox* functions in patterning and integration but does not function in specification of the connective tissue elements. Additionally, the migration of muscle precursors into the limb occurs normally and dorsal and ventral muscle masses are present. However, the subsequent splitting of the masses into individual muscle bundles is abnormal and loss or fusion of various muscle groups is observed [80]. Loss of *Hox11* function does not appear to affect muscle differentiation.

Development and patterning of the skeletal elements remains normal in *Hox11* compound mutants where one of the four functional *Hox11* alleles of the forelimb (either *Hoxa11* or *Hoxd11*) is still expressed [16, 21, 80, 83]. The question of whether the muscle and tendon defects represent an independent role for *Hox11* in patterning these tissues, or whether the phenotypes are simply a consequence of the severely disrupted skeletal patterning can, thus, be addressed. In *Hox11* compound mutants, skeletal patterning is preserved but regional mis-patterning of the muscles and tendons is still observed, demonstrating that the muscle and tendon phenotype is independent of skeletal pattern [80]. Therefore, *Hox11* genes function in patterning and integration all of the tissues of the musculoskeletal unit beyond just skeleton development. These analyses also demonstrate that skeletal patterning and muscle/tendon patterning can be uncoupled. Analysis of limb muscle and tendon phenotypes in other posterior *Hox* gene paralogous mutants has not been performed in detail, but given the conserved skeletal defects comparing loss-of-function of the 5' Hox paralogs, I hypothesize that similar muscle and tendon phenotypes will be observed.

The observation that *Hox11* is not expressed in differentiated cartilage, bone, or muscle tissues but in the connective tissues of the limb including the perichondrium, tendon, and muscle connective tissue, significantly alters predictions for the mechanism of *Hox11* function in patterning the limb. Consistent with the body of work establishing essential roles for connective tissue elements in musculoskeletal patterning and integration, these data support a model whereby all Hox-mediated regional patterning information is contained within the stromal populations of the limb. *Tcf4*-Cre lineage-tracing experiments revealed that muscle connective tissue, tendon, and eminence cells were all derived from the *Tcf4*-lineage and suggested the possibility that all the connective tissues of the limb are derived from a single progenitor population that integrates the musculoskeletal system [66, 84]. The continuum of Hoxa11eGFP-expression throughout the connective tissue elements is consistent with Hox-expression defining this putative progenitor population in the zeugopod region.

Hox Function Beyond Embryogenesis

Complete loss of an entire paralogous *Hox* group are generally embryonically lethal and are not observed in human patients, however mutations in specific *Hox* genes have been associated with several congenital disorders. For example, hand-foot-genital syndrome, a rare autosomal dominant disorder, is likely caused by a predicted loss-of-function mutation of *Hoxa13* due to a polyalanine tract expansion [85, 86]. Additionally, patients with cognitive dysfunction associated with Bosley-Salih-Alorainy syndrome and Athabascan brainstem dysgenesis syndrome are linked to mutations in *Hoxa1* [87]. Beyond development, there is growing evidence for continuing functions for *Hox* genes in multiple organ systems in adult tissue homeostasis and in cancer. *Hox* genes continue to be expressed at adult stages in many tissues and the regional domains established during development appear to be maintained [88, 89]. In the lung, loss of the *Hox5* paralogs results in severely hypoplastic lungs and ongoing work has implicated continuing functions for the *Hox5* genes in alveolar development in the lung, a process that occurs exclusively after birth in mice [[90, 91], Hrycaj *et al. in preparation*]. In the hematopoietic system, multiple *Hox* genes are expressed in hematopoietic stem cells (HSCs) and other immature myeloid sub-population and have been implicated in

regulating proliferation and differentiation [92-97]. Despite abundant genetic evidence for *H0ox* gene function in the hematopoietic system, their mechanism of action remains unclear. There is substantial evidence for deregulation of *Hox* gene expression in numerous adult solid tumor and blood cancers including; colorectal, breast, prostate, ovarian, bladder/kidney, thyroid, lung, acute myeloid leukemia (AML), and mixed-lineage leukemia (MLL) [reviewed [98-100]]. General principles of *Hox* function in cancer have not been established and the mechanism of action is highly context dependent. Additionally, both oncogenic and tumor suppressive roles have been attributed to different *Hox* genes, sometimes even the same *Hox* gene, in specific contexts. In breast cancer, high levels of *Hoxb13* is associated with increased tumor cell invasiveness; thereby acting as an oncogene [101]. These patient observations are recapitulated *in vitro* where forced expression of *Hoxb13* in breast epithelial cells results in increased cell motility and invasiveness [102]. While in the prostate, forced expression of *Hoxb13* in prostate cancer cell lines inhibits activation of the androgen receptor, slowing cell growth, and thereby preventing tumorigenesis [103, 104]. The role of *Hox* genes in cancer has, perhaps, been most significantly investigated for *Hoxa9* in leukemias [100]. High levels of *Hoxa9* expression are correlated with poor prognosis in acute leukemia, and clinically Hoxa9 is used as a biomarker [100]. Multiple upstream genetic alterations have been described resulting in upregulation of *Hoxa9* including translocations and fusion events, sometimes even with the C-terminal *Hox* homeodomain, as well as deregulation of polycomb gene expression [100]. Ongoing study into the function of *Hox* in both the healthy and disease state will be important given clear functions for *Hox* in a diverse array of cancers and the therapeutic potential for targeting *Hox* genes or their downstream effectors.

As mentioned previously, *Hox11* compound mutants display largely normal skeletal development during embryogenesis however these animals begin to display morphological defects during the postnatal growth period [21, 105]. Expression analysis of fracture calluses indicated increased levels of several homeodomain containing proteins including *Msx1, Msx2, Prx1, Hoxa2 and Hoxd9* [106]. A different group performed microarray analyses on femur fracture callus samples throughout the healing process and observed increased *Hox* gene expression throughout the whole time course of

repair [107]. These observations strongly suggest continuing functions for *Hox* genes in the skeleton.

Our group recently used an ulnar fracture model to elucidate the function of *Hox11* during skeletal repair [108]. These studies utilized *Hox11* compound loss-of-function mutants (*Hoxa11+/-;Hoxd11-/-* or *Hoxa11-/-;Hoxd11+/-*) to assess *Hox* function during the course of injury repair. *Hox11* compound mutants display defects at multiple stages of injury repair suggesting functions for *Hox* throughout the processes. During early stages of fracture repair, *Hox11* compound mutants exhibit reduced endochondral ossification and generate significantly less cartilage volume within the callus, resulting in incomplete bridging of the fracture gap [108]. At later stages, *Hox11* compound mutants display incomplete bone remodeling with the bone never recovering back to its original structure and form [108]. There is a clear similarity between the apparent chondrogenesis defects observed in fracture repair and the early arrest of chondrocyte differentiation within the skeletal anlagen during development of *Hox11* mutants suggesting potentially conserved functions for Hox throughout life.

To provide insight into the mechanism of *Hox* function at adult stages, significant effort was devoted to establishing the identity of adult Hoxa11eGFP-expressing cells at homeostasis and during injury repair. Characterization of Hox11eGFP expression throughout postnatal and adult stages demonstrated that Hox11-expressing cells remain regionally restricted to the zeugopod throughout life [109, 110]. During fracture healing, Hox11-expressing cells expand immediately throughout the fracture callus and stay localized to the bone surfaces throughout the repair process [108]. Extensive co-expression studies determined that, similar to embryonic development, Hoxa11eGFP was not expressed in any differentiated cell type within the skeleton including chondrocytes, osteoblasts, osteocytes, blood vessels, hematopoietic cells, or neurons [80, 110]. Flow cytometry analyses determined that Hoxa11eGFP-positive cells were restricted to the non-hematopoietic, non-endothelial stromal compartment within the bone marrow space and in the perichondrium [110]. Through the use of cell surface markers and genetic lineage-tracing models, Hox11-expressing cells were identified as exclusively labeled by the bone marrow mesenchymal stem/stromal cell (MSC) surface markers PDGFRα/CD51 and Leptin Receptor (LepR) and by LepR-Cre [110].

Skeletal Mesenchymal Stem Cells

The existence of multi-potent mesenchymal stromal cells (MSCs) in the skeleton was first demonstrated by Friedenstein and colleagues when they established that plastic adherent cells isolated from bone marrow could form fibroblastic colonies (CFU-F) in cell culture, differentiate into bone, and reconstitute the hematopoietic microenvironment when transplanted *in vivo* [111-115]. Two main functions have been attributed to skeletal MSCs. The first function is to serve as a reservoir of new cellular material to maintain skeletal integrity throughout the life of the animal [116, 117]. The second function is as a component of the HSC niche [118-121]. The niche refers to the physical environment where HSCs reside within the bone marrow space and functions to preserve the stem cell state both through direct cell-cell contact and through paracrine production of specific signaling factors [122]. Bone marrow stromal cells express several important HSC niche factors including *C-X-C motif chemokine 12* (*CXCL12*), *stem cell factor* (*Scf*), and *angiopoietin 1* (*Ang1*) that are necessary for HSC maintenance [123]. Elimination of MSC populations or deletion of HSC niche factor expression in MSCs through genetic or pharmaceutical methods leads to reductions of long-term HSCs [120, 121, 124-127]. Today, several overlapping mesenchymal stromal populations of cells have been defined that enrich, to varying degrees, for cells with stem cell capacity [reviewed in extensive detail [119, 128, 129]. However, unlike the hematopoietic system where the HSC has been unequivocally defined, an analogous cell has not been precisely described in the mesenchymal compartment. It is important to highlight here that the existence of a self-renewing mesenchymal stem cell capable of giving rise to bone, cartilage, and fat has, thus far, only been demonstrated clonally through *in vitro* differentiation assays or via transplantation of a cultured clonal population. Single-cell clonal tracing to demonstrate both multi-lineage contribution and self-renewal has yet to be performed *in vivo*.

The earliest genetically marked population to be rigorously tested to enrich for progenitor-enriched MSCs was defined by GFP expression driven by the *Nestin* promoter. *Nestin*-GFP-positive cells were shown to be rare, perivascularly-localized stromal cells within the bone marrow space [121]. The *Nestin*-GFP positive population was shown to contain all the CFU-F capacity in the bone marrow and these cells undergo multi-lineage differentiation into the skeletal mesenchymal lineages; osteoblasts,

chondrocytes, and adipocytes [121]. Self-renewal was demonstrated clonally through serial transplantation supporting that this population enriches for cells with multi-potent stem cell activity [120, 121]. When the lineage capacity of the *Nestin*-GFP positive population was tested *in vivo u*sing an inducible lineage-tracing model, *Nestin*-CreER, the *Nestin*-lineage marked cells were shown to contribute to bone and cartilage lineages *in vivo* [Figure 1.4 and [121, 130]]. Interestingly, contribution to adipocytes was not reported following adult-lineage induction, and no contribution was observed from postnatal *Nestin*-lineage marked cells [130]. This apparent contradiction in multi-lineage capacity of *Nestin*-GFP expressing stromal cells and *Nestin*-lineage marked cells has not been resolved, but conflicting results suggests assays in which cells have been placed *in vitro* and subsequently transplanted may not represent *in vivo* functions. It is important to note that *Nestin*-GFP is also expressed in endothelial cells within bone marrow, and *Nestin*-CreER lineage tracing reveals substantial contributions to the endothelial lineage particularly from fetal and early postnatal stages [130]. Curiously, several *Nestin* transgenes have been generated and they do not identify completely overlapping populations. Cells expressing the *Nestin*-GFP transgene discussed above express little endogenous *Nestin*, *Nestin*-CreER, or *Nestin*-mCherry, obfuscating the identity of the marked population [125, 130]. *Nestin*-CreER was additionally shown to preferentially label *Nestin*-GFP expressing endothelial cells during developmental stages [130]. These differences in expression could explain some of the discrepancies between the clonal *in vivo*/*in vitro* analyses and the genetic models.

Bone marrow stromal cells expressing the combination of cell surface markers PDGFRα/CD51 or Leptin Receptor (LepR) identify a largely overlapping population within the cells marked by *Nestin*-GFP [131, 132]. As expected, the stromal cell population identified by these markers also encompasses the majority of CFU-F in the bone marrow, undergoes tri-lineage differentiation into bone, cartilage and fat *in vitro*, and is capable of self-renewal by CFU-F culture analyses and serial clonal transplantation [131, 132]. It is important to note that only ~10% of LepR cells form CFU-F and only ~10% of clonal colonies undergo tri-lineage differentiation with the remaining clones showing a bias towards osteogenic-forming colonies, highlighting the heterogeneity within this population [132]. While CFU-F capacity is not a direct measure of stem cell

number, and clonal *in vitro* differentiation experiments are technically challenging, these data suggest that the true mesenchymal stem cell is only a fraction of the total population and remains to be more specifically defined.

Additional sub-populations have been identified that enrich for progenitor-enriched MSCs with varying characteristics. Cells co-expressing PDGFRα and Sca1 represent a very small fraction of the PDGFRα/CD51 population that is highly enriched for CFU-F, however does not contain all CFU-F in the bone marrow [132, 133]. PDGFRα/Sca1 cells are clonally capable of tri-lineage differentiation *in vitro* [133]. Stromal cells expressing CXCL12, otherwise known as CAR cells, are bi-potent osteo-adipo progenitors *in vitro* [134]. CAR cells appear to be mutually exclusive from PDGFRα/Sca1 cells as there is no expression of CXCL12 within the PDGFRα/Sca1 population [133]. Through extensive fractionation of the bone marrow stroma using markers CD51 (AlphaV integrin), CD105, Thy, 6C3 and CD200, cells co-expressing CD51 and CD200 were demonstrated to sit at the top of a stromal hierarchy giving rise to all seven of the other identified sub-populations *in vitro* and *in vivo* [135]. For these experiments, each sub-population of stromal cells was either clonally cultured *in vitro* or transplanted into the renal capsule *in vivo* and the lineage hierarchy was determined by flow cytometry analysis of the expanded population following a period of colony expansion [135]. CD51/CD200 cells, termed mouse skeletal stem cells (mSSCs) are multi-potent *in vivo* and *in vitro* and self-renewal was demonstrated through serial transplantation [135]. During development, PDGFRα/Sca1 cells and CD200-positive mSSCs arise as two mutually exclusive sub-populations from within the PDGFRα/CD51 population [136]. Most recently, *Hoxa11eGFP*-expressing cells were found to be exclusively identified as a sub-population of PDGFRα/CD51- and LepR-positive bone marrow stromal cells [110]. The Hoxa11eGFP-positive sub-population was shown to further enrich for CFU-F potential as compared to the total PDGFRα/CD51 population, suggestive of even further enrichment for progenitor-enriched MSCs, and Hox-positive cells undergo tri-lineage differentiation *in vitro* [110]. As mentioned above, Hox expression is regionally restricted within the skeleton during development. Using *LepR-Cre* lineage-marked stromal cells isolated from different regions of the skeleton, Rux and colleagues demonstrated that Hox expression is exclusive to the *LepR*-lineage marked

stromal fraction, and that *LepR*-lineage marked cells isolated from different regions of the body express a Hox profile consistent with the expression domains established during embryonic development [110].

Ubiquitous and inducible lineage-tracing alleles have been used to interrogate the multi-lineage potential of progenitor-enriched MSC populations *in vivo*. Adult bone marrow stromal cells marked by Cre driven by the LepR promoter (*LepR-Cre*) faithfully mark the PDGFRα/CD51 and LepR-positive progenitor-enriched MSC population, and are the major source of bone and fat in the adult mouse [Figure 1.4 and [132]]. *LepR*-lineage marked cells did not give rise to chondrocytes during homeostasis but were capable of giving rise to cartilage within the callus following fracture injury [132, 137]. Interestingly, *LepR*-lineage marked cells begin to appear around E17.5 but do not make any substantial contribution to osteoblasts and osteocytes until at least 2 months of age, suggesting this lineage gives rise to adult MSCs but does not support embryonic development and postnatal growth [132, 137]. It is important to note that *LepR*-Cre is not a temporally controlled model and, therefore, new cells will continuously be marked by this allele as LepR, and thus *LepR*-Cre, is expressed. This precludes the unequivocal identification of a single MSC population. While this allele has been helpful in assessing the dynamics of adult progenitor-enriched MSC populations, the critical caveats of this model must be remembered and care taken to appropriately assess these data.

The timing of lineage-contribution to differentiated cells in the *LepR*-Cre model revealed that embryonic bone development and postnatal growth is not supported by the cells marked by *LepR*-Cre. Numerous genetic models have been explored to identify earlier skeletal progenitors. *Prx1*-Cre labels the entire early limb bud mesenchyme, derived from the lateral plate mesoderm, and gives rise to CAR cells, periosteal cells, and LepR-positive stromal cells demonstrating that adult MSCs arise from cells within the early limb bud [Figure 1.4 [134, 138]]. It was unclear from these data whether a more precise stem cell origin could be identified.

Multiple groups have investigated this question and proposed some unique insights into the nature of developmental progenitors of the skeleton. The most rigorously investigated inducible model is *Osterix*-CreER [137, 139, 140]. *Osterix* (*Osx*) is a critical

early transcription factor required for osteoblast differentiation. *Osx*-lineage marked cells behave differently depending on the timing of lineage induction [Figure 1.4]. Cells marked by *Osx*-CreER at embryonic stages contribute substantially to bone formation during development and postnatal growth, but contribution ceases by adult stages and this population is depleted with time [139, 140]. Embryonic cells marked by *Gli1*-CreER at similar stages exhibit multi-lineage contribution to the skeleton at adult stages (8 weeks), but the long-term persistence of this population was not reported [Figure 1.4 and [141]]. The same *Gli1*-CreER marked population at later stages functions as an osteo-lineage restricted progenitor with no stromal cell contribution [141]. In contrast, early postnatal *Osx*-lineage marked cells contribute to bone during growth and adult homeostasis and persist as bone marrow stromal cells out beyond 1 year of age [137, 140]. Interestingly, the contribution of postnatal *Osx*-lineage marked cells to bone decreases as the animal ages despite the persistence of a marked stromal population suggesting heterogeneity within the initially marked population [140]. Long-lived *Osx*-lineage marked stromal cells are *Nes*tin-GFP-, LepR-, and PDGFRα-positive [137, 140]. There is more significant *Osx*-lineage contribution to CAR cells over PDGFRα/Sca1 cells in the bone marrow following chasing to adult stages [140]. Lineage-tracing of perichondrial/periosteal cells by *Col2*-CreER or chondrocyte lineage cells by *Sox9*-CreER or *Aggrecan*-CreER demonstrated similar capacity to give rise to long-lived bone marrow stromal cell populations from postnatal stages, but not other stages [Figure 1.4 and [140]]. Postnatal and adult cells labeled by *Gremlin 1*-CreER (*Grem1*-CreER) also exhibit long-term persistence, but function as lineage-restricted osteo-chondro progenitors [Figure 1.4 and [142]]. The embryonic *Grem1*-lineage was not examined beyond birth. Finally, adult *Osx*-CreER lineage-marked cells are osteo-lineage restricted and only contribute to bone for a short period of time before they are depleted [140]. From these collective data, a model for skeletal progenitors was proposed whereby embryonic development is supported by early skeletal progenitors which are replaced by definitive skeletal progenitor-enriched MSCs that arise during postnatal stages [118, 128].

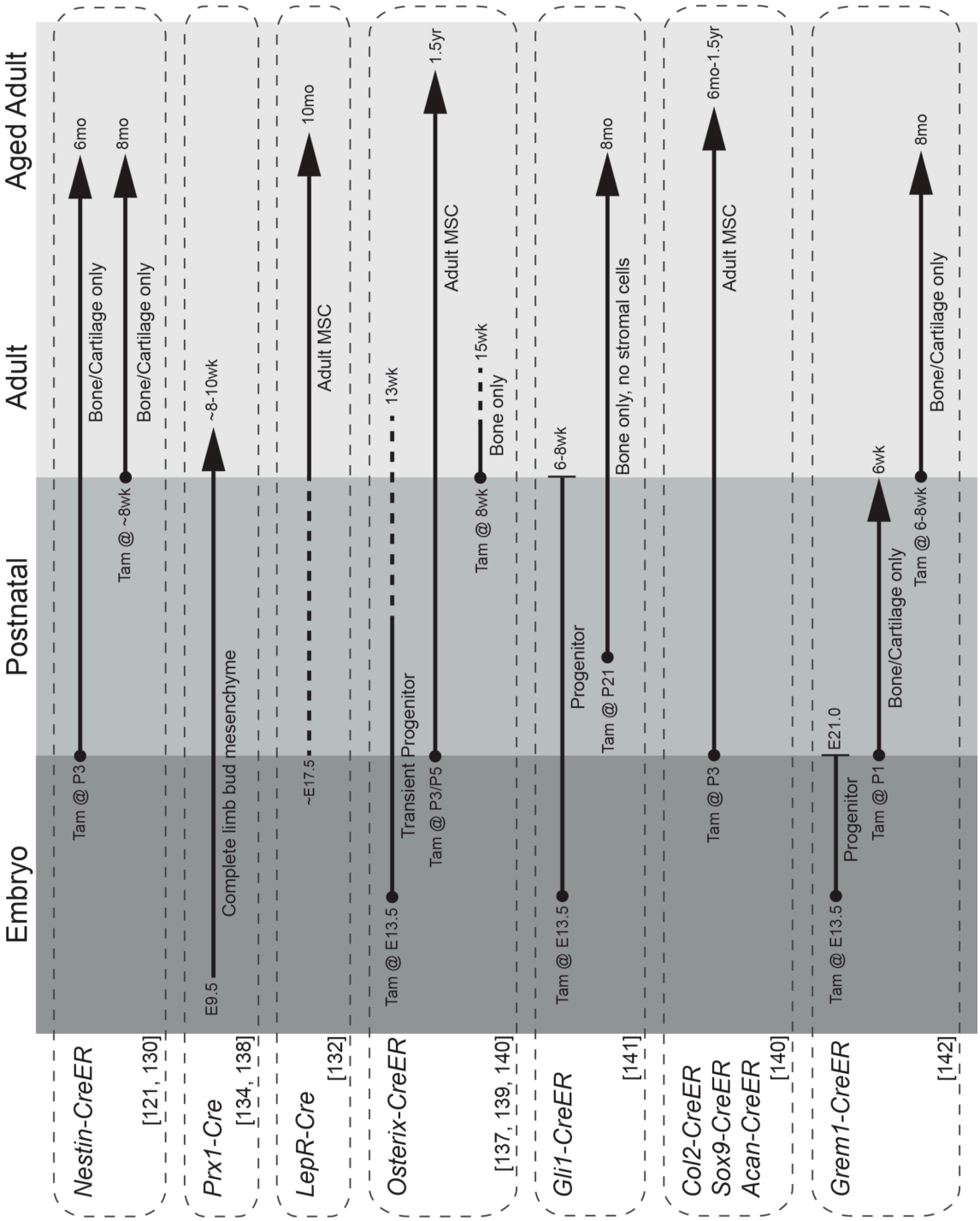

Figure 1.4: Comparison of genetic MSC lineage populations. MSC populations genetically marked by various Cre/CreER models display different lineage dynamics over time. The appearance of each population or the time point of tamoxifen induction (black circle) and the analysis end point (arrow) for each model is noted. Lineage contribution not reported beyond a certain stage is indicated by vertical bar. Brief summary of the skeletal contribution and MSC-like behavior is indicated.

One important critique of the 'two-waves-of-progenitors' model comes from the nature of the genetic models utilized to generate this hypothesis. The majority of the mouse models analyzed employ an inducible CreER driven by promoter of genes known to be involved in early chondrogenic (Sox9 and Aggrecan) or osteogenic (Osterix) differentiation. Additionally, as has been shown for many stem cell populations, skeletal stem cells are thought to be primed to differentiate into multiple lineages and therefore have initiated expression of multiple early commitment factors despite not committing to a given lineage [143]. One interpretation of these results is that most of the cells marked by these inducible CreER alleles will be committed cartilage or bone progenitors, respectively, while the true progenitors will be inefficiently and stochastically labeled. Therefore, the interesting dynamics of the Osx-CreER lineage-marked population, for instance, may be more representative of the behavior of early osteo-progenitors and less indicative of the true skeletal stem cell.

Summary of thesis work

The work presented in this thesis aims to understand the mechanism of Hox11 function in the skeletal system, to define the nature of Hox11-expressing cells in the skeleton at all stages, and to assess the stem/progenitor potential of Hox11-expressing cells throughout life. *Hox11* compound mutant skeletons are indistinguishable from controls at birth, but by adult stages the bones display an abnormal morphology characterized by shorter elements and an anterior bowing of the radius [21, 80, 83]. I first characterized the postnatal growth defects displayed by *Hox11* compound mutants as the development of this phenotype has not been assessed in great detail prior to this work. I characterized the progression of the *Hox11* compound mutant bone phenotype from birth to 8 weeks of age and demonstrated a reduced growth rate in both bones. Interestingly, the ulna growth rate was disproportionately reduced potentially contributing to the abnormal bowed morphology of the radius. Defects in the rate of chondrocyte proliferation within the reserve and proliferative zones were observed resulting in depletion of the immature chondrocyte pool and premature growth plate collapse. The proliferative defects additionally uncouple the growth rate between the radius and ulna thereby contributing to the abnormal skeletal morphology by adult stages. These data

provide evidence for continuing functions for Hox11 genes in the skeleton outside of development and support an important role for Hox11 in regulating chondrocyte proliferating and differentiation within the growth plate.

Previous work from the Wellik lab identified adult Hoxa11eGFP-expressing stromal cells to be identified by markers for bone marrow MSCs [110]. However, these data did not establish whether Hox11-expressing cells function as MSCs *in vivo*. Additionally, given the continuum of Hox11eGFP-expression throughout life and genetic evidence supporting Hox11 function in the skeleton throughout life, I hypothesized Hox11-expressing cells represent a continuous skeletal progenitor population. To test the stem/progenitor potential of the Hox11-expressing population *in vivo*, I generated *Hoxa11* lineage-tracing allele using Cas9/CRISPR. The first allele contains a tamoxifen inducible $CreER^{T2}$ knock-in to the endogenous *Hoxa11* locus, *Hoxa11-*$CreER^{T2}$. I show that *Hoxa11*-lineage marked cells give rise to all the skeletal mesenchymal lineages (cartilage, bone, and adipose) and provide evidence that Hox11-expressing MSCs self-renew for the life of the animal. These data reconcile conflicting data in the field and demonstrate for the first time that long-lived skeletal stem cells population arise during embryonic development and persist throughout life.

There is evidence supporting continuing functions for *Hox11* genes in the skeleton during embryonic development, postnatal growth, and adult fracture repair [80, 109, 110]. However, paralogous *Hox11* loss-of-function mutants are embryonic lethal precluding study of complete mutants at postnatal and adult stages. I additionally generated a *Hoxd11*-conditional allele which, when combined with *Hoxa11* loss-of-function, will allow for generation of complete *Hox11* loss-of-function mutants in a stage-specific and/or cell type-specific manner through the use of various *Cre/CreER* models. I show preliminary data confirming the functionality of this new allele and this work will be continued by other members of the Wellik lab.

Finally, I present data exploring potential mechanisms for Hox11 function during the early stages of skeletal development. *Hox11* mutants display chondrogenic differentiation defects that first manifest around E12.5, however the mechanism of Hox11 function regulating the early stages of skeletal patterning and development are

unknown [83]. Careful comparative expression analyses of three genes with critical functions in early skeletal development, *Indian Hedgehog* (*Ihh*), *Runx2*, and *Wnt5a*, were performed in *Hox11* control and mutant embryo forelimbs. Hox11-expressing cells in the perichondrium appear to respond to IHH ligand through up-regulation of *Gli1*-lacZ signal. These data are consistent with the hypothesis that Hox11 cooperates with the Hedgehog signaling pathway in the perichondrium to pattern the developing skeletal elements. These studies provide a foundation for future experiments to determine the nature of the Hox and Hedgehog pathway interactions.

CHAPTER II

Hox11 genes regulate postnatal longitudinal bone growth and growth plate proliferation.

Summary

Hox genes are critical regulators of skeletal development and *Hox9-13* paralogs, specifically, are necessary for appendicular development along the proximal to distal axis. Loss of function of both *Hoxa11* and *Hoxd11* results in severe malformation of the forelimb zeugopod. In the radius and ulna of these mutants, chondrocyte development is perturbed, growth plates are not established, and skeletal growth and maturation fails. In compound mutants in which one of the four *Hox11* alleles remains wild-type, establishment of a growth plate is preserved and embryos develop normally through newborn stages, however, skeletal phenotypes become evident postnatally. During postnatal development, the radial and ulnar growth rate slows compared to wild-type controls and terminal bone length is reduced. Growth plate height is decreased in mutants and premature growth plate senescence occurs along with abnormally high levels of chondrocyte proliferation in the reserve and proliferative zones. Compound mutants additionally develop an abnormal curvature of the radius, which causes significant distortion of the carpal elements. The progressive bowing of the radius appears to result from physical constraint caused by the disproportionately slower growth of the ulna than the radius. Collectively, these data are consistent with premature depletion of forelimb zeugopod progenitor cells in the growth plate of *Hox11* compound mutants, and demonstrate a continued function for *Hox* genes in postnatal bone growth and patterning.

Introduction

The proximodistal elongation of long bones occurs through the process of endochondral ossification within the growth plate. The growth plate is organized into distinct cellular zones: the reserve or resting zone (RZ), the proliferative zone (PZ), and the prehypertrophic/hypertrophic zone (HZ). Chondrocytes at the epiphyseal end of the growth plate make up the RZ. RZ chondrocytes are slow dividing, stem/progenitor cells which give rise to flattened columns of PZ chondrocytes [144]. Chondrocytes in the PZ proliferate rapidly and undergo morphological changes to become oriented into columns of cells arranged parallel to the long axis of the bone [145]. As cells in the columns reach the metaphyseal side of the growth plate and enter the HZ, it has been reported that chondrocytes exit the cell cycle, undergo hypertrophy and initiate apoptosis [146]. Concomitantly, hypertrophic chondrocytes secrete significant amounts of extracellular matrix which becomes mineralized and provides a template for new bone formation [147]. The cartilage matrix of the growth plate is subsequently remodeled and replaced by bone through the function of osteoclasts and osteoblasts.

Longitudinal bone growth is regulated both locally and systemically by a host of hormones and growth factors that coordinate proliferation, matrix synthesis and differentiation of chondrocytes [148, 149]. While the differentiation program of growth plate chondrocytes is similar in all long bones, elongation occurs at different rates to allow each element to achieve correct proportionate lengths for the adult animal [150]. These rates of growth can vary dramatically. Indeed, growth plates at opposite ends of the same long bone can differ by a factor of two- to three-fold [150]. These differences in growth rate contribute to final bone lengths and morphology, however the processes that govern these differential rates of growth are poorly understood.

Hox genes are a family of highly conserved, homeodomain-containing transcription factors crucial for axial and appendicular patterning. In the limb skeleton, *Hox9-13* genes pattern the proximodistal axis and loss-of-function mutations of paralogous genes result in dramatic, region-specific perturbations of skeletal development. Loss of *Hox9* and/or *Hox10* genes results in mispatterning primarily of the stylopod element (humerus or femur) [16, 22]. Loss of *Hox11* function leads to severely

truncated zeugopod skeletal elements (radius/ulna or tibia/fibula) [16, 21, 83]. In *Hoxa13/Hoxd13* mutants, the autopod skeletal elements (hand or foot bones) are affected [23, 151, 152]. The genetic requirement for *Hox* genes during development is well documented, but continuing roles for these genes postnatally is less explored.

A high degree of functional redundancy exists between members of a *Hox* paralogous group. For example, single allele mutants of *Hoxa11* or *Hoxd11* exhibit minor developmental defects, which include fusion of various carpal bones, minor malformations of the distal epiphyseal end and a slight thickening of the radius and ulna [153-155]. These phenotypes are in stark contrast to the dramatic mispatterning observed when all *Hox11* paralogous genes are lost ($Hoxa11^{-/-};Hoxd11^{-/-}$ in the forelimb or $Hoxa11^{-/-};Hoxc11^{-/-};Hoxd11^{-/-}$ in the hindlimb). In these mutants, the cartilage anlage condense normally, however, the subsequent maturation of the chondrocytes fails, an organized growth plate is not established and no skeletal pattern is elaborated [83]. Interestingly, maintenance of a single functional allele of *Hoxa11* or *Hoxd11* is sufficient to allow for normal embryonic skeletal development in the forelimb [21, 80, 83]. In these *Hox11* compound mutant embryos, no differences in proliferation, apoptosis, or overall skeletal growth was observed [83]. However, by adult stages, *Hox11* compound mutant animals exhibit a significant reduction in zeugopod skeletal length [21]. The purpose of this study was to define the morphological and cellular processes that contribute to the postnatal growth defects in *Hox11* compound mutants during postnatal development.

We show that *Hoxa11* and *Hoxd11* continue to be expressed in the forelimb zeugopod throughout postnatal stages. Consistent with previous reports, the skeletal morphology of *Hox11* compound mutants is indistinguishable from controls at birth. However, during postnatal growth, the compound mutant radius and ulna grow at slower rates than controls at all time points examined and growth arrests at earlier stages. Despite total bone lengths being comparable to controls at birth, growth plate length is shortened in compound mutants. Chondrocytes are prematurely depleted in the mutant growth plate during postnatal growth correlated with increased levels of proliferation in the RZ and PZ. Additionally, the longitudinal growth of the compound mutant ulna is more severely affected than the radius resulting in a bone that is disproportionately shorter. The altered proportions of the radius and ulna contribute to an anterior bowing of

the compound mutant radius in adult animals. Together, these results demonstrate a continuing role for *Hox11* genes in postnatal bone growth.

RESULTS

Hox11 genes remain expressed through postnatal and adult stages

We previously published detailed developmental expression analysis of *Hoxa11* in the embryo utilizing a *Hoxa11eGFP* knock-in allele [80, 81]. Embryonically, *Hoxa11eGFP* is expressed in the connective tissue elements of the forelimb including the perichondrium/periosteum, tendon and muscle connective tissue with the strongest expression surrounding the distal end of the radius and ulna [80]. Utilizing this *Hoxa11eGFP* allele, we show that *Hoxa11eGFP* continues to be expressed at birth and through postnatal stages. *Hoxa11eGFP* is expressed strongly in the perichondrium and along the trabecular bone surface, with lower expression observed within the most distal RZ chondrocytes [Figure 2.1A-D]. Expression of *Hoxd11* is observed in the connective tissue surrounding the distal radius and ulna in a pattern similar to *Hoxa11eGFP* expression [Figure 2.1E-F and data not shown]. qPCR analysis for both *Hoxa11* and *Hoxd11* on whole bones (radius and ulna) at E12.5, E18.5 and 1, 2, and 4 weeks of age demonstrates continued expression of both genes through adult stages. Interestingly, *Hoxd11* shows higher relative expression at embryonic stages, but both *Hoxa11* and *Hoxd11* remain expressed through adult stages.

Abnormal postnatal skeletal growth in *Hox11* compound mutants

To assess the development of the compound mutant skeletal phenotype during postnatal stages, we performed micro-computed tomography (μCT) analysis at 0, 2, 4, 6 and 8 weeks of age on *Hox11Aadd* animals. The humerus was measured as an internal control for animal size as the length, bone quality, and bone morphology and was indistinguishable between *Hox11* compound mutants and controls [Figure 2.2]. Skeletal preparations and isosurface renderings of μCT scans allow visualization of the morphology of the radius and ulna of control and *Hox11* compound mutants throughout postnatal growth [Figure 2.3A]. While no statistical difference in mineralized bone length is measurable at birth, the length of the ulna is trending towards being shorter in mutants compared to controls and slight morphological differences in the radius and ulna can already be observed [Figure 2.3A-C]. Abnormal curvature of the radius in compound mutants is readily apparent at two weeks of age and becomes

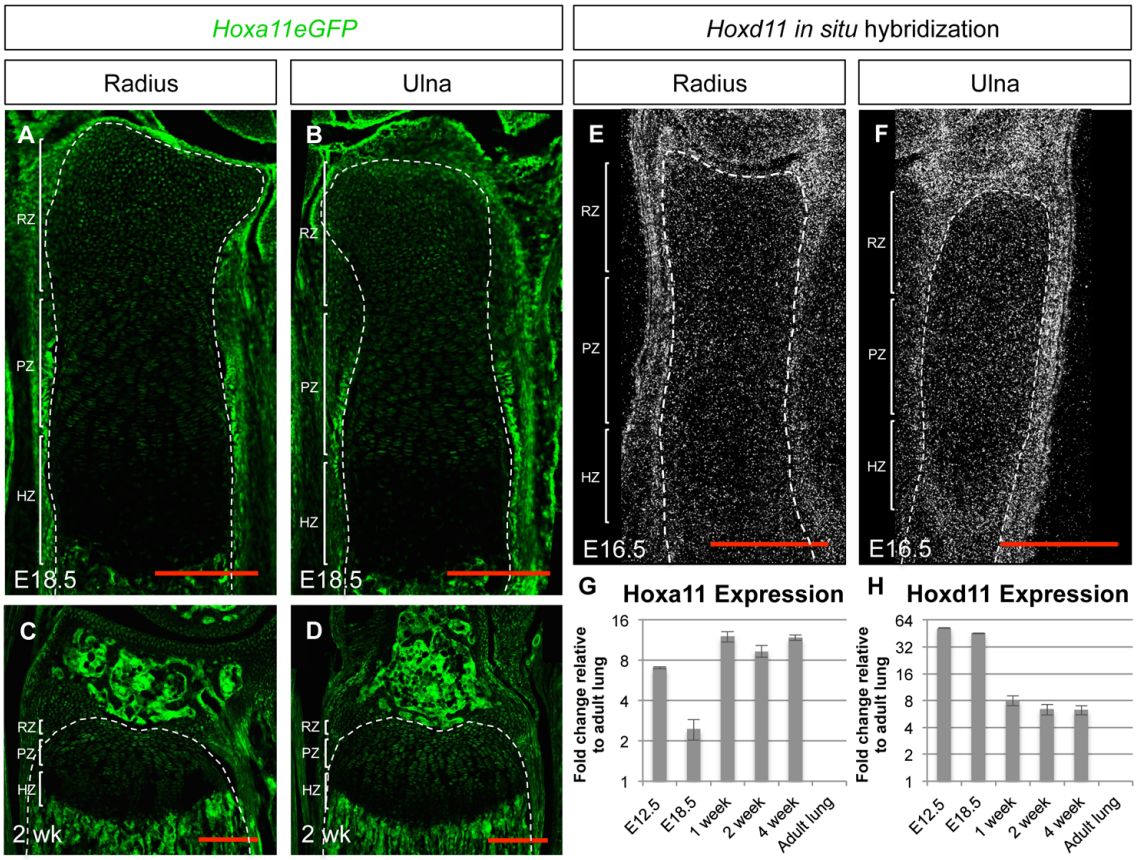

Figure 2.1: Expression of *Hoxa11* and *Hoxd11* in postnatal development. (**A-D**) Expression of *Hoxa11eGFP* in E18.5 radius (**A**) and ulna (**B**) and in 2-week old radius (**C**) and ulna (**D**). *In situ* hybridization of *Hoxd11* in E16.5 radius (**E**) and ulna (**F**). Dashed white line outlines the distal growth plate and brackets demarcate the zones of the growth plate. (**G**) qPCR analysis of *Hoxa11* expression at E12.5, 18.5 and 1, 2, and 4 weeks of age. (**H**) qPCR analysis of *Hoxd11* expression at E12.5, E18.5 and at 1, 2, and 4 weeks of age. (**G-H**) Expression values are relative to *Hoxa11* or *Hoxd11* expression in adult lung, which is set to '1'. All data presented as mean ± standard deviation. RZ: reserve zone, PZ: proliferative zone, HZ: hypertrophic zone. N=3-5, Scale bar = 200μm

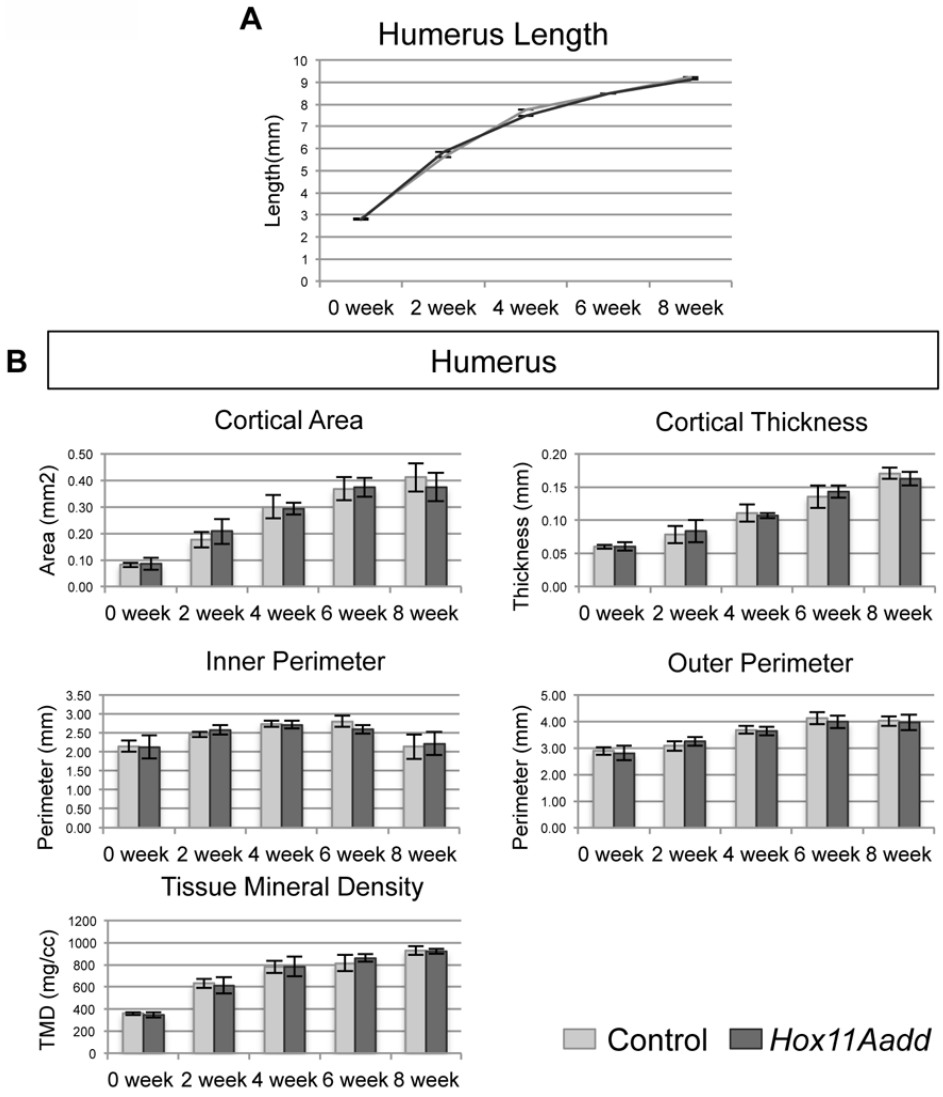

Figure 2.2: Development of the humerus is unaffected in *Hox11* compound mutants. (**A**) Mineralized length of the humerus in control (light grey) and *Hox11* compound mutant (dark grey) at 0, 2, 4, 6, and 8 weeks of age was measured along the central curvature of the element. (**B**) µCT analysis of bone morphology and quality of the humerus of control (light grey) and *Hox11* compound mutant (dark grey). Cortical area and thickness, inner and outer perimeter, and tissue mineral density was measured at 0, 2, 4, 6, and 8 weeks of age. All data presented as mean ± standard deviation. N=5-10.

progressively more severe through postnatal development. In addition, the distal radioulnar joint is dysmorphic and the radius of compound mutants progressively extends ectopically into the carpal bones [Figure 2.3A, arrows]. The overgrowth of the radius results in a forward subluxation of the hand and outwards rotation of the autopod.

To begin to dissect the onset of the postnatal phenotypes, the mineralized lengths of the radius and ulna were measured along the central curvature of the bone at 0, 2, 4, 6, and 8 weeks of age [Figure 2.3A, solid and dashed lines]. No significant differences in mineralized length of the radius or ulna was observed at newborn stages between controls and compound mutants, consistent with previous reports [Figure 2.3B,C, [83]]. Differences in bone length are observed early in postnatal development and by 2 weeks of age, both the radius and ulna of the compound mutant are shorter compared to controls: the radius is 15% reduced and ulna 20% reduced. By 4 weeks of age, the differences in length between the compound mutant and controls are exacerbated further (radius 17%, ulna 27% reduced). Longitudinal bone growth has slowed dramatically or stopped in all bones in both controls and mutants by 8 weeks of age, and at this stage the *Hox11* mutant radius is 22% shorter and the ulna is 30% shorter than their analogous control counterparts [Figure 2.3B,C].

In both controls and mutants, the rate of bone growth decreases with age. Consistent with the reduction in total bone length, the growth rate of both the mutant radius and ulna is reduced compared to controls at all time points examined [Figure 2.3D, solid bars vs. open bars]. Interestingly, the rate of growth of the mutant ulna slows noticeably faster than the mutant radius, and growth of both elements has essentially stopped by 6 weeks of age in mutants [Figure 2.3D, solid blue bars vs. solid green bar]. While the compound mutant radius grows slower than controls throughout development, the decrease in growth rate over time is comparable to controls [Figure 2.3D, solid green bar vs. open green bar].

Bone mineral quality is not affected in *Hox11* compound mutants

Bone quality of both *Hox11* compound mutants and controls was analyzed by μCT analyses at 0, 2, 4, 6 and 8 weeks of age. No differences in any of the parameters measured, including cortical area and thickness, inner and outer perimeter, and tissue

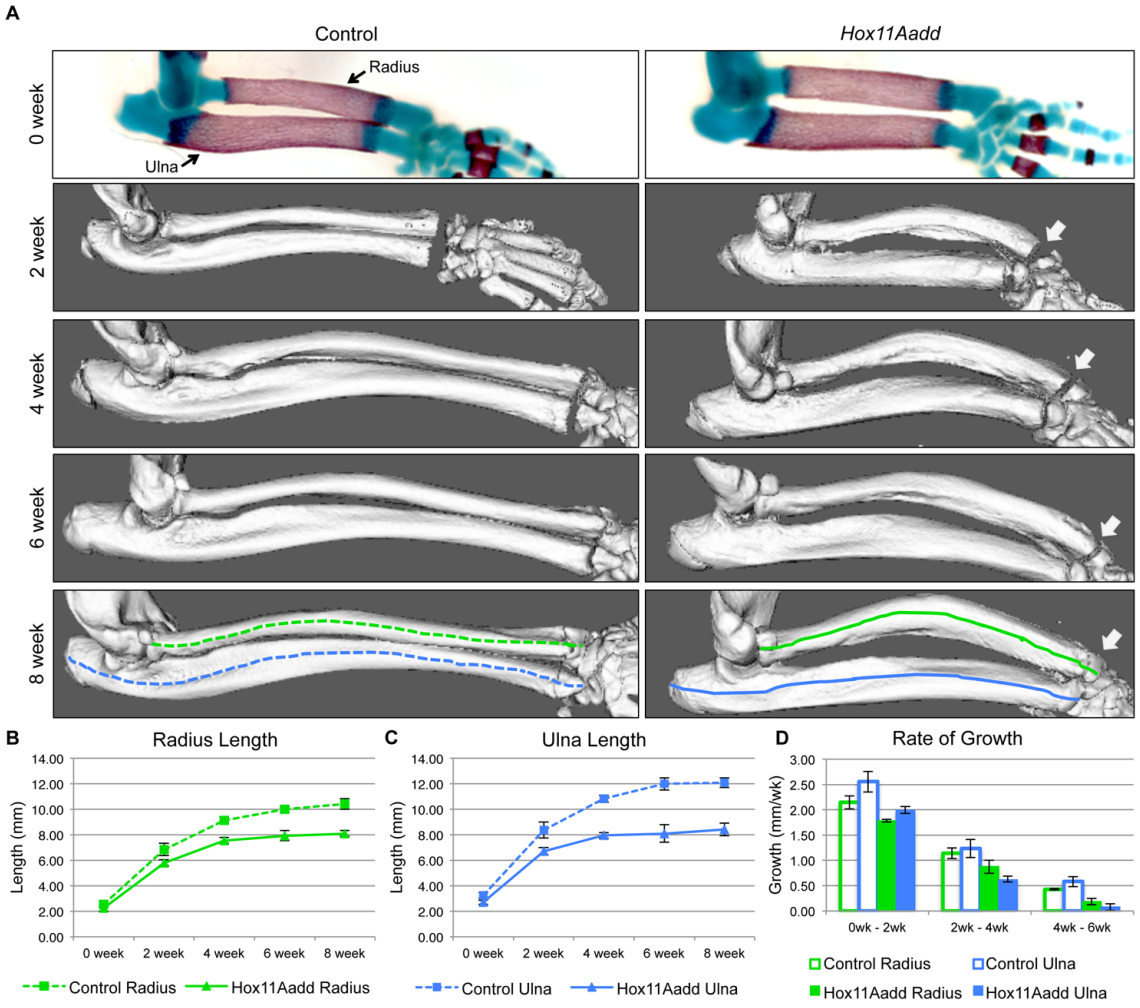

Figure 2.3: Postnatal development of wild-type control and *Hox11* compound mutant forelimb zeugopod. (**A**) Skeletal preparation of newborn (0 week) forelimb and 3D rendering of µCT scans of 2, 4, 6 and 8 week forelimb from control and *Hox11* compound mutant. Dashed and solid lines indicate central curvature of the element. White arrows highlight distortion of the carpal bones by the radius in the compound mutant. (**B-C**) Mineralized length of the radius (**B**) and ulna (**C**) at 0, 2, 4, 6 and 8 weeks of age was measured along the central curvature of the element. (**D**) The rate of growth of the radius and ulna of controls and compound mutants was calculated between 0-2 week, 2-4 week, and 4-6 week of age. All data presented as mean ± standard deviation. N=5-10.

mineral density were observed in the humerus of *Hox11* mutants [Figure 2.2B]. In contrast, cross-sectional views of the radius and ulna through the mid-diaphysis of control and *Hox11* mutants at 8 weeks of age highlight morphological differences in these animals. Note the bowing phenotype leads to a larger distance between the radius and ulna in compound mutants compared to controls [Figure 2.4A,B]. Compound mutant bones are show measured increases in cortical area, cortical thickness, and bone perimeter compared to controls [Figure 2.4C,D]. No differences in tissue mineral density are observed between control and *Hox11* compound mutants demonstrating that, despite differences in bone thickness and size, bone quality appears to be comparable by this measure [Figure 2.4C,D].

Appositional bone growth is not coordinated in *Hox11* compound mutant radius and ulna.

To investigate bone growth and remodeling, we utilized dynamic histomorphometry to examine appositional growth patterns in the radius and ulna of control and compound mutants. New mineral deposition was analyzed by injection of dye at 2 weeks (xylenol orange label), 3 weeks (calcein label), and 4 weeks (alizarin complexone label) of age. Animals were assessed two days after the last injection. Growth patterns of control and compound mutants were analyzed at the mid-diaphysis where peak curvature is observed in mutant radii. Both xylenol orange (2 weeks) and alizarin complexone (4 weeks) are detected in the red channel, and new bone formed at these two time points can be distinguished by the presence of a green calcein label between the two labels. Rapid growth rates and high bone turnover make quantification of appositional growth rates unfeasible at these time points, however, qualitative differences in overall growth patterns between *Hox11* compound mutants and controls can be assessed. Within the cortical bone of wild-type controls, there are relatively large distances between labels indicating significant amounts of growth between time points [Figure 2.5A-C]. Additionally, the distance between labels is not uniform, highlighting the dynamic nature of postnatal skeletal growth. The 3-week label (green) is present as a mostly uninterrupted layer throughout both zeugopod bones, the 4-week label (surface red layer) is observed uniformly on the endosteum of both bones in the control, while the 2-week label (cortical red label) has been largely remodeled away by the time point of

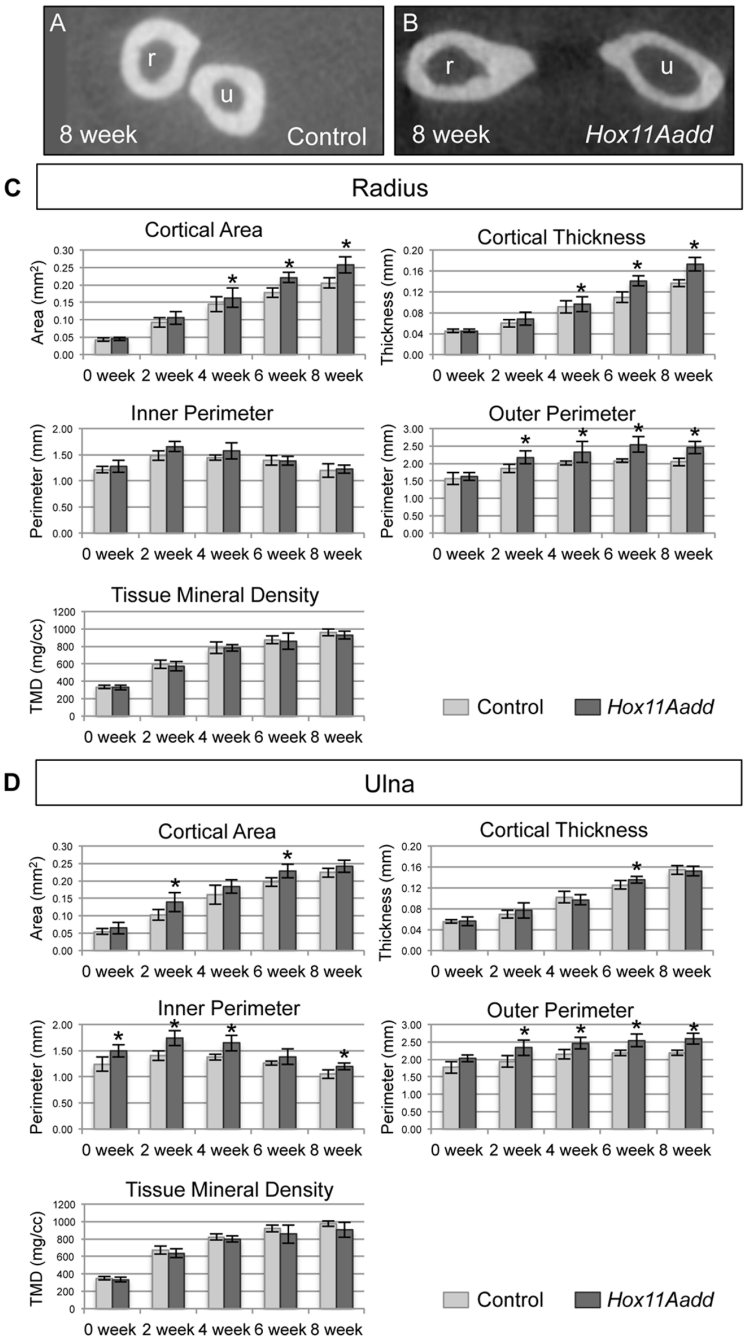

Figure 2.4: µCT analysis of bone morphology and quality. (**A-B**) Cross-sectional view of µCT scans at 8 weeks of age for control (**A**) and *Hox11* compound mutant (**B**) forelimb zeugopod. Cortical area and thickness, inner and outer perimeter, and tissue mineral density of the radius (**C**) and ulna (**D**) of control (light grey) and compound mutant (dark grey) animals were measured at 0, 2, 4, 6 and 8 weeks of age. All data presented as mean ± standard deviation. N=5-10 *p ‹ 0.05.

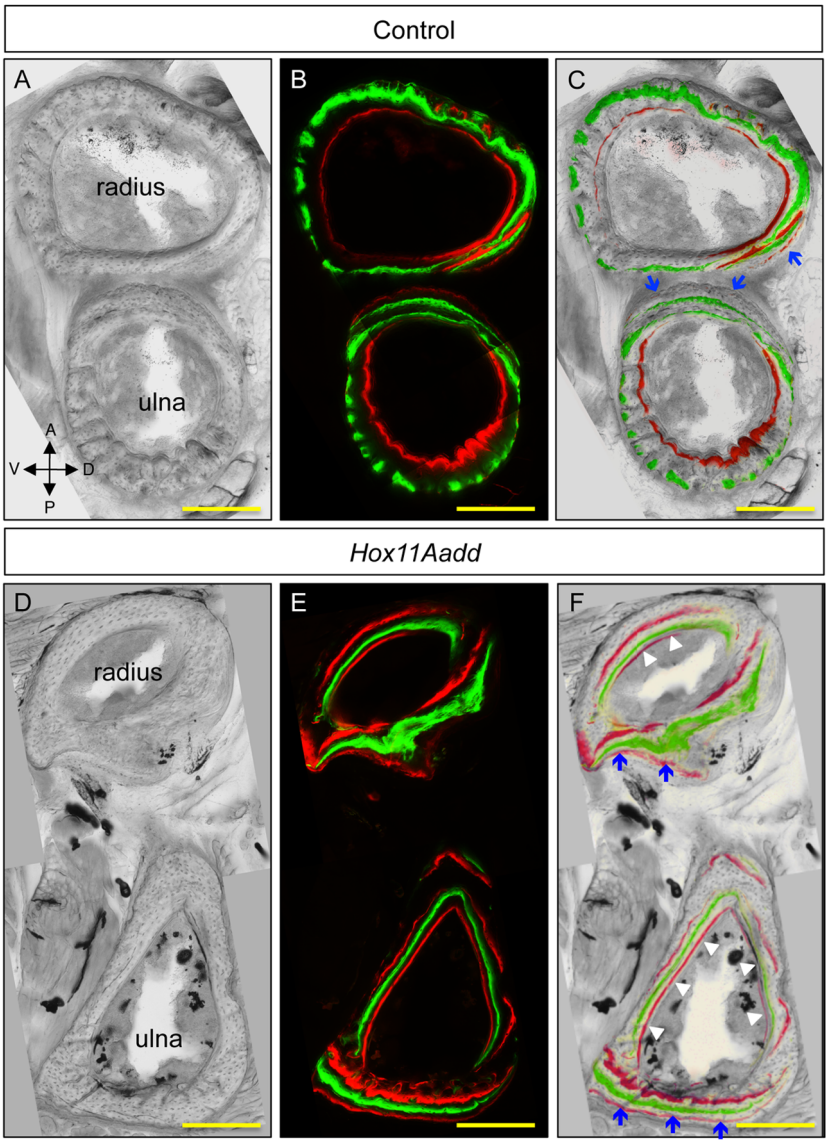

Figure 2.5: Appositional bone growth examined by dynamic histomorphometry. Wild-type control (**A-C**) and *Hox11* compound mutant (**D-F**) animals were injected with xylenol orange (red), calcein (green), and alizarin complexone (red) at 2 weeks, 3 weeks and 4 weeks of age respectively. Representative bright field (**A, D**) and fluorescent (**B, E**) cross-sectional images of the mid-diaphysis were overlaid (**C, F**) to examine appositional growth patterns. Areas of appositional growth of the periosteal (blue arrows) and endosteal (white arrowheads) bone surface are highlighted. Scale bar = 100 μm.

analyses [Figure 2.5A-C]. Appositional growth in control animals is observed only on the posterior-distal periosteal surface of the radius and the anterior periosteal surface of the ulna corresponding to ridges that are being patterned on the bone surface [Figure 2.5A-C, blue arrows].

In contrast to control animals, appositional growth in *Hox11* compound mutants is consistently unidirectional in both the radius and ulna. Posterior growth is observed endosteally [Figure 2.5D-F, white arrowheads] and periosteally [Figure 2.5D-F, blue arrows] in both the radius and ulna. This strong unidirectional growth pattern is established by 2 weeks of age and continues through 4 weeks as demonstrated by incorporation and retention of all three labels [Figure 2.5D-F]. Minimal incorporation of label on the anterior surface of the compound mutant radius and ulna indicates a lack of new bone formation or high levels of remodeling on this surface. Taken together, the data demonstrate that *Hox11* mutants enact active bone growth in opposition to the direction of anterior radial bowing, consistent with correctional growth.

Hox11 compound mutant growth plates are morphologically abnormal and chondrocytes are prematurely depleted

Growth plate morphology was analyzed at 0, 2, 4, 6, and 8 weeks of age in controls and compound mutants to investigate whether premature depletion of chondrocytes contributes to the reduction in bone length in mutants. The growth plate length of the mutant radius and ulna is significantly shorter than controls at newborn stages despite the absence of significant differences in bone length at this stage, and the growth plate remains shorter throughout postnatal development [Figure 2.6A,B]. By 6 weeks of age and beyond, differences in growth plate length are no longer statistically significant, likely due to physiological growth plate collapse in both controls and mutants by these stages [Figure 2.6A-B,O-V].

All three zones of the growth plate: the reserve zone, proliferative zone, and hypertrophic zone, are established in the compound mutant, however, cellular organization of the growth plate is disorganized compared to controls. This is noted particularly in the PZ of the compound mutants. PZ chondrocytes are visualized histologically in clusters in the mutant animals, in contrast to the normal vertical columns

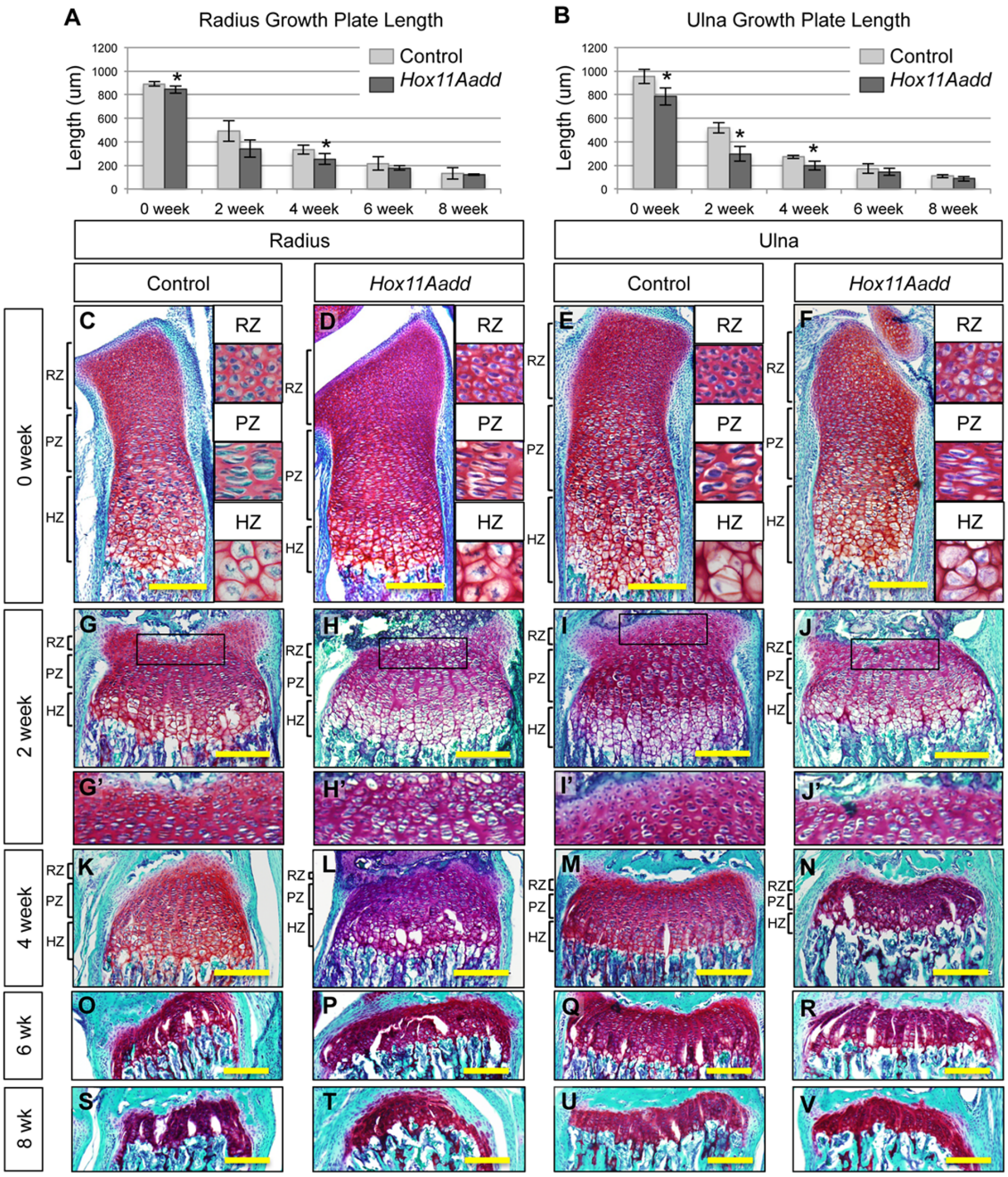

Figure 2.6: The distal growth plate of *Hox11* compound mutant forelimb zeugopod bones undergoes premature senescence. (**A-B**) Total growth plate length of the radius (**A**) and ulna (**B**) from control (light grey) and compound mutant (dark grey) animals was measured from Safranin-O/Fast Green stained sections. Representative images of Safranin-O/Fast Green/Hematoxylin stained distal forelimb growth plates at 0 week (**C-F**), 2 week (**G-J'**), 4 week (**K-N**), 6 week (**O-R**) and 8 week (**S-V**) old controls and compound mutants. Black brackets demarcate zones of the growth plate at 0, 2, and 4 weeks (**C-J**). RZ: reserve zone, PZ: proliferative zone, HZ: hypertrophic zone. All data presented as mean ± standard deviation. N=4-5. *p ‹ 0.05, paired Student's t-tests. Scale bar = 200 μm.

of flattened chondrocytes seen in controls [Figure 2.6D, PZ vs. Figure 2.6C, PZ and Figure 2.6F, PZ vs. Figure 2.6E, PZ]. While matrix secreted by the PZ chondrocytes is not uniformly organized vertically in *Hox11* compound mutants, there are no apparent differences in the amount of matrix produced compared to controls [Figure 2.6D, PZ vs. Figure 2.6C, PZ and Figure 2.6F, PZ vs. Figure 2.6E, PZ]. Additionally, RZ chondrocytes are depleted more rapidly in mutants compared to controls; there are noticeably fewer cells in this zone by 2 weeks of age [Figure 2.6H' vs. G' and Figure 2.6J' vs. I'].

To examine the cause of the premature shortening of the growth plate in *Hox11* compound mutants, we examined proliferation rates in the RZ and PZ of the growth plate using BrdU labeling analysis. By histological analysis, the number of RZ chondrocytes is reduced by 2 weeks of age in mutants and therefore we focused our analysis to 0, 1, and 2 weeks of age. Proliferation of growth plate chondrocytes in the mutant radius and ulna is higher in both the RZ and PZ than in controls, reaching statistical significance at 1 week in the ulna and 2 weeks in the radius [Figure 2.7A,B]. Representative images at E18.5, 1 week and 2 weeks highlight the regional differences in proliferation in the growth plates of controls and *Hox11* compound mutants [Figure 2.7C,D].

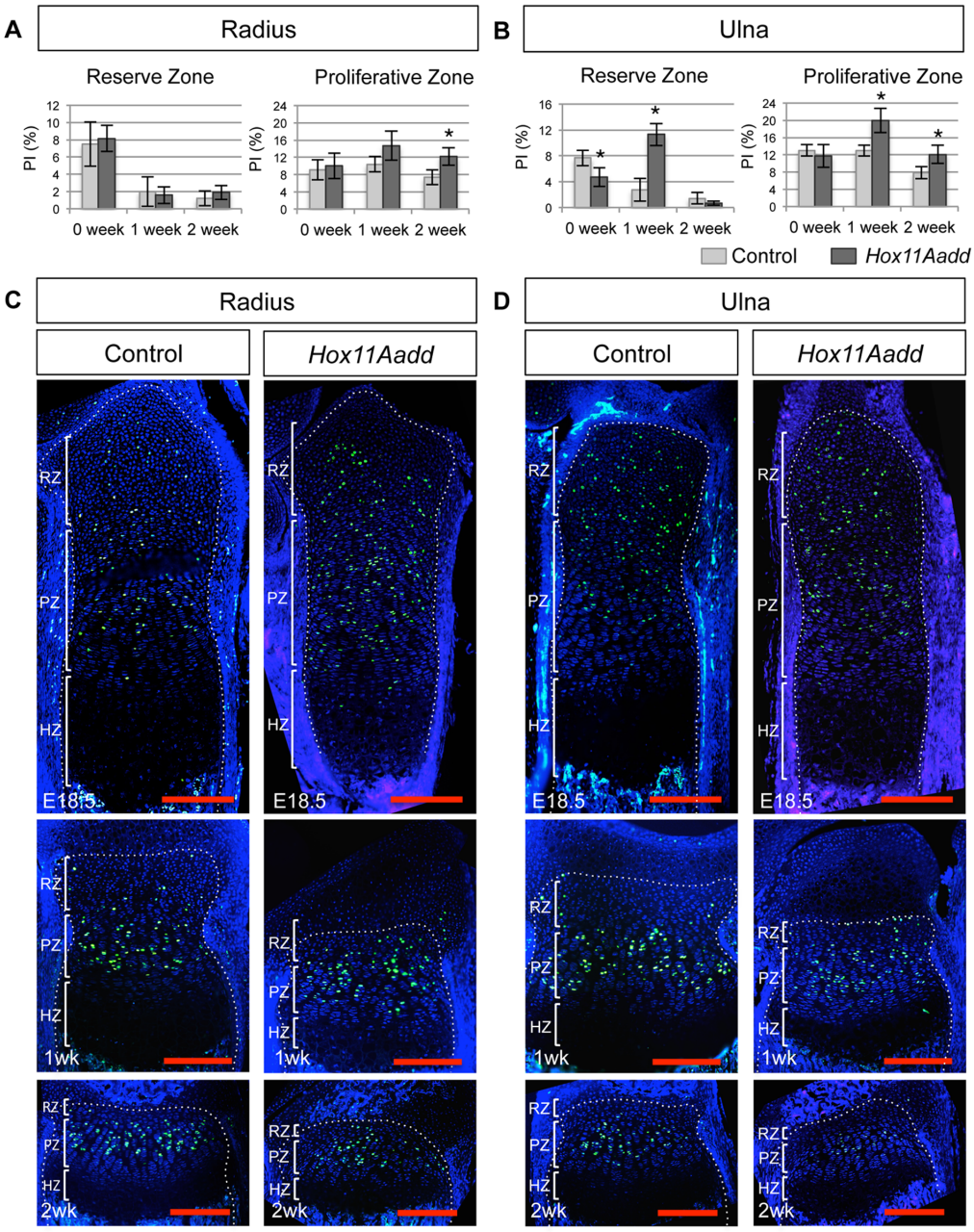

Figure 2.7: Proliferation defects are observed in the distal growth plate of *Hox11* compound mutant forelimb zeugopod bones. Proliferative index (PI) was calculated from total BrdU-positive nuclei relative to total nuclei in the reserve and proliferative zone at 0, 1 and 2 week in the radius (**A**) and ulna (**B**) of control (light grey) and compound mutant (dark grey) animals. Representative images of BrdU staining in the distal growth plate of the radius (**C**) and ulna (**D**) at E18.5, 1 week, and 2 weeks of control and *Hox11* compound mutant. White brackets demarcate zones of the growth plate (**C-D**). RZ: reserve zone, PZ: proliferative zone, HZ: hypertrophic zone. All data presented as mean ± standard deviation. N=3-4. *p ‹ 0.05, paired Student's t-tests. Scale bar = 200 μm.

Discussion

Herein, we show that *Hox11* genes continue to be expressed and function during postnatal skeletal development. While preserving a single functional allele of *Hoxa11* or *Hoxd11* is sufficient for normal embryonic bone development, the radius and ulna of *Hox11* compound mutant animals develop abnormal skeletal morphology postnatally compared to controls. The progressive anterior bowing of the mutant radius does not appear to be due to inferior bone quality or mis-directed appositional growth. In fact, both the compound mutant radius and ulna exhibit appositional growth consistent with compensatory growth. We demonstrate that the anterior radius bowing phenotype is likely to be the result of disproportionate longitudinal growth of the radius and ulna, with the ulna lagging in growth rate compare to the radius. Uncoordinated growth leads to bowing of the faster growing element, the radius. These data suggest that *Hox11* genes function to coordinate the longitudinal growth of the distal growth plate of the radius and ulna.

Why the radius grows faster than the ulna in the *Hox11* compound mutant is unclear. The genotype of the *Hox11* compound mutant alone cannot explain the loss of coordinated growth of the radius and ulna since the radial bowing phenotype occurs to a similar extent in both compound mutant genotypes; *Hox11Aadd* or *Hox11aaDd* [21]. Embryonically, a single *Hoxa11* or *Hoxd11* allele is sufficient to support normal forelimb development. Therefore, both elements of the zeugopod clearly require *Hox11* function for proper patterning during development. These observations highlight that *Hoxa11* and *Hoxd11* genes perform similar and highly overlapping functions during embryonic development and in regulating postnatal growth. *Hoxa11* and *Hoxd11* are strongly expressed in the mesenchymal tissue surrounding the distal ends of the radius and ulna embryonically and postnatally. One hypothesis to explain why the ulna is more severely affected than the radius during postnatal growth is that there is a differential requirement for *Hox11* function in the ulna compared to the radius. However, the nature of this differential function has not been investigated in this work. Future studies utilizing conditional alleles of *Hox11* for complete loss of *Hox* function in postnatal development will further clarify the function of *Hox11* in regulating longitudinal skeletal growth.

During longitudinal skeletal growth, there is tight regulation of proliferation and chondrocyte maturation within the growth plate. The majority of proliferation occurs within the columns of PZ chondrocytes, while RZ chondrocytes proliferate at a much reduced rate to contribute new cells to the PZ [144, 146, 156, 157]. Through postnatal development, there is a reduction in proliferation within the growth plate and a decrease in the height of the growth plate, a process termed growth plate senescence [158]. Senescence is a complex process; chondrocytes within the growth plate are only capable of a finite number of cell divisions and the balance of chondrocyte proliferation and timing of maturation determines bone length [158-161]. We show that there is a loss of proliferative regulation within the growth plate coupled with premature senescence in *Hox11* compound mutants. Abnormally high levels of proliferation in both RZ and PZ chondrocytes are measured in the compound mutant ulna and radius, however longitudinal growth arrests earlier in these mutants. These observations provide evidence that the regulation of chondrocyte proliferation and maturation is no longer linked in *Hox11* compound mutants. These data are consistent with a model whereby loss of *Hox11* function results in premature depletion of RZ chondrocytes and, perhaps, accelerated differentiation resulting in overall shortened zeugopod bones.

We and others have demonstrated that *Hox11* gene expression is restricted to the perichondrium and RZ chondrocytes and that *Hox11* genes are not expressed within the PZ and HZ chondrocytes themselves [80, 83]. Since *Hox* genes encode for transcription factors, this raises the possibility that *Hox* functions to maintain an undifferentiated state within the RZ chondrocyte progenitor pool and regulates when RZ chondrocytes enter the PZ and begin to differentiate. Loss of *Hox* within RZ chondrocytes may result in a loss of progenitor identity, and thus, premature differentiation and depletion of the chondrocyte progenitor pool. This hypothesis is consistent with the phenotypes observed in embryonic *Hox11* loss of function limbs. $Hoxa11^{-/-};Hoxd11^{-/-}$ mutant limbs are severely shortened, growth plates do not form, and chondrocyte maturation is perturbed [83]. Additionally, proliferation analysis in the *Hox11* mutant radius and ulna show proliferation throughout the cartilage anlage in contrast to control limbs where proliferation is restricted to the distal growing ends. Similar to the postnatal limb, *Hox11* genes are expressed at the distal end of the growing cartilage anlage embryonically; suggesting that *Hox11* contributes to

maintaining progenitor identity and regulating the rate of proliferation and differentiation of chondrocytes in both the embryonic and adult context.

Growth plate chondrocytes undergo a well-characterized differentiation program that is common to all long bones, however, the rate of growth between growth plates of different bones vary substantially [150, 162]. Neither systemic regulation nor local feedback loops can easily account for these differences since these factors are present in all growth plates. Our current data are consistent with a model whereby the differential growth rates across the skeleton are controlled, at least in part, by the HOX proteins expressed in each region. It is well documented that during development *Hox9-13* paralogs function in a highly region-specific fashion to pattern the appendages. We demonstrate that *Hox11* function remains region-specific during postnatal development and regulates long bone growth through controlling chondrocyte maturation within the growth plate.

Materials and Methods

Animals

Male and female mice heterozygous for both the *Hoxa11* and *Hoxd11* null alleles and the *Hoxa11eGFP* knock-in allele were previously described [16, 81]. All procedures followed protocols reviewed and approved by the University of Michigan's Committee on Use and Care of Animals.

qPCR Analysis

Specimens were dissected in PBS on ice. Forelimbs/forelimb buds were removed and soft tissues were dissected away from the radius and ulna. The whole embryonic day (E) 12.5 limb bud or whole radius and ulna at E18.5, 1wk, 2wk and 4wk were collected into Trizol. Adult lung tissue was collected into Trizol as a control. qPCR for *Hox11* genes was performed with the following primer sets: Hoxa11F – CCTTTTCCAAGTCGCAATGT, Hoxa11R – AGGCTCCAGCCTACTGGAAT, Hoxd11F – AGTGAGGTTGAGCATCCGAG, Hoxd11R – ACACCAAGTACCAGATCCGC. Delta Ct values were calculated for each primer set relative to GAPDH at each time point assessed and normalized to expression in the adult lung which was set to '1'. Error bars represent standard deviation. A minimum of three animals were analyzed at each age.

Histology, immunohistochemistry, *in situ* hybridization

All specimens were dissected in PBS on ice. Right limbs were wrapped in PBS-soaked gauze and stored at -20°C prior to μCT analysis. Left limbs were immediately processed for histology. For histological analyses, limbs were fixed for 3 days in 4% paraformaldehyde in PBS at 4°C and then decalcified in 14% EDTA for one week prior to embedding into OCT media. Newborn limbs did not require decalcification and were embedded in OCT immediately after fixation. Cryosections were collected at 16 μm through the radius/ulna.

Endogenous *Hoxa11eGFP* expression at E18.5 was visualized without the use of an antibody, however the decalcification process results in high auto-fluorescence in adult tissues and an antibody against GFP was required to visualize expression at 2wk.

Immunohistochemical staining was performed by blocking with donkey serum and incubation with primary antibody against GFP (Invitrogen, A-11122, 1:200) overnight at 4˚C. Secondary antibody was incubated at room temperature: donkey anti-rabbit alexafluor488 (Invitrogen, A21206, 1:1000). Section *in situ* hybridization was performed using ^{35}S-labeled riboprobes using standard techniques [163]. *Hoxd11 in situ* probes were previously described [164].

For skeletal preparations, newborn animals were skinned and fixed in 95% ethanol. Fixed skeletons were stained in Alcian Blue (76% ethanol:20% acetic acid) at 37°C for 48 hours, rinsed in 95% ethanol, treated with 1% KOH for 4-5 hours and stained with Alizarin Red in 2% KOH for 1 hour. Stained skeleton were cleared successively in 20% glycerol:1% KOH, 50% glycerol:1% KOH and 100% glycerol. Forelimbs were removed and imaged on a Leica MZ125 stereo microscope (Buffalo Grove, IL, USA).

To visualize growth plate morphology, cryosections were stained with Safranin-O/Fast Green/Hematoxylin as previously described [165]. Images were captured on an Olympus BX-51 upright light microscope with an Olympus DP70 camera (Center Valley, PA, USA). Measurements of the total growth plate length were performed using ImageJ software [166].

Micro-computed tomography (μCT) analysis

Samples were scanned using an eXplore Locus SP microCT system (GE Healthcare, Pittsburgh, PA, USA). All specimens were scanned in water using the following parameters: voltage 80 kVp; current 80 μA; exposure time 1600 ms; voxel size in the reconstructed image 18 μm, isotropic. The data were processed and analyzed using MicroView (v 2.1.2 Advanced Bone Application; GE Healthcare Preclinical Imaging). First, the image was reoriented so that the anterior-posterior and longitudinal axes were aligned with the principal image axes. Next, the bone was manually segmented starting with a frame at the center of the bone and extending 72 μm on either side to identify a 144 μm region of interest (ROI). The tissue mineral density (TMD), cortical area, cortical thickness, and inner and outer perimeters were calculated. The total length of the radius, ulna and humerus was measured along the central curvature of the bone. A minimum of five animals were analyzed at each age.

Bone histomorphometry

Five animals each of control and *Hox11* compound mutant were injected with xylenol orange (90 mg/kg) (Sigma, St. Louis, MO, USA) , calcein (15 mg/kg) (Sigma, St. Louis, MO, USA), and alizarin complexone (30 mg/kg) (Sigma, St. Louis, MO, USA) in PBS at 2 weeks, 3 weeks and 4 weeks of age respectively. Animals were sacrificed two days following the final injection and limbs were collected. Un-decalcified bones were processed and embedded into plastic as previously published [167]. 200 μm thick sections were collected, mounted to plastic slides and polished to approximately 30 μm thickness. Images were captured at 20X magnification using a Zeiss Axiovert 200 M inverted microscope equipped with Apotome imaging system (Zeiss, Thornwood, NY, USA).

BrdU incorporation

Timed pregnant females, 1 week, and 2 week pups were injected intraperitoneally with bromodeoxyuridine (100mg/kg)/fluorodeoxyuridine (12mg/kg) (Sigma, St. Louis, MO, USA) in DPBS. Pregnant females were sacrificed 2 hours after injection and 1 and 2 week pups were sacrificed 4 hours after injection. Specimens were dissected in PBS on ice. Forelimbs were collected and the soft tissues were removed. Limbs were fixed for 3 days in 4% paraformaldehyde in PBS at 4°C, decalcified in 14% EDTA for one week, and then washed into 70% ethanol prior to processing into paraffin. Microtome sections were collected at 7 μm through the radius/ulna. BrdU signal was visualized utilizing a BrdU immunostaining kit (Life Technologies, Grand Island, NY, USA). Total number of cells, as counted by Dapi positive nuclei, and BrdU-positive cells were counted using ImageJ software and proliferation rates were calculated as number of BrdU-positive cells divided by total number of cells. A minimum of three animals were analyzed at each age.

CHAPTER III

Hox expressing cells serve as skeletal stem/progenitor cells throughout life

Summary

Multipotent mesenchymal stromal cells (MSCs) are necessary to support skeletal function throughout life, however, the lineage relationships between developmental progenitors and adult progenitors is unclear. Current models suggest distinct waves of progenitors, with postnatally arising adult MSCs replacing embryonic progenitors. We previously reported exclusive expression and function of the embryonic patterning transcription factor, *Hox11*, in adult skeletal progenitor-enriched MSCs. Here, using a *Hoxa11-CreER*^{T2} lineage-tracing system, we show Hox-expressing cells give rise to all skeletal lineages throughout life and persist as adult MSCs. Further, *Hoxa11* lineage-positive cells are capable of life-long self-renewal, even from embryonic stages. Hox11-expressing cells additionally give rise to previously described progenitor-enriched MSC populations marked by *LepR-Cre* and *Osx-CreER.* Our studies establish Hox-expressing cells as a life-long, skeletal stem cell population arising from the earliest stages of skeletal development.

Introduction

Hox genes are well known for their roles in patterning the embryonic skeleton. *Hox1* through *Hox13* paralogs are expressed and function regionally along the anterior-posterior axis of the axial skeleton, with the *Hox9-Hox13* paralogs co-opted to also pattern along the proximal to distal axis of the appendicular skeleton [16, 21-23, 37]. The *Hox11* paralogs pattern the sacral region of the spine and the zeugopod region of the limb (radius/ulna and tibia/fibula). Loss of *Hox11* function during development results in dramatic mis-patterning of the zeugopod skeletal elements [16, 83]. In addition to developmental roles, compound *Hox11* mutants exhibit defects in skeletal growth during postnatal stages and in adult fracture repair [108-110].

Despite clear genetic evidence for *Hox* function in the skeleton, Hox expression is excluded from all differentiated cell types at all stages, including chondrocytes and osteoblasts [80, 109, 110]. Embryonically, Hox11 expression is observed in the developing zeugopod perichondrium/periosteum immediately adjacent to Sox9-positive chondrocytes or Osterix-positive pre-osteoblasts [80]. At postnatal and adult stages, Hox11-expressing cells remain in the outer periosteal stroma adjacent to the osteoblast layer, and are additionally observed in the bone marrow and endosteal (inner) bone surface [109, 110]. Adult Hox11-expressing stromal cells from all skeletal compartments are exclusively identified by antibodies that mark progenitor-enriched mesenchymal stem/stromal cell (MSC) populations: PDGFRα/CD51 and Leptin-Receptor (LepR) [110, 131, 132]. Hox-expressing cells also overlap with *Leptin Receptor-Cre* (*LepR-Cre*) lineage-labeled bone marrow MSCs [110, 132]. *In vitro, Hox11* mutant MSCs are unable to differentiate into chondrogenic and osteogenic lineages indicating that *Hox11* genes are functional within this population [110].

The progenitor-enriched MSC population genetically marked by *LepR-Cre* contains the majority of bone marrow CFU-F activity and gives rise to most (61%-81%) osteoblasts and some (13%) osteocytes in cortical bone by 14 months of age [132]. Despite first appearing in the skeleton at late embryonic/early postnatal stages, *LepR-Cre* lineage-marked cells only begin to make a substantial contribution to the osteoblast lineage at 6 months of age, demonstrating this constitutive Cre does not mark progenitors

that support embryonic skeleton development or postnatal growth [132, 137]. A variety of genetic lineage-tracing models have been utilized to investigate the skeletal stem/progenitor potential of distinct cell populations throughout the life of the animal. *Prx1-Cre* lineage-marked lateral plate mesodermal cells contribute to all cells of skeleton during development and overlap with PDGFRα/Sca1 and LepR cells in adult bone marrow, providing evidence that MSC populations come from cells that arise from the lateral plate mesoderm [132, 134, 138, 168]. However, this genetic model is not inducible and broadly marks all limb mesenchyme. Thus, it is unclear when long-term progenitors arise or if there is a more specific population that constitutes embryonic skeletal progenitors.

Several more recently published inducible Cre alleles revealed differences in lineage contribution of cells marked at embryonic or postnatal stages. Induction of *Osx-CreER* lineage during embryonic stages demonstrates that these cells behave as skeletal progenitors during development and postnatal growth but are depleted by adult stages [137, 140]. Postnatal induction of *Osx-CreER* leads to labeling of a small proportion of long-lived bone marrow MSCs. [137, 140]. Embryonic induction of *Gli1-CreER*^{T2} lineage marks perichondrial/periosteal cells that contribute to the skeleton and give rise to LepR-positive stromal cells up to 8-weeks of age however, this lineage was not reported at later stages [141]. Postnatal *Gli1-CreER*^{T2} lineage-marked cells only give rise to osteoblasts with no contribution to bone marrow MSCs or other skeletal lineages [141]. Postnatal induction of *Gremlin1-CreER* demonstrates lineage contribution to chondrocytes, osteoblasts, and bone marrow stromal cells out to 8 weeks [142]. In these studies, embryonically-induced *Gremlin1*-lineage contribution beyond newborn stages was not reported. Collectively, these data have led to a model that asserts the existence a primitive embryonic progenitor population that supports embryonic and postnatal skeletal development that is replaced by the establishment of a long-term adult MSC pool arising during postnatal life [117, 118].

Previous work has genetically established the importance of *Hox11* genes in embryonic skeletal development, postnatal growth, and adult fracture repair [80, 108-110]. Given the continuity in Hoxa11eGFP expression in undifferentiated stromal cells throughout life and the recent identification of adult Hox11-expressing cells as skeletal

MSCs, we sought to test the progenitor capacity of the Hox11-expressing population throughout life [80, 110]. Using a *Hoxa11-CreER*^{T2} lineage-tracing allele, we find that *Hoxa11*-lineage marked cells continuously give rise to all the skeletal mesenchymal lineages (cartilage, bone, and fat) throughout life. By adult stages, *Hoxa11*-lineage marked stromal cells co-express MSC markers PDGFRα+/CD51+ and LepR+ and, in contrast to other reported genetically-marked progenitor populations, persist to at least one year of age even when lineage labeling is initiated at embryonic stages. Further, we demonstrate that *Hoxa11*-lineage marked MSCs continue to express Hoxa11eGFP at all stages examined, consistent with *in vivo* self-renewal of this population. To understand the lineage relationships between Hox11-expressing cells and other genetically marked progenitor/MSC populations from embryonic to adult stages, we compared Hoxa11eGFP expression to cells genetically marked by *LepR-Cre* and *Osx-CreER* [132, 137, 140]. We provide evidence that Hox11-expressing cells are upstream progenitors that give rise to the cells marked by the other genetic models. These data support that the Hox-expressing stromal cell population specifically enriches for skeletal mesenchymal stem cells and demonstrate the presence of a lineage-continuous MSC population from the earliest stages of skeleton development.

Results

Hoxa11eGFP expression defines a continuous PDGFRα+/CD51+ population in the skeleton

Hox11 expression is regionally-restricted in the limb to the embryonic zeugopod (radius/ulna and tibia/fibula) within the perichondrium surrounding the chondrocyte anlage and within the outer periosteum immediately adjacent to developing Osterix-positive pre-osteoblasts at later stages [Figure 3.1A-B]. Throughout life, Hoxa11eGFP-expressing cells persist on the periosteal surface, and are also observed on endosteal bone surfaces and as stromal cells within the bone marrow space from postnatal stages [Figure 3.1C-F]. At adult stages, Hoxa11eGFP-expressing cells are exclusively identified by co-expression of PDGFRα/CD51 and of LepR, cell surface markers for progenitor-enriched MSCs [110, 131, 132]. Consistent with the possibility that Hox11 expression defines skeletal mesenchymal progenitors throughout life, Hoxa11eGFP-expressing cells are observed in several regions that have been demonstrated to contain progenitors including the distal growth plate, the perichondrium/periosteum, and the trabecular bone. [Figure 3.1A-F and [144, 169-171]].

We analyzed Hoxa11eGFP-expressing cells from embryonic, postnatal, and adult stages for co-expression of adult MSC markers PDGFRα/CD51 and LepR by flow cytometry. At embryonic stages, analyses were performed on the entire skeletal anlage, while at postnatal and adult stages, the bone marrow and bone adherent fractions were analyzed separately. PDGFRα/CD51 co-labels the majority of Hoxa11eGFP-expressing cells from embryonic stages out to one year of age [Figure 3.1G and Sup Figure 3.1]. In agreement with previous reports, LepR expression does not initiate until approximately newborn stages [Figure 3.5 and [132, 137]]. Consistent with increasing expression in stromal progenitors during postnatal life, co-expression of Hoxa11eGFP with LepR increases during this time; by adult stages the majority of Hox-expressing cells are LepR-positive [Figure 3.1G and Sup Figure 3.1B]. While it has not been established whether adult MSC cell surface markers label progenitors during embryogenesis, these data demonstrate that Hoxa11eGFP-expressing stromal cells maintain a constant cell surface signature from when each marker is first expressed.

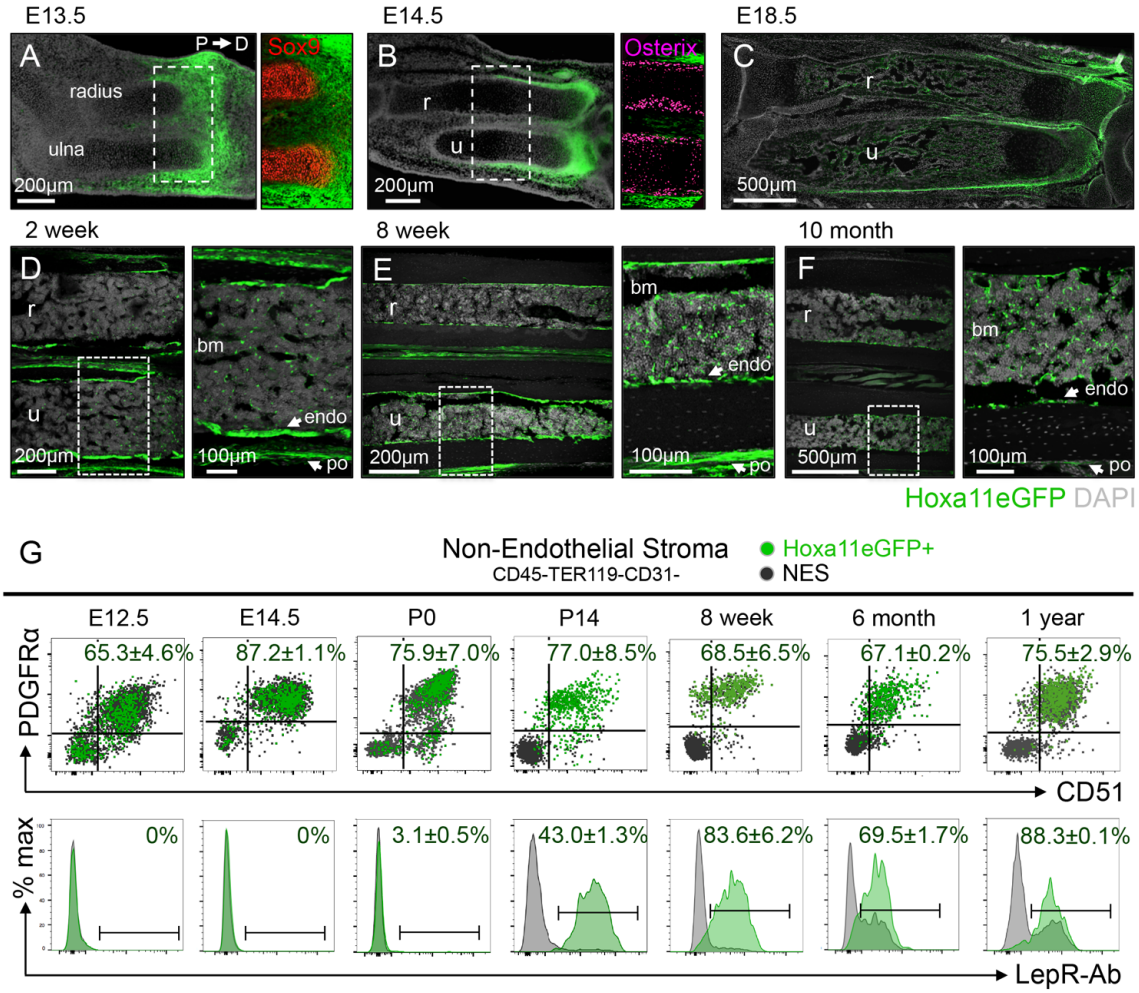

Figure 3.1: Skeletal Hoxa11eGFP expression defines a continuous PDGFRα/CD51 population throughout life. (**A-F**) Hoxa11eGFP expression in the forelimb zeugopod (radius and ulna) shown from embryonic to adult stages. Hoxa11eGFP expression (green) in radius and ulna (**A-C**), with higher magnification image showing cartilage marker, Sox9 at E13.5 (**A**, red) and osteoblast marker, Osterix at E14.5 (**B**, magenta). (**D-F**) mid-diaphysis radius (r) and ulna (u) with proximal on left and distal on right (higher magnification images of mid-diaphysis ulna shown on right). In all images, grey: DAPI. Bone marrow: bm, periosteum: po, endosteum: endo (**G**) Flow cytometry analyses of whole skeletal anlage (E12.5, E14.5, and P0) or flushed bone marrow (P14, 8 week, 6 month, and 1 year). Gating strategy and bone surface analyses shown in Sup Figure 3.1. Non-hematopoietic, non-endothelial stromal compartment (CD45-TER119-CD31-) was gated on PDGFRα/CD51 (top) or Leptin Receptor (LepR-Ab, bottom). Percentages reflect proportion of Hoxa11eGFP-positive population within double-positive gate (top) or bracketed region of histogram (bottom). Grey dots or grey histogram: total non-endothelial stroma (NES), green dots or green histogram: Hoxa11eGFP-expressing non-endothelial stroma (Hoxa11eGFP+). n=3-7 mice per group. All data presented as mean ± standard deviation.

Cas9/CRISPR generation of a *Hoxa11-CreER^{T2}* allele

To rigorously examine the lineage potential of Hox11-expressing cells *in vivo*, we generated a tamoxifen inducible *Cre* knock-in at the *Hoxa11* locus using Cas9/CRISPR mediated gene editing [Sup Figure 3.2A]. Briefly, two guide RNA sequences were designed to cut near the boundaries of exon 1 and a recombination plasmid was generated containing a tamoxifen-inducible Cre cassette (*CreER^{T2}*) with the rabbit β-globin poly-adenylation sequence [172]. This insertion cassette was flanked by 1.3kb of homology upstream and downstream of exon 1. The editing strategy resulted in replacement of exon 1 with *CreER^{T2}*, including a strong stop, while maintaining the endogenous *Hoxa11* upstream and surrounding sequences. Founder animals were screened by PCR for insertion of *CreER^{T2}* sequence [Sup Figure 3.2B]. Targeting to the *Hoxa11* locus was validated by Southern Blot analyses using 5' and 3' flanking probes as well as an internal probe for *CreER* [Sup Figure 3.2C]. *Hoxa11-CreER^{T2}* mice were crossed to *ROSA26-LSL-tdTomato* reporter mice and no tdTomato expression was observed in the absence of tamoxifen administration [Sup Figure 3.2D].

Hoxa11-lineage marked cells contribute to all skeletal mesenchymal lineages throughout life

The *in vivo* lineage potential of Hox11-expressing cells was assessed by generating mice that carried *Hoxa11CreER^{T2};ROSA26-LSL-tdTomato* to report lineage contribution to the skeleton in combination with a *Hoxa11eGFP* real-time reporter to determine if *Hoxa11*-lineage marked cells persist as Hox11-expressing MSCs [81]. Lineage-tracing was initiated by administering tamoxifen at E13.5, a time point at which embryonic Hoxa11eGFP expression has become restricted to the stromal population surrounding the developing zeugopod, but several days prior to the formation of a bone marrow cavity [Figure 3.1A and [80]]. Embryonic *Hoxa11*-lineage marked cells (*Hoxa11$^{E13.5}$*) closely matched Hoxa11eGFP expression further confirming the integrity of the *Hoxa11-CreER^{T2}* allele [Figure 3.2A]. Two days after injection, at E15.5, the embryonic skeletal anlage has begun to mature, with cartilaginous growth plates on the distal ends and ossification initiating in the center of each element. *Hoxa11$^{E13.5}$*-lineage marked cells are observed throughout the perichondrium/periosteum surrounding the

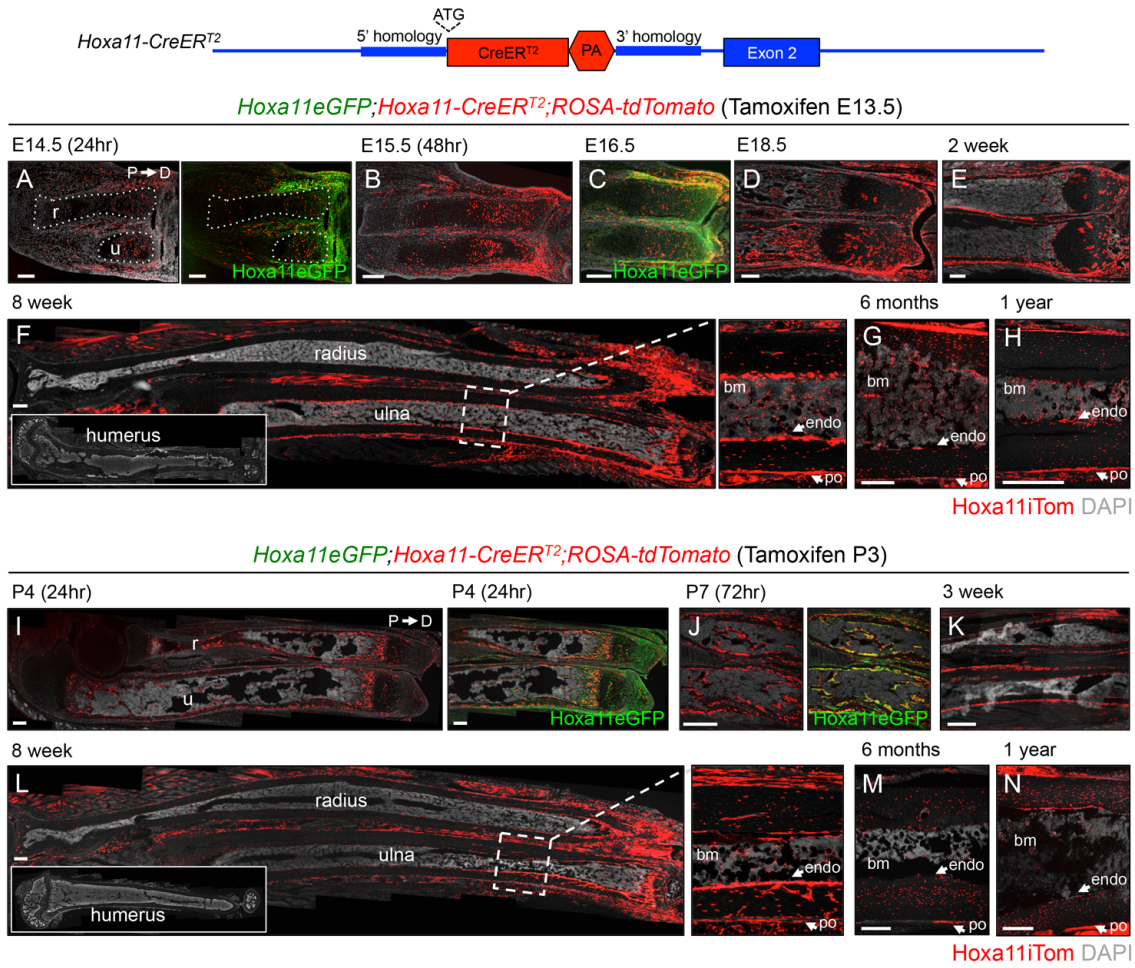

Figure 3.2: *Hoxa11*-lineage marked cells contribute to the zeugopod skeleton throughout life. Schematic of *Hoxa11-CreER^{T2}* allele. Exon 1 of *Hoxa11* was replaced with *CreER^{T2}* followed by a rabbit β-globin poly-adenylation stop sequence (see materials and methods). Endogenous sequence in blue, edited sequence in red, start site marked by 'ATG'. (**A-H**) Pregnant females were given 2mg of tamoxifen intraperitoneally at E13.5 and resulting *Hoxa11eGFP;Hoxa11-CreER^{T2};ROSA-tdTomato* animals were examined at indicated ages. *Hoxa11* lineage-marked cells (Hoxa11iTom) are red, Hoxa11eGFP-expressing cells are green. Shown are complete (**A-B, F**) or distal radius (r) and ulna (u) (**C-E**) or distal diaphysis region of tibia (**G-H**). (**A**) right panel shows image overlaid with Hoxa11eGFP. 24 hours after tamoxifen induction tdTomato expression is dim and visualized using an anti-RFP antibody. (**C**) Co-expression of Hoxa11eGFP and Hoxa11iTom. (**I-N**) P3 pups were given 0.25mg of tamoxifen intragastrically and *Hoxa11eGFP;Hoxa11-CreER^{T2};ROSA-tdTomato* mice were examined at indicated ages. Shown are complete (**I** left, **L**), distal (**I** right) or mid-diaphysis (**J-K**) radius and ulna, or distal region of tibia (**M-N**). (**I-J**) Right panel shows Hoxa11iTom with Hoxa11eGFP (**F, L**) Inset shows complete humerus. Region boxed with dashed white line shown magnified on right; view of mid-diaphysis ulna. Bone marrow: bm, periosteum: po, endosteum: endo. All images shown with distal end of bone to right. In all images, grey: DAPI. All scale bars = 200μm.

zeugopod elements and additionally within the growth plate and on the bony surfaces [Figure 3.2B]. Significant overlap of *Hoxa11*$^{E13.5}$-lineage marked cells and Hoxa11eGFP-expressing cells continues to be observed while the *Hoxa11*-lineage marked population has expanded [Figure 3.2C and Sup Figure 3.3A]. By E18.5, *Hoxa11*$^{E13.5}$-lineage marked cells are observed throughout the zeugopod growth plate, within the primary spongiosa, and in the outer periosteal region [Figure 3.2D]. *Hoxa11*$^{E13.5}$-lineage marked cells contribute to both chondrocytes and osteoblasts at E18.5, demonstrating that the Hox11-expressing population marks multipotent skeletal progenitors that function during embryogenesis [Sup. Figure 3.3B].

Following the *Hoxa11*$^{E13.5}$-lineage marked population after birth revealed lineage labeling throughout the periosteum, the endosteum, and within the now-established bone marrow space [Figure 3.2E]. This pattern of distribution continues to adult stages and extensive lineage-labeling is observed [Figure 3.2F]. Consistent with the regional expression of Hoxa11eGFP, *Hoxa11*$^{E13.5}$-lineage marked cells only contribute to the zeugopod skeleton and no lineage-labeling is seen in the stylopod (humerus) and other regions that do not express *Hox11,* demonstrating that this progenitor is a regionally persistent stromal population [Figure 3.2F, inset and data not shown]. Remarkably, *Hoxa11*$^{E13.5}$-lineage marked cells continue to show remarkably strong contribution to the skeleton as late as one year of age [Figure 3.2G-H].

Lineage-labeling was next performed beginning at postnatal stages, a time when other genetic models demonstrate contribution to long-lived stromal cells, to test whether Hox11-expressing stromal cells function similarly at this stage. Tamoxifen was administered at postnatal day 3 (P3) and contribution of *Hoxa11* lineage-marked cells (*Hoxa11*^{P3}) was examined. During the first days following tamoxifen administration, *Hoxa11*^{P3}-lineage marked cells are observed within the reserve zone chondrocytes at the distal growth plate and on the periosteal, the endosteal, and the trabecular bone surfaces consistent with the pattern of Hoxa11eGFP expression [Figure 3.2I-J]. Following an eight-week chase, *Hoxa11*^{P3}-lineage marked cells contribute extensively to the skeleton and are observed on periosteal and endosteal bone surfaces as well as throughout the bone marrow space. [Figure 3.2L]. Similar to E13.5 lineage-induction, *Hoxa11*^{P3}-lineage marked cells give rise to the skeletal lineages within the zeugopod and lineage

contribution is not observed in the stylopod [Figure 3.2L, inset]. *Hoxa11*^{P3}-lineage marked cells persist and continue to contribute to the skeleton through one year of age [Figure 3.2M-N]. Of note, lineage induction at postnatal stages looks indistinguishable from embryonic labeling, consistent with the Hox11-expressing population representing skeletal progenitors with equivalent capacity at both stages.

Hox11-expressing cells become cartilage, bone, and adipose cells and are maintained as a continuous, self-renewing skeletal progenitor throughout life

To examine the contribution of *Hoxa11-CreER*^{T2} lineage cells to differentiated mesenchymal skeletal cell types, we performed co-labeling with markers for cartilage, bone, and adipose tissues. *Hoxa11*$^{E13.5}$-lineage marked cells differentiate into chondrocytes within the growth plate, osteoblasts on the trabecular and endosteal bone surfaces, osteocytes embedded within the cortical bone, and to bone marrow adipocytes [Figure 3.3A]. Analysis out to one year of age shows that *Hoxa11*$^{E13.5}$-linege marked cells continue to give rise to all skeletal lineages; osteoblasts, osteocytes, and bone marrow adipocytes [Figure 3.3B]. In adult mice, osteoblasts are reported to live for one month, therefore multiple rounds of osteoblast turnover will have occurred between E13.5 and 1 year of age [173, 174]. Additionally, bone marrow adiposity increases with age [175]. Thus, the presence of *Hoxa11*$^{E13.5}$-linege marked osteoblasts and adipocytes at one year of age is consistent with continued contribution to newly differentiated cells, not simply the persistence of differentiated cells over time.

We next performed flow cytometry analyses on *Hoxa11*$^{E13.5}$-linege marked stromal cells from the zeugopod bone marrow and bone surfaces to assess the identity of these cells. The majority of *Hoxa11*$^{E13.5}$-linege marked stromal cells from both compartments were confined to the non-hematopoietic, non-endothelial stromal compartment (CD45-TER119-CD31-) [Figure 3.3C and Sup Figure 3.3C]. Adult, *Hoxa11*$^{E13.5}$-linege marked bone marrow stromal cells specifically express MSC markers PDGFRα/CD51 and LepR, demonstrating that the embryonically labeled *Hoxa11*-expressing cells give rise to an adult, progenitor-enriched MSCs that are maintained throughout life [Figure 3.3C]. Similar flow cytometry profiles are observed for *Hoxa11*$^{E13.5}$-lineage marked cells that persist on the cortical bone surfaces, with the

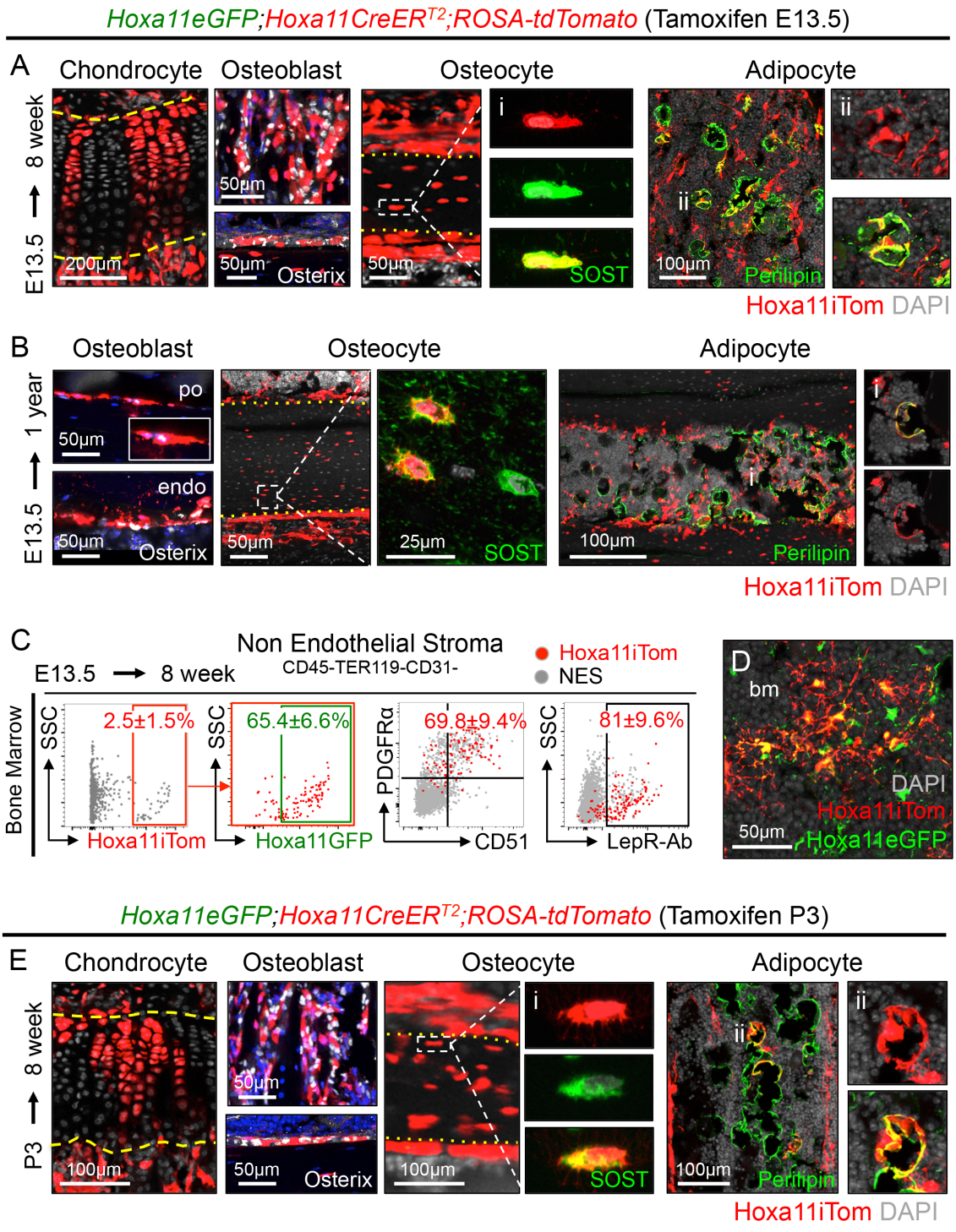

Figure 3.3: *Hoxa11-CreER^{T2}* lineage-marked cells become cartilage, bone, and adipose cells and are maintained as a continuous, self-renewing skeletal progenitor throughout life. (**A-D**) Pregnant dams received 2mg tamoxifen intraperitoneally at E13.5 and resulting *Hoxa11eGFP;Hoxa11-CreER^{T2};ROSA-tdTomato* mice were chased to (**A, C-D**) 8 weeks or (**B**) 1 year. (**E**) P3 pups were given 0.25mg tamoxifen intragastrically and *Hoxa11eGFP;Hoxa11-CreER^{T2};ROSA-tdTomato* mice were chased to 8 weeks. (**A,**

E) *Hoxa11* lineage-labeled cells (Hoxa11iTom, red) and co-expression with markers for each differentiated cell type. Shown are chondrocytes with characteristic columnar morphology at distal end of growth plate, osteoblasts stained with Osterix (white) on trabecular (top) and endosteal bone (bottom), osteocytes within the cortical bone stained with SOST (green), and bone marrow adipocytes stained with Perilipin (green). Upper and lower boundaries of growth plate and periosteal and endosteal boundaries of cortical bone marked by dashed and dotted yellow lines, respectively, white boxed region of single osteocyte magnified to right (i), and single adipocyte (ii) magnified to right. (**B**) Hoxa11iTom, red and immunolabeling for osteoblasts (Osterix, white) on periosteal (po, top) and endosteal (eo, bottom) bone surfaces, osteocytes (SOST, green) in cortical bone, and adipocytes (Perilipin, green) in bone marrow. Periosteal and endosteal boundaries of cortical bone marked by dotted yellow line, white boxed region of osteocytes magnified to right, and single adipocyte (i) magnified to right. (**C**) Flow cytometry analyses of non-hematopoietic, non-endothelial stromal compartment (CD45-TER119-CD31-) in bone marrow. First panel: *Hoxa11* lineage-marked cells (x-axis: Hoxa11iTom), second panel: analysis of Hoxa11iTom positive gate (red) for Hoxa11eGFP expression, third panel: co-expression analysis of PDGFRα/CD51, fourth panel: co-expression analysis of Leptin Receptor (LepR-Ab). Percentages reflect proportion of Hoxa11iTom population in identified gate. Grey dots: total non-endothelial stroma (NES), red dots: Hoxa11iTom. n=3-5 mice per group. All data presented as mean ± standard deviation. (**D**) Co-expression of Hoxa11iTom (red) and Hoxa11eGFP (green) in bone marrow. In all images, grey or blue: DAPI.

majority of labeled bone surface cells co-expressing PDGFRα/CD51 and LepR as we have previously reported for real-time Hoxa11eGFP [Sup Figure 3.3E and [110]]. A majority of *Hoxa11*$^{E13.5}$-lineage marked cells additionally co-express Hoxa11eGFP up to one year of age [Figure 3.3C-D and Sup Figure 3.3D-F]. Collectively these data provide evidence that the embryonic Hoxa11-expressing cell population gives rise to adult Hoxa11eGFP-expressing MSCs and persists throughout life.

The same analyses were performed on *Hoxa11*^{P3}-lineage marked stromal cells where essentially identical results are observed. *Hoxa11*^{P3}-lineage marked cells differentiate into all mesenchymal skeletal cell types, including chondrocytes, osteoblasts, osteocytes, and bone marrow adipocytes [Figure 3.3E]. *Hoxa11*^{P3}-lineage marked cells also continue this contribution through one year of age [Sup Figure 4A]. Flow cytometry analyses on *Hoxa11*^{P3}-lineage marked bone marrow and bone surface stromal cells following an eight-week chase demonstrate that *Hoxa11*^{P3}-lineage marked cells are contained within the non-hematopoietic, non-endothelial stromal compartment and co-express progenitor-enriched MSC markers PDGFRα/CD51 and LepR in both the bone marrow and bone surface compartments [Sup Figure 3.4B-D]. *Hoxa11*^{P3}-lineage marked cells also express Hoxa11eGFP in both compartments, again consistent with the Hox11-expressing stromal population containing skeletal MSCs [Sup Figure 3.4C-D].

Hoxa11-lineage marked cells contribute to regenerating cartilage and bone following fracture injury

To examine whether *Hoxa11*-lineage marked cells serve as progenitors in regeneration of the skeleton following injury, *Hoxa11CreER*^{T2}*;ROSA26-LSL-tdTomato* animals were administered tamoxifen at E13.5 or at P3 to initiate lineage-labeling and the ulna was fractured at adult stages (8-10 weeks of age). Contribution to regenerating cartilage and bone was analyzed 10 days post-injury (10DPI). *Hox11*$^{E13.5}$- and *Hoxa11*^{P3}-lineage marked cells expand in response to fracture and are observed throughout the callus [Figure 3.4A,D]. Apparent expansion of both the lineage-marked periosteal stromal compartment and lineage-marked the bone marrow stromal compartment is observed. *Hoxa11*-lineage marked cells give rise to both Sox9-positive chondrocytes within the cartilaginous regions of the callus and to Osx-expressing osteoblasts within the

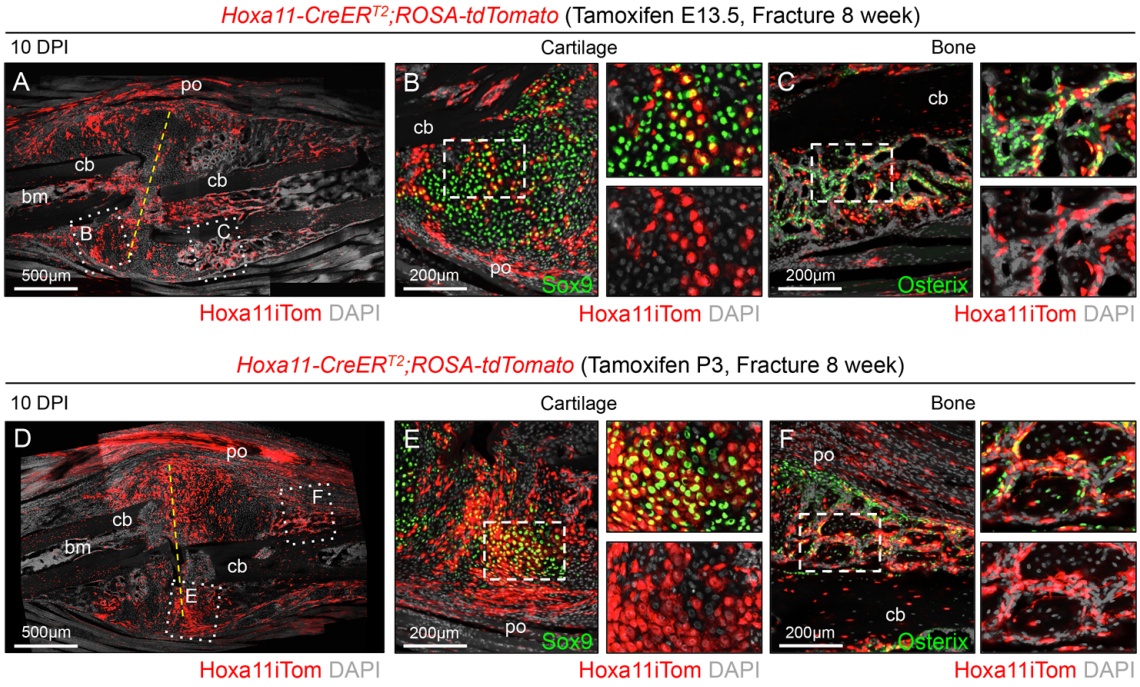

Figure 3.4: The *Hoxa11*-lineage marked cells contribute to regenerating cartilage and bone following fracture injury. An ulnar fracture was performed at 8 weeks of age on *Hoxa11-CreERt2;ROSA-tdTomato* mice following tamoxifen dosing at (**A-C**) E13.5 – 2mg intraperitoneally to pregnant female, or (**D-F**) P3 – 0.25mg intragastrically to pup. (**A, D**) *Hoxa11* lineage-positive cells (Hoxa11iTom, red) are observed throughout the fracture callus 10 days post-injury (DPI). Expansion from bone marrow (bm) and periosteal (po) compartments is observed. Fracture line marked with dashed yellow line and cortical bone (cb) is labeled. Dashed white lines indicates regions visualized with antibodies for cartilage (Sox9, **B, E**) and bone (Osx, **C, F**). In all images, grey: DAPI.

woven bone regions of the callus [Figure 3.4B-C,E-F]. Contribution of *Hoxa11*-lineage marked cells to the regenerating skeletal tissues is qualitatively equivalent whether lineage-tracing was initiated at embryonic or postnatal stages, demonstrating that Hoxa11-positive cells from both stages label functional adult skeletal MSCs.

Comparison of Hoxa11eGFP expressing cells to other MSC lineage populations

A critical knowledge gap in the field is understanding of the relationships between various identified stromal populations. Significant differences exist in the lineage-dynamics of these populations at different stages throughout life, yet it is not clearly understood why. We sought to establish the relationship between Hox11-expressing cells and previously reported MSC populations genetically labeled by *LepR-Cre* and *Osx-CreER* using our *Hoxa11eGFP* real-time reporter crossed to *LepR-Cre;ROSA26-LSL-tdTomato* mice or *Osx-CreER;ROSA26-LSL-tdTomato* mice.

LepR-Cre lineage-marked cells first appear during late embryonic stages as rare cells within the primary spongiosa [Figure 3.5A and [132, 137]]. At this stage, Hoxa11eGFP-expressing cells are found throughout the periosteum and along the bone surfaces of the primary spongiosa. There is virtually no overlap between *LepR-Cre* lineage-marked cells and Hoxa11eGFP at early stages [Figure 3.5A, arrowheads]. The number of *LepR-Cre* lineage-marked cells increases with age. In the bone marrow, the overlap between Hoxa11eGFP and *LepR* lineage-marked cells progressively increases with age until, by 15 weeks, the majority Hoxa11eGFP-expressing bone marrow stromal cells are also *LepR* lineage-positive [Figure 3.5B-E and Sup Figure 3.5, [110]]. Interestingly, there is a population of Hoxa11eGFP-expressing cells on the outer periosteal surface that remains *LepR-Cre* lineage-negative at all stages examined [Figure 3.5D'-E']. Thus, the Hoxa11eGFP population progressively overlaps with *LepR*-lineage marked cells, consistent with LepR-lineage labeling continuing to initiate in Hox-positive cells [Figure 3.5F]. Differences in the overlap between the bone marrow and bone adherent populations reveal a unique Hox11-expressing population in the periosteum.

Previous reports demonstrate *Osx*-lineage contribution to MSCs at postnatal but not embryonic stages. We induced *Osx*-lineage labeling in *Hoxa11eGFP;Osx-CreER;ROSA26-LSL-tdTomato* animals at E13.5 or at P3 to compare these populations.

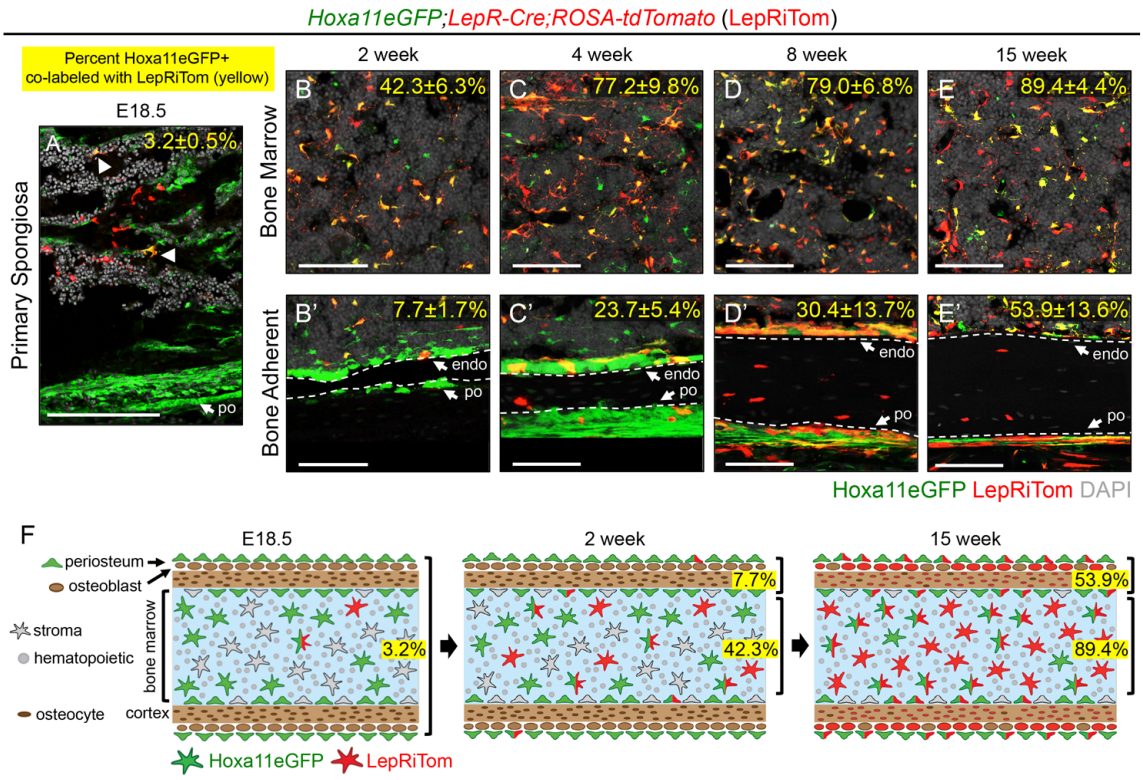

Figure 3.5: *LepR*-Cre lineage-marked cells progressively co-express in existing Hoxa11eGFP-expressing population in bone marrow; much less overlap in periosteum. Analysis of the co-expression of Hoxa11eGFP (green) and LepR-Cre lineage-marked cells (LepRiTom, red) in *Hoxa11eGFP;LepR-Cre;ROSA-tdTomato* mice. Percentages (yellow) reflect proportion of Hoxa11eGFP-positive cells that also express LepRiTom. Flow cytometry analyses shown in Sup Figure 3.5. (**A**) LepRiTom is first observed at late embryonic stages. (**B-E'**) High magnification view of mid-diaphysis of ulna, (**B-E**), cortical bone (**B'-E'**). In all images; grey: DAPI. Data presented as mean ± standard deviation. n=3-5 mice per group. (**F**) Diagram of data at E18.5, 2 week, and 15 week.

One day following tamoxifen administration at E13.5, embryonic *Osx*-lineage marked cells ($Osx^{E13.5}$) are restricted to the inner periosteal, pre-osteoblast layer, while Hox11-expressing cells are restricted to the outer periosteal layer with little to no overlap observed [Figure 3.6A]. *Osx-CreER* lineage induced at E13.5 also labels hypertrophic chondrocytes in the developing bone. The pattern of $Osx^{E13.5}$-lineage marked cells is consistent with Osterix protein expression using an anti-Osterix antibody [Figure 3.1B]. By E18.5, $Osx^{E13.5}$-lineage marked cells are observed throughout the primary spongiosa and minimal co-expression with Hoxa11eGFP is observed [Figure 3.6B (i), arrows]. Hoxa11eGFP-expressing cells and $Osx^{E13.5}$-lineage marked cells continue to exhibit a mutually exclusive stratified expression pattern in the periosteum, with $Osx^{E13.5}$-lineage marked cells in the inner pre-osteoblast layer and Hoxa11eGFP-expressing cells in an adjacent outer periosteal layer. [Figure 3.6B (ii)]. Minimal overlap of these populations is observed through adult stages [Figure 3.6C]. $Osx^{E13.5}$-lineage marked cells are rare and represent only 2.7±0.3% of the total Hoxa11eGFP-expressing population [Figure 3.6E]. Flow cytometry analyses of the few bone marrow $Osx^{E13.5}$-lineage marked cells shows 74.0±3.4% of cells co-express PDGFRα/CD51 and 69.3±8.3% co-express Hoxa11eGFP [Figure 3.6C-E]. Virtually no $Osx^{E13.5}$-lineage marked cells remain on the bone surfaces by adult stages, having presumably all differentiated into osteoblasts and osteocytes [Figure 3.6C (i)]. These data reveal Hoxa11eGFP-expressing perichondrial/periosteal population that is distinct from $Osx^{E13.5}$-lineage marked cells. Further, these populations do not become overlapping with age, consistent with embryonic *Osx*-lineage labeled cells not being MSCs [Figure 3.6D].

The *Hoxa11*-lineage contribution to bone and the stratified periosteal expression pattern of Hoxa11eGFP and $Osx^{E13.5}$-lineage marked cells led us to investigate whether Hox11-expressing stromal cells give rise to the population marked by *Osx-CreER*. Tamoxifen was administered to *Hoxa11-CreER*^{T2}*;ROSA-tdTomato* reporters at E11.5 ($Hoxa11^{E11.5}$), two days prior to induction of Osterix expression in the developing skeleton, and the contribution of the $Hox11^{E11.5}$-lineage marked cells was assessed at E18.5. $Hoxa11^{E11.5}$-lineage-marked cells contribute extensively to the skeleton at E18.5, giving rise to many Osterix-positive osteoblasts within the cortical bone and primary spongiosa [Figure 3.6A and Sup Figure 3.6]. Comparable contribution to the osteoblast

lineage at birth is observed from *Hoxa11*$^{E13.5}$ [compare Sup Figure 3.6B sup to Sup Figure 3.3B]. These data show that the *Hox11*-lineage arises before the *Osx-CreER* lineage, and that Hox11-expressing cells serve as progenitors that give rise to the osteoblast lineage.

Consistent with the reported broader mesenchymal progenitor capacity of the postnatal *Osx*-lineage marked population (*Osx*^{P3}), some overlap is observed between Hoxa11eGFP-expressing cells and *Osx*^{P3}-lineage marked cells at this stage. Three days following tamoxifen administration, *Osx*^{P3}-lineage marked cells are localized to the bone surfaces (periosteal, endosteal, and trabecular) [Figure 3.6F]. Hoxa11eGFP-expressing cells are also observed in the periosteum, but overlap with *Osx*^{P3}-lineage marked cells is restricted to the innermost layer [Figure 3.6F (i)]. Hoxa11eGFP-expressing cells are already present at this stage throughout the bone marrow space and no co-expression with rare *Osx*^{P3}-lineage marked bone marrow cells is observed [Figure 3.6F (ii), arrow]. Following an 8-week chase, *Osx*^{P3}-lineage marked cells contribute to bone, fat, and bone marrow stromal cells, consistent with previous reports [Figure 3.6G and [137]]. Most *Osx*^{P3}-lineage marked cells in the bone marrow co-express Hoxa11eGFP and progenitor-enriched MSC markers PDGFRα/CD51 [Figure 3.6G-I]. On the bone surfaces, only about half of *Osx*^{P3}-lineage marked cells co-express PDGFRα/CD51 and Hoxa11eGFP [Figure 3.6I]. The remaining population likely reflects lineage-marked cells actively undergoing osteoblast differentiation. Interestingly, the majority of overlap of Hoxa11eGFP-expressing cells and *Osx*^{P3}-lineage marked cells is observed on the endosteal surface, while a stratified, non-overlapping expression pattern continues to be observed on the periosteal surface [Figure 3.6G (i)]. Of note, *Osx*^{P3}-lineage marked cells represent only a small fraction of the total Hoxa11eGFP-expressing population, ~11% [Figure 3.6I]. These data show that *Osx-CreER* marks a sub-population of Hox11-expressing MSCs at postnatal stages that persist to adult stages [Figure 3.6H]. These data additionally highlight a unique Hox11-expressing population in the outer periosteum, adjacent to the Osx-positive inner pre-osteoblast periosteal layer that does not overlap with *Osx*-lineage marked cells at any stage.

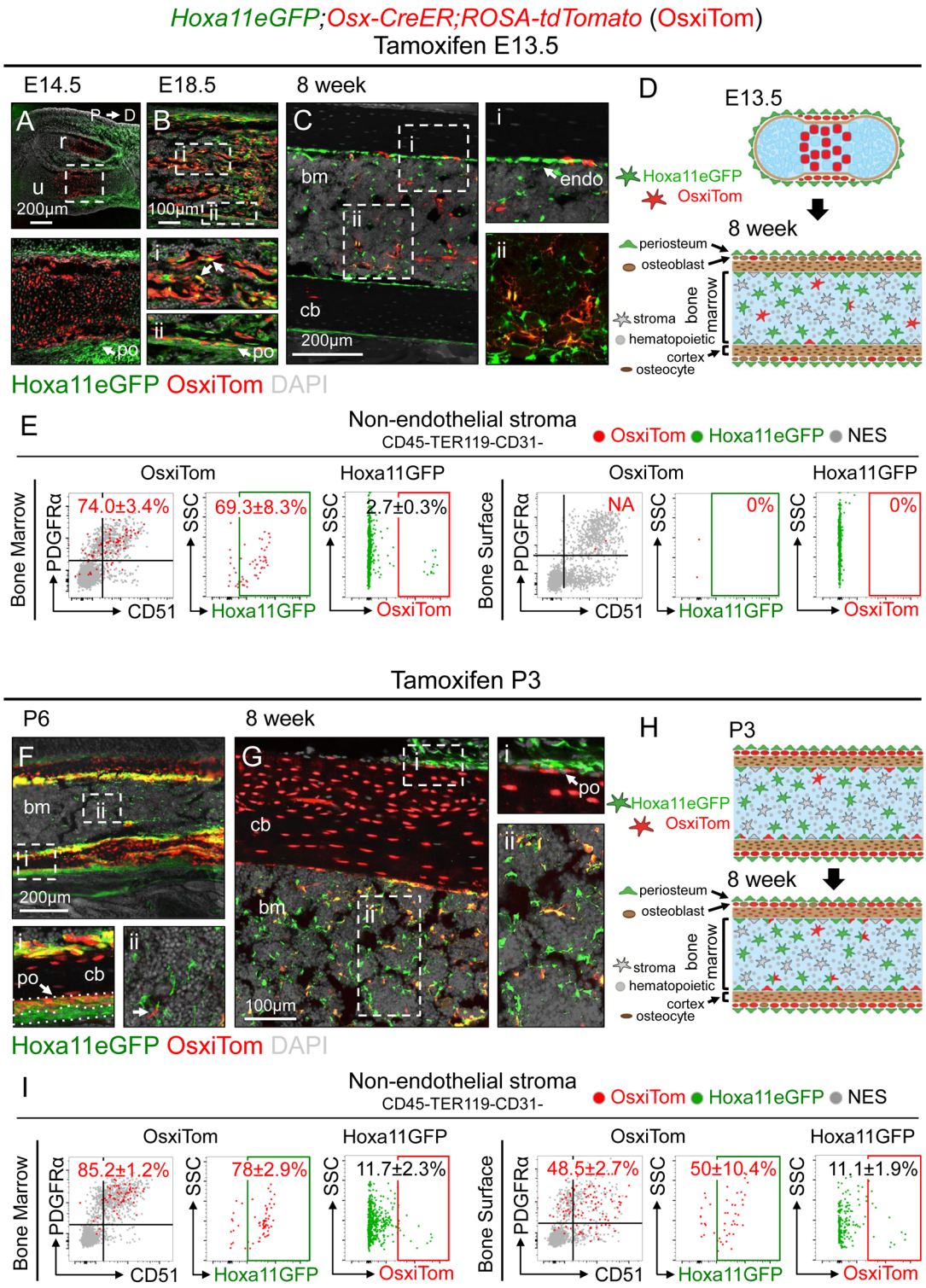

Figure 3.6: Hoxa11eGFP-expressing MSCs are distinct from embryonic *Osx*-CreER lineage-marked cells; postnatal *Osx*-CreER lineage-marked cells only marginally overlap in bone marrow and do not overlap in outer periosteum. Comparison of Hoxa11eGFP (green) and *Osx-CreER* lineage-marked cells (OsxiTom, red) was

performed in *Hoxa11eGFP;Osx-CreER;ROSA-tdTomato* mice. (**A-E**) Pregnant females received 2mg tamoxifen intraperitoneally at E13.5 and co-expression of Hoxa11eGFP and embryonic *Osx*-lineage was examined at (**A**) E14.5, (**B**) E18.5 and (**C, E**) 8 weeks. (**A**) Complete radius (r) and ulna (u) 24 hours after tamoxifen with proximal to the left and distal to the right. High magnification of region marked by dashed white line (below). Periosteum: po (**B**) Mid-diaphysis ulna; below, high magnification image of primary spongiosa (i) and periosteum (ii). (**C**) Mid-diaphysis ulna; on right, high magnification images of (i) endosteum (endo) and (ii) bone marrow (bm). Cortical bone: cb. (**D**) Diagrammatic representations of data. (**E**) Flow cytometry analysis of non-hematopoietic, non-endothelial stroma (CD45-TER119-CD31-, NES) in bone marrow (left panels) and bone adherent (right panels) compartments. First panel: analysis of OsxiTom population for PDGFRα/CD51, second panel: analysis of OsxiTom for Hoxa11eGFP, third panel: analysis of Hoxa11eGFP-positive cells (green) for OsxiTom expression. OsxiTom cells are very rare (0.018±0.03 of total NES) on bone surface (left panels) and do not express Hoxa11eGFP. (**F-I**) P3 pups were given 0.25 mg tamoxifen intragastrically and co-expression of Hoxa11eGFP and postnatal *Osx*-lineage was examined at (**F**) P6 and (**G-H**) 8 weeks. (**F**) Mid-diaphysis ulna, high magnification images (below) of cortical bone (i) and bone marrow (ii), rare OsxiTom stromal cell (arrow). (**G**) Mid-diaphysis tibia, high magnification images (right) of periosteum (i) and bone marrow (ii). (**H**) Diagrammatic representations of data. (**I**) Flow cytometry analysis of non-hematopoietic, non-endothelial stroma (CD45-TER119-CD31-) in bone marrow (left panels) and bone surface (right panels) compartments. First panel: analysis of OsxiTom population for PDGFRα/CD51, second panel: analysis of OsxiTom for Hoxa11eGFP, third panel: analysis of Hoxa11eGFP-positive cells (green) for OsxiTom expression. All fluorescent images, grey: DAPI. Flow cytometry dot plots, grey dots: total non-endothelial stroma (NES). n=3-5 mice per group. Data presented as mean ± standard deviation.

Discussion

Previous lineage-tracing analyses have supported a model whereby transient, embryonic skeletal progenitor populations are later replaced with bona fide adult skeletal stem cells arising during early postnatal life [117, 118]. A substantial caveat to many of the genetic tools used in previous analyses is that tamoxifen-inducible *Cre* expression is driven by promoters for genes that function in early lineage commitment to skeletal cell types (chondrocyte – *Sox9-CreER*, or osteoblast – *Osx-CreER*), for instance [137, 140] [reviewed by [143]]. Therefore, the bulk of *Sox9-CreER* lineage-marked cells will be committed to the chondrocyte fate and the bulk of *Osx-CreER* lineage-marked cells to the osteoblast fate, while only a small population of putative progenitors that perhaps did not fully commit to differentiation are likely to be marked by these alleles. Labeling of long-term skeletal progenitors with these alleles is non-specific and incomplete, and temporal differences in MSC capacity observed likely reflects exhaustion of early committed progenitors over time. A subset of genetic models, driven by promoters of genes involved in key signaling pathways such as Hedgehog (*Gli1-CreER*) or BMP (*Gremlin1-CreER*), also demonstrate temporal differences in progenitor capacity over time [141, 142]. Hedgehog and BMP signaling are both critically important pathways in chondrogenic and osteogenic differentiation [176-178]. Differences in the progenitor capacity of these lineage-marked populations may reflect changes in the signaling environment of the skeleton with age. These caveats collectively suggest that the proposed waves of skeletal progenitors may be an artifact of the genetic models and not a physiologically relevant property of skeletal MSCs.

Prior reports establish Hox expression is excluded from differentiated skeletal cell types at all stages and genetically demonstrate *Hox* gene function in the skeleton throughout life [80, 108-110]. Further, real-time expression of Hoxa11eGFP marks only progenitor-enriched MSCs and no other differentiating cell types. Herein, we present evidence that the Hox11-expressing stromal population, marked by *Hoxa11-CreER*^{T2} from both embryonic and postnatal stages, specifically enriches for a population of skeletal stem cells throughout the life of the animal and are likely to represent the true MSC compartment. In contrast to models suggesting developmental progenitors are later

replaced by postnatally arising, long-lived adult MSCs, these data reveal a lineage-continuous skeletal MSC population throughout life from embryonic stages. *Hoxa11* lineage-marked cells contribute extensively to the skeleton, giving rise to all skeletal cell types including chondrocytes, osteoblasts, osteocytes, and bone marrow adipocytes at all stages examined. Further, *Hoxa11* lineage-marked cells expand and contribute to regenerating cartilage and bone following fracture injury. In addition to contributing to differentiated skeletal cells, *Hoxa11* lineage-marked cells persist within the bone marrow space and on the cortical bone surfaces throughout life and maintain co-express MSC markers PDGFRα/CD51 and LepR. The majority of lineage-marked stromal cells additionally express Hoxa11eGFP, establishing a continuous lineage relationship between the embryonic and the adult Hox11-expressing skeletal progenitor population. The collective data establishing the contribution of *Hoxa11* lineage-marked cells to the skeleton and the persistence of *Hoxa11* lineage-marked stromal cells at all stages provides *in vivo* evidence that the Hox11-expressing stromal population enriches for life-long skeletal MSCs.

Assessing the relationship between different genetically defined populations of skeletal progenitors is critical for understanding how these populations behave and can provide information on the spatiotemporal dynamics of skeletal stem cells throughout life. *Hoxa11-CreER*^{T2} lineage-tracing data demonstrates that Hox11-positive progenitors arise days prior to the appearance of *Osx-CreER* lineage-marked cells (around E13.5) or *LepR-Cre* (around E17.5). In all of these comparative analyses, there is consistently a unique Hox-expressing population in the periosteum that does not overlap with the *Osx*- or *LepR*-lineage marked cells after short- or long-term lineage-tracing. The periosteal compartment has been shown to contain skeletal stem cells with greater capacity to regenerate bone compared to bone marrow MSCs, suggesting this unique Hox-positive population may represent the true skeleton stem cell [179]. Embryonic *Osx*-lineage marked cells only function as progenitors transiently, and little to no overlap is observed with Hoxa11eGFP-expressing cells, consistent with these populations being entirely distinct. In contrast, postnatal *Osx*-lineage marked cells give rise to a small population of long-lived stromal cells. Shortly following postnatal induction of the *Osx*-lineage marked cells, overlap of Hoxa11eGFP-expressing cells and *Osx*-lineage marked cells is observed

on the bone surfaces while a unique Hoxa11eGFP-expressing cell population remains on the outer periosteum and within the bone marrow. By adult stages, only a fraction of Hoxa11eGFP-expressing bone marrow MSCs are *Osx* lineage-marked, however most *Osx* lineage-marked cells overlap with Hoxa11eGFP-expression. These data are consistent with Hox-expressing progenitors in the outer periosteum giving rise to the population marked by *Osx-CreER*, and thereby the complete osteo-lineage, and suggests a temporal window during development and early postnatal life where the bone marrow stroma is likely established from cells within the periosteum.

We also show that Hox11-expressing MSCs are progressively *LepR*-lineage-marked with time and, by adult stages, the majority of Hoxa11eGFP-expressing, progenitor-enriched MSCs overlap with the *LepR*-lineage marked cells. Given *LepR-Cre* is not a temporally controlled Cre, these data suggest that LepR expression, and thus the *LepR*-Cre, is increasingly initiated within the Hoxa11eGFP-expressing population beginning around birth. Interestingly, *LepR*-Cre progressively marks Hoxa11eGFP-expressing bone marrow progenitors more rapidly and more completely than Hoxa11eGFP-expressing cells within the bone adherent compartment. *LepR-Cre* lineage labeling in the bone adherent (endosteal and periosteal) compartment correlates with the onset of *LepR*-lineage marked cell contribution to bone [132, 137]. These data lead to speculation that *LepR-Cre* is expressed only gradually, and perhaps never completely, within the true skeletal mesenchymal stem cell population. Together, our comparative studies provide strong evidence that Hox-positive MSCs give rise to *Osx-CreER* and *LepR-Cre* lineage-marked populations and establish a unique Hox-expressing periosteal origin for skeletal stem cells.

Rux, *et al*. reported that adult bone marrow MSCs from different anatomical regions display a Hox expression profile consistent with regionally-restricted expression domains established during embryonic development [110]. *Hoxa11-CreER*^{T2} allows for the unique labeling of a zeugopod-restricted MSC population and shows that skeletal contributions of MSCs remain regional throughout life. Together, these data provide strong support for a model whereby regional, Hox-expressing stem cell populations in the skeleton are established during embryonic development and give rise to regionally-restricted mesenchymal stem cells that function throughout life. It is increasingly

important to understand whether differences in the Hox expression profile in MSCs from different skeletal regions results in functionally distinct stem cell populations. This could have critical implications for the optimal therapeutic and tissue engineering use of bone marrow MSCs.

Supplemental Information

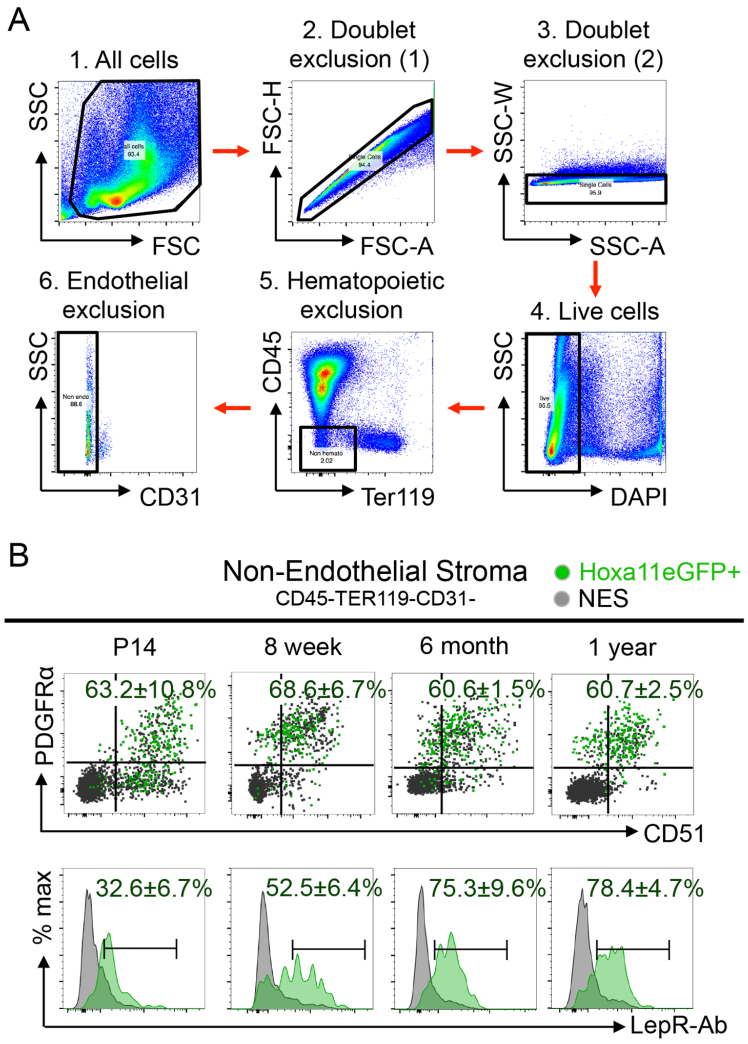

Supplemental Figure 3.1: Bone adherent Hoxa11eGFP-expressing cells express MSC markers PDGFRα/CD51 and Leptin Receptor. (**A**) Gating strategy to obtain non-hematopoietic, non-endothelial stromal compartment. Example from adult (8-10wk) bone marrow. (**B**) Compliment to Figure 3.1G, flow cytometry analyses of bone adherent compartment (P14, 8 week, 6 month, and 1 year). Non-hematopoietic, non-endothelial stromal compartment (CD45-TER119-CD31-) was gated on PDGFRα/CD51 (top) or Leptin Receptor (LepR-Ab, bottom). Percentages reflect proportion of Hoxa11eGFP-positive population within double positive gate (top) or bracketed region of histogram (bottom). Grey dots or grey histogram: total non-endothelial stroma (NES), green dots or green histogram: Hoxa11eGFP-expressing non-endothelial stroma (Hoxa11eGFP+). n=3-5 mice per group. All data presented as mean ± standard deviation.

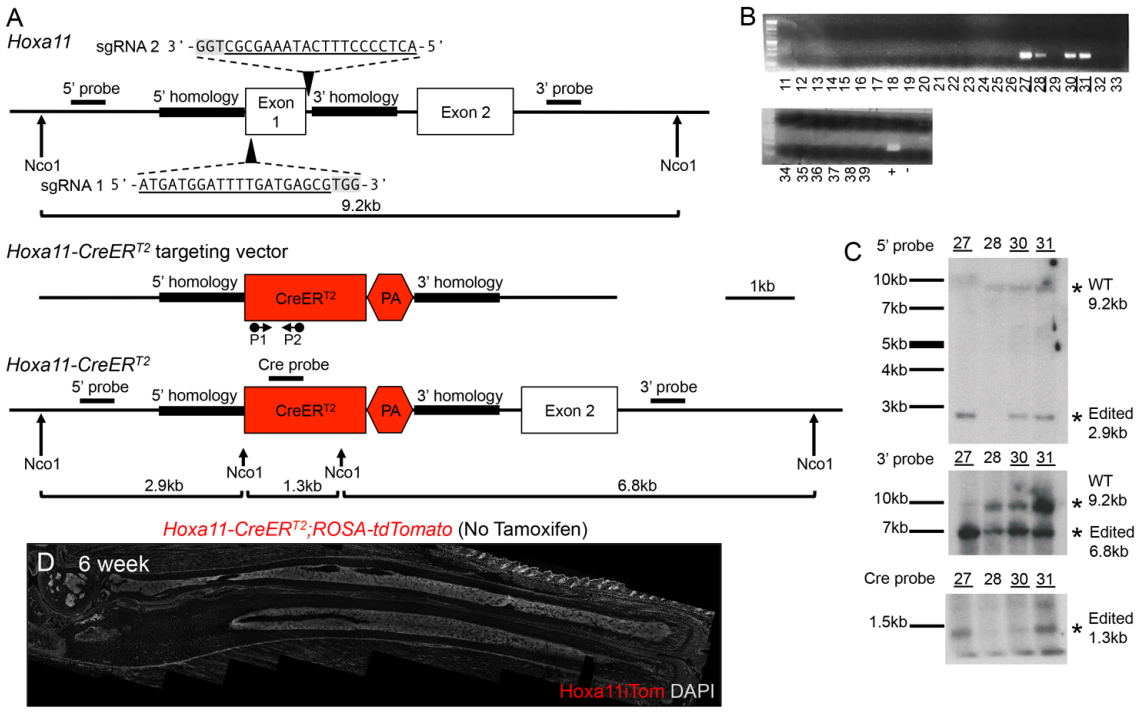

Supplemental Figure 3.2: Cas9/CRISPR generation of a *Hoxa11-CreER^{T2}* allele: (**A**) Schematic of Cas9/CRISPR targeting of *Hoxa11* locus for generation of *Hoxa11-CreER^{T2}* allele. Top: *Hoxa11* locus, positions and sequence of sgRNAs (grey box: PAM), Nco1 restriction sites, positions for 5' and 3' Southern Blot probes and size of wild-type (WT) fragment generated. Middle: *Hoxa11-CreER^{T2}* targeting vector, 5' and 3' homology regions (thick black line), CreER^{T2} and rabbit globin poly-adenylation (PA) insertion (red), and location of Cre PCR primers. Bottom: *Hoxa11-CreER^{T2}* allele, Nco1 restriction sites, positions for 5', 3' and Cre Southern Blot probes and size of edited fragments generated. (**B**) PCR analysis for Cre sequence on 29 live births. (**C**) Southern Blot on four Cre-positive animals using 5' probe (top), 3' probe (middle) and Cre probe (bottom). Wild-type and edited bands and sizes as marked. (**D**) *CreER^{T2}* recombination in the absence of tamoxifen in *Hoxa11-CreER^{T2};ROSA-tdTomato* mice at 6 weeks of age. Fluorescent image - red: *Hoxa11* lineage-marked cells (Hoxa11iTom), grey: DAPI.

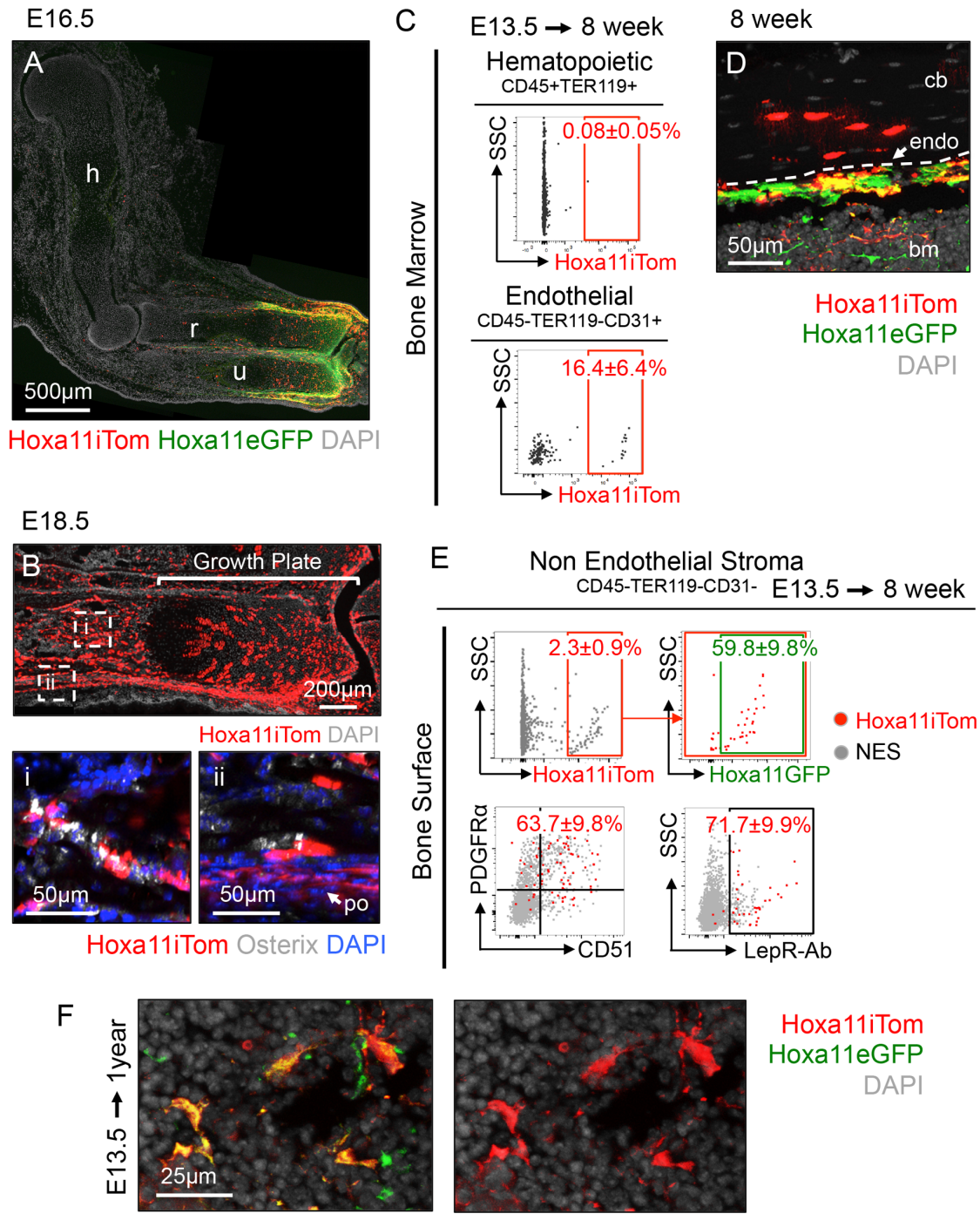

Supplemental Figure 3.3: Embryonic *Hoxa11* lineage-marked cells contribute to all skeletal lineages during development and give rise to self-renewing skeletal MSCs on the bone surface. Pregnant dams received 2mg tamoxifen intraperitoneally at E13.5 and resulting *Hoxa11eGFP;Hoxa11-CreER^{T2};ROSA-tdTomato* mice were chased to (**A**)

E16.5, (**B**) E18.5 (**C-E**) 8 weeks or (**F**) 1 year. (**A**) Hoxa11eGFP (green) expression and lineage contribution of *Hoxa11* lineage-marked cells (Hoxa11iTom, red) in forelimb (humerus (h), radius (r), and ulna (u)). Compliment to Figure 2C. (**B**) High magnification view of ulna growth plate from Figure 2D. Dashed white boxes show approximate location of high magnification images (below). Co-expression of Hoxa11iTom and Osterix (white) in (i) primary spongiosa (ii) periosteum (po). (**C**) Flow cytometry analyses of Hoxa11iTom cells in the hematopoietic (top, CD45+TER119+) and endothelial (bottom, CD45-TER119-CD31+) compartments in the bone marrow. Percentages reflect proportion of Hoxa11iTom population in indicated gate. Data presented as mean ± standard deviation. n=3-5 mice per group (**D**) Co-expression of Hoxa11iTom and Hoxa11eGFP on the bone surface. Cortical bone: cb, bone marrow: bm, dashed white line marks endosteal (endo) bone surface. (**E**) Flow cytometry analysis of non-hematopoietic, non-endothelial stromal compartment (CD45-TER119-CD31-) on bone surface, compliment to Figure 3.3C. Top left panel: *Hoxa11*-lineage (x-axis: Hoxa11iTom), top right panel: analysis of Hoxa11iTom by Hoxa11eGFP, bottom left panel: co-expression analysis of PDGFRα/CD51, bottom right panel: co-expression analysis of Leptin Receptor (LepR-Ab). Percentages reflect proportion of Hoxa11iTom population within identified gate. Grey dots: total non-endothelial stroma (NES), red dots: Hoxa11iTom. n=3-5 mice per group. All data presented as mean ± standard deviation. (**F**) Hoxa11eGFP in Hoxa11iTom bone marrow stromal cells after one year chase. All images, grey or blue: DAPI.

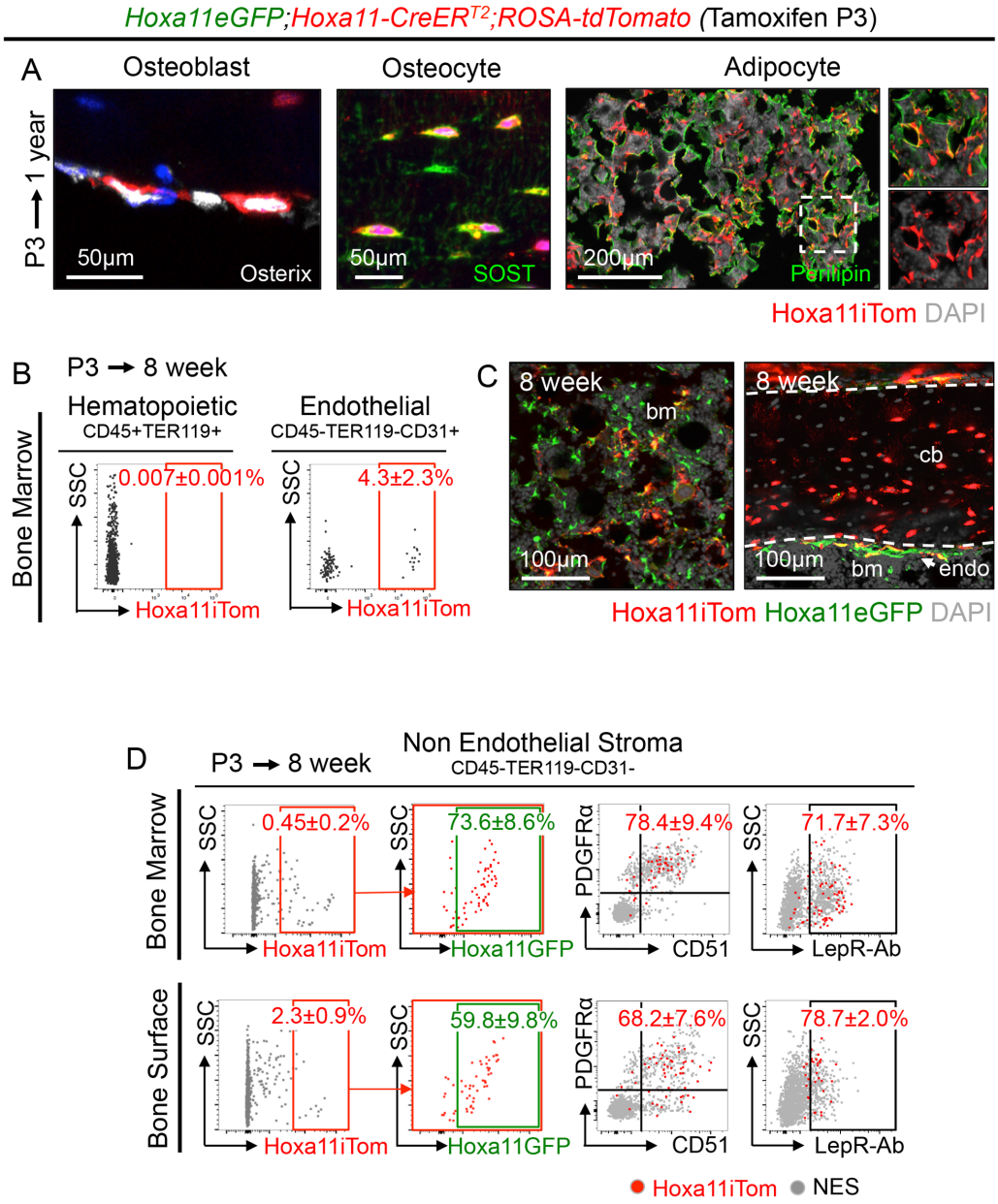

Supplemental Figure 3.4: Postnatal *Hoxa11* lineage-marked cells contribute to all skeletal lineages and give rise to self-renewing skeletal MSCs. P3 pups received 0.25mg tamoxifen intragastrically and *Hoxa11eGFP;Hoxa11-CreER^{T2};ROSA-tdTomato* mice were chased to (**A**) 1 year or (**B-C**) 8 weeks. (**A**) *Hoxa11* lineage-marked cells (Hoxa11iTom, red) and immunolabeling for osteoblasts (Osterix, white) on endosteal bone surface, osteocytes (SOST, green) in cortical bone, and adipocytes (Perilipin, green) in bone marrow. All images, grey: DAPI (**B**) Flow cytometry analyses of Hoxa11iTom cells in the hematopoietic (left, CD45+TER119+) and endothelial (right, CD45-TER119-CD31+) compartments in the bone marrow. Percentages reflect proportion of Hoxa11iTom population within gate. Data presented as mean ± standard deviation. n=3-5 mice per group. (**C**) Hoxa11iTom and Hoxa11eGFP (green) in bone marrow (left) and on bone surface (right). Bone marrow: bm, cortical bone: cb, white dashed lines mark

periosteal and endosteal (endo) surfaces. All images, blue or grey: DAPI (**D**) Flow cytometry analyses of non-hematopoietic, non-endothelial stromal compartment (CD45-TER119-CD31-) in bone marrow (top) or on bone surface (bottom). First panel: *Hoxa11*-lineage (x-axis: Hoxa11iTom), second panel: analysis of Hoxa11iTom positive gate for Hoxa11eGFP, third panel: co-expression analysis of PDGFRα/CD51, fourth panel: co-expression analysis of Leptin Receptor (LepR-Ab). Grey dots: total non-endothelial stroma (NES), red dots: Hoxa11iTom. Percentages reflect proportion of Hoxa11iTom population in marked gate. n=3-5 mice per group. All data presented as mean ± standard deviation.

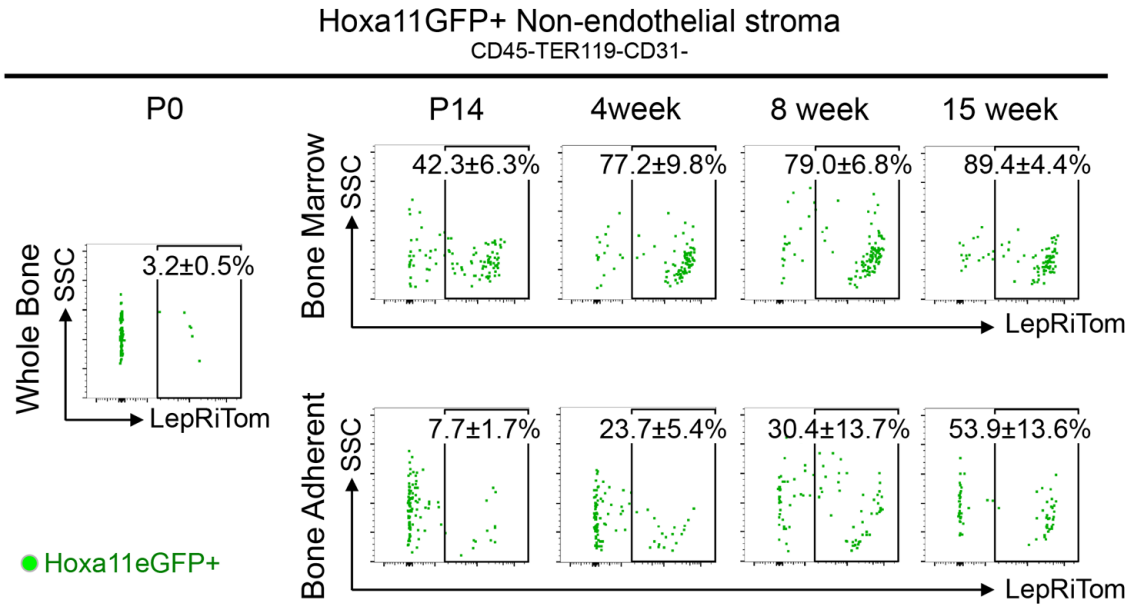

Supplemental Figure 3.5: Hoxa11eGFP-expressing population progressively overlaps with *LepR*-Cre lineage-marked cells. Compliment to Figure 3.5. Flow cytometry analyses of Hoxa11eGFP-expressing stromal cells (green) and *LepR*-Cre lineage (LepRiTom) in whole bone at P0, or bone marrow (top) and bone adherent (bottom) compartments from P14 to 15 weeks. Analysis in non-hematopoietic, non-endothelial (CD45-TER119-CD31-) compartment. Percentages reflect proportion of Hoxa11eGFP-positive population within indicated gate. n=3-5 mice per group. All data presented as mean ± standard deviation.

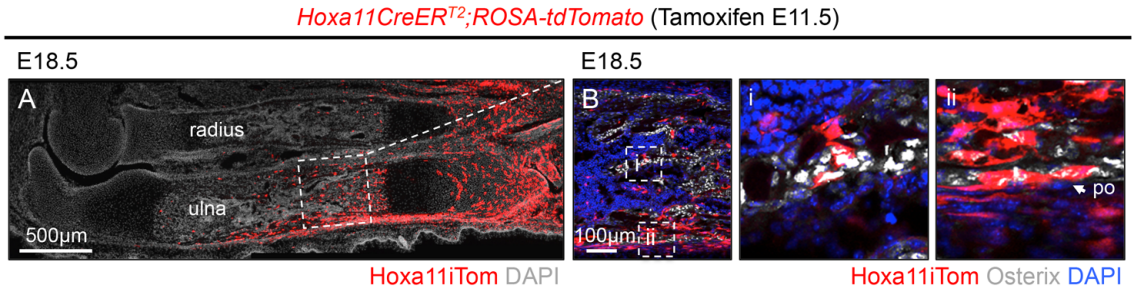

Supplemental Figure 3.6: Induction of *Hoxa11-CreER^{T2}* at E11.5 leads to lineage-marked Osterix-positive osteoblasts in zeugopod. Pregnant dams received 2mg tamoxifen intraperitoneally at E11.5 and resulting *Hoxa11-CreER^{T2};ROSA-tdTomato* mice were chased to E18.5. (**A**) *Hoxa11* lineage-marked cells (Hoxa11iTom, red) within complete radius and ulna. White dashed line marks region shown in **B**. Grey: DAPI. (**B**) Hoxa11iTom and immunostaining for osteoblasts (Osterix, white) in mid-diaphysis ulna. To right, high magnification images of boxed regions in (i) primary spongiosa and (ii) periosteum (po). Blue: DAPI.

Methods

Mouse models

All mice were maintained in a C57BL/6 background. *Hoxa11eGFP* [81], *Leptin Receptor-Cre* [180], *Osterix-CreER^{T2}* [170] mice have been described elsewhere. Rosa26-CAG-loxp-stop-loxp-tdTomato ([181], JAX stock #007909) were obtained from Jackson Laboratory. Both male and female mice were used for experiments. Animals were euthanized for experiments through CO_2 exposure followed by removal of a vital organ. All procedures described here were conducted in compliance with the University of Michigan's Committee on Use and Care of Animals, protocol PRO00006651 (Wellik) and protocol PRO00006763 (Goldstein).

Generation of *Hoxa11-CreER^{T2}* mice

Production of sgRNAs and Cas9 mRNA:

Two guide sequences targeting exon 1 of *Hoxa11* were designed and cloned into the pT7-Guide Vector (Blue Heron Biotech, LLC). The guide sequence and approximate locations of both sgRNAs, including the corresponding PAM sequence, are illustrated in Sup Figure 2A. MEGAshortscript T7 kit (Life Technologies) was used to generate *in vitro* transcribed sgRNAs from the pT7-Guide Vector and products were subsequently purified using the MEGAclear kit (Life Technologies). Using the pT7-Cas9-Nuclease vector (gift from Dr. Moises Mallo), Cas9 mRNA was *in vitro* transcribed using the mMESSAGE mMACHINE T7 ULTRA kit (Life Technologies) and purified using the MEGAclear kit (Life Technologies).

Production of targeting plasmid:

Homologous sequence flanking exon 1 of *Hoxa11* were synthesized by Blue Heron Biotech, LLC into the pUCminusMCS vector as a continuous insert separated by sequence containing restriction sites for EcoRI, NotI, and HindIII to allow for sub-cloning of *CreER^{T2}* and rabbit β-globin poly-adenylation signal. The 5' homology arm contained 1.3kb immediately upstream of the endogenous *Hoxa11* start site and 3' homology arm contained 1.3kb of sequence immediately downstream of sgRNA 2 as illustrated in Sup Figure 2A. Sequence for CreERT2 and rabbit β-globin poly(A) signal

was sub-cloned from pCAG-CreERT2 vector (gift from Connie Cepko, Addgene plasmid #14797, [172]). Targeting of CreERT2 to *Hoxa11* locus preserves endogenous upstream and downstream sequence and creates a null allele; expressing CreERT2 in place of Hoxa11.

Zygote injection and confirmation of targeting:

Zygote injections were performed as previously described with minor modifications [182]. C57BL/6 female mice were superovulated and mated with C57Bl/6 male mice and one-cell stage embryos were collected for microinjection. CRISPR reagents were microinjected at the following concentrations: Cas9 mRNA (100ng/μL), each sgRNA (50ng/μL), and targeting plasmid (20ng/μL). Freshly injected eggs were transferred into pseudopregnant females and resulting progeny were initially screened for potential $CreER^{T2}$ insertion via PCR. The following internal primers for CreER sequence were used: Cre Fwd: 5' GGACATGTTCAGGGATCGCCAGGC 3', Cre Rev: 5' CGACGATGAAGCATGTTTAGCTG 3'. Approximate location of primers indicated in Sup Figure 2A. Cre-positive animals by PCR were analyzed by Southern Blotting to confirm targeting using 5' and 3' flanking probes and a Cre internal probe with Nco1 digested DNA. Approximate locations of probes are illustrated in Sup Figure 2A. The 453 bp 5' probe was generated using primers: 5' TTTCGGTTCTCCTAGACGCC 3' and 5' CACGGCGTTTGCATGAGATT 3', the 533 bp 3' probe was generated using primers: 5' TCTGTAGTGAGCGCCTTTGG 3' and 5' GAGGTTCCCGAGAGACTCCT 3', and the 408 bp Cre probe was generated using primers: 5' GCATTACCGGTCGATGCAACGAGTGATGAG 3' and 5' GAGTGAACGAACCTGGTCGAAATCAGTGCG 3', that were randomly labeled with ^{32}P-dCTP. Four animals were CreER positive via PCR and three animals showed correct targeting via Southern Blot [Sup Figure 2B-C]. Animal #27 displayed germline transmission of the allele. Animals from this founder were used in all subsequent experiments.

Tamoxifen treatment

For embryonic induction, *Hoxa11-CreERT2* or *Osx-CreERT2* male mice were mated to $Rosa^{tdTomato/tdTomato}$ or $Hoxa11eGFP;ROSA^{tdTomato/tdTomato}$ female mice and the

vaginal plug was checked every morning. Pregnant mice received 2mg of tamoxifen (Sigma T5648) and 1mg/mL progesterone (Sigma P0130) dissolved in corn oil intraperitoneally at indicated embryonic day. For postnatal induction, pups of the genotype indicated in figures received 0.25mg of tamoxifen intragastrically at P3. At least three embryos, pups, or adult animals of the indicated genotypes were examined at time points shown in figures.

Ulnar fracture

Following procedure previously described in detail [108, 110]. Tamoxifen was administered as described above, and animals were aged to adult stages (8-10 weeks). Briefly, animals were anesthetized with isoflurane during procedure and provided buprenorphine pre- and postoperatively and carprofen during recovery period. A small incision was made along the posterior ulnar surface and the bone was exposed via blunt dissection. Using fine wire cutters, the ulna was cut at the mid-shaft. Skin was closed using sutures. Animals were euthanized for analysis at 10 days post injury. At least three animals from each tamoxifen induction time point were examined.

Immunohistochemistry

Limb skeletal tissues were collected at the indicated ages or time point following fracture injury. All specimens were dissected in PBS on ice and skin was removed prior to fixation for postnatal and adult tissues. Samples were fixed in 4% paraformaldehyde in PBS (embryo: 1-3 hours, postnatal (P3-P7): 4-6 hours, adult (2wk+): 1-2 days) rocking at 4°C. Postnatal and adult tissues were decalcified in 14% EDTA for 1-7 days depending on age. Samples were equilibrated in 30% sucrose overnight prior to embedding into optimal cutting temperature medium. Cryosections were collected at 12-30 μm through indicated segments of the limb or fracture callus using the Kawamoto tape method [183].

Immunohistochemical staining was performed using standard methods. Sections were blocked with donkey serum and incubated with primary antibodies overnight at 4°C against Sox9 (Millipore, AB5535, 1:500), Osterix (Abcam, ab22552, 1:300), and Perilipin (Sigma, P1873, 1:100). Secondary antibodies were incubated at room temperature for 2 hr: donkey-anti-rabbit-Alexa Fluor 647 (Thermo Fisher, A31573, 1:1000) and donkey-anti-rabbit-Alexa Fluor 488 (Thermo Fisher, A21206, 1:1000). A

modified signal amplification protocol was used to visualize SOST. Following blocking, primary antibody against SOST (R&D Systems, AF1589, 1:100) was incubated overnight at 4°C followed by donkey-anti-goat-biotin secondary (Jackson ImmunoResearch, 705-067-003, 1:400). The biotinylated secondary was detected using Vectastain Elite ABC kit (Vector Laboratories, PK-6100) and signal was amplified by Alexa Fluor 488 Tyramide reagent (Thermo Fisher, B40853). To minimize imaging complications from autofluorescence in postnatal and adult tissues, Hoxa11eGFP was visualized using chicken-anti-GFP (Abcam, ab13970, 1:2000) and donkey-anti-chicken-Alexa Fluor 488 (Invitrogen, A11039, 1:1000) in combination with aforementioned antibodies. tdTomato expression was dim at 24-72hr post-tamoxifen induction and was visualized using rabbit-anti-RFP (Rockland, 600401379, 1:1000) and donkey-anti-rabbit-Alexa Fluor 555 (Invitrogen, A31572, 1:1000). Following longer chases, tdTomato was imaged directly without the use of an antibody.

Fluorescent images were captured on an Olympus BX-51 microscope with an Olympus DP-70 camera or Leica Upright Sp5x 2-photon confocal microscope. Confocal z-stacks were obtained through entire sections at a thickness of 2 μm and images were stacked using ImageJ software. When applicable, 10x images were stitched together using Photoshop software to obtained images of entire limbs and fracture calluses.

Flow cytometry analysis

Bone marrow cells were harvested by flushing the marrow cavity with digestion buffer (2 mg/mL collagenase IV and 3 mg/mL dispase in 1X PBS) using a 30G needle for both the radius and ulna. To obtain bone adherent cells, the remaining bone following bone marrow flushing was minced in digestion buffer and subjected to subsequent digestion. The digestion of all samples was carried out at 37°C with three rounds of agitation to achieve a single cell suspension. After each cycle of digestion/agitation, cells in suspension were collected into media (DMEM, 5% calf serum) and kept at 37°C until the entire digestion protocol was finished. Red blood cells were lysed on ice using lysis buffer at a final concentration of 0.5X. For staining, cells were resuspended in staining buffer (1X PBS, 0.5% BSA, 2mM EDTA) at a concentration of 1 x 10^6 cells/30μl in a solution containing the following antibodies. For hematopoietic exclusion: CD45-AF700

(eBioscience, clone 30-F11, 1:100) and TER119-APC-Cy7 (Becton Dickinson, clone TER119, 1:100). For endothelial cell exclusion: CD31-PerCPCy5.5 (Becton Dickinson, clone MEC13.3, 1:100). For MSC identification: PDGFRα/CD140a-APC (eBioscence, clone APA5, 1:100) and biotinylated rat-anti-CD51 (Biolegend, clone RMV-7, 1:100) or biotinylated goat-anti-leptin receptor (R&D, BAF497, 1:50) and streptavidin-Brilliant Violet 605 (Biolegend, 405229, 1:500). Following staining on ice, all samples were washed twice with staining buffer and resuspended in staining buffer containing DAPI (1:10,000) for analysis. All analyses were carried out on an LSRII Fortessa flow cytometer (BD) and results were analyzed with FlowJo (v10.2) software. Results are presented as mean values ± standard error of the mean (SEM). No statistical method was used to predetermine sample size. Sample size was determined on the basis of previous literature and our previous experiments to give sufficient standard error of the mean, and feasible generation of experimental animals. The experiments were not randomized and investigators were not blinded during experiments and assessment of results.

CHAPTER IV

Interaction of *Hox11*, *Ihh*, *Runx2*, and *Wnt5a* in early limb development

Summary

Long bone growth is driven by chondrocyte proliferation and differentiation within highly organized structures at the distal ends of the bone termed the growth plate. Numerous signaling pathways and transcription factor networks function both cooperatively and in parallel to regulate chondrocyte proliferation differentiation to effect proper bone growth. The *Hox* transcription factors regulate skeletal patterning during development. Loss-of-function of the *Hox11* paralogs results in dramatic mispatterning of the zeugopod skeletal elements characterized by significantly short elements composed of immature and disorganized chondrocytes. Loss-of-function of the Hedgehog pathway ligand *Indian hedgehog* (*Ihh*), the Wnt ligand *Wnt5a*, or the transcription factor *Runx2* results in skeletal phenotypes that are remarkably similar to *Hox11* mutants suggesting potential functional relationships between Hox11 and one or more of these factors. We show that expression of *Ihh*, *Runx2*, and *Wnt5a* is reduced or absent in *Hox11* mutants during early skeletal development. Using a *Gli1*-lacZ reporter allele we show that Hox11-expressing perichondrial cells respond to Hedgehog signaling, and that *Hox11* mutants display dramatically reduced levels of *Gli1*-lacZ signal. Interestingly, in an *ex vivo* limb culture system, activation of the Hedgehog pathway using a pharmacologic Smoothened agonist demonstrates that *Hox11* mutant cells are capable of responding to Hedgehog signaling. These studies provide preliminary evidence suggesting a relationship between Hedgehog signaling and Hox11 function in the skeleton.

Introduction

Long bones of the appendicular skeleton form through the process of endochondral ossification whereby a cartilaginous template is first established and is progressively replaced by bone. In the limb bud, Sox9-expressing chondrocyte progenitors condense along the proximal to distal axis of the limb to form the skeletal anlage with the stylopod containing one element (humerus or femur), the zeugopod containing two elements (radius/ulan or tibia/fibula), and the autopod containing many elements (carpals/metacarpals and tarsals/metatarsals) [52-55]. At the borders of the condensations, a layer of elongated fibroblasts, the perichondrium, forms surrounding the cartilage template [184]. This tissue is thought to provide mechanical cues to control the ratio of lengthwise to girthwise growth of the skeletal elements. Longitudinal bone growth is driven by the highly ordered processes of chondrocyte proliferation and differentiation. All chondrocytes of the skeletal anlage are initially highly proliferative. As the element grows in size, chondrocytes at the center of the anlage stop proliferating, undergo hypertrophic differentiation, and switch from secreting a type II collagen matrix to a type X collagen matrix [185]. Signaling from the hypertrophic chondrocytes to the perichondrium initiates osteoblast differentiation of the adjacent perichondrial cells and invasion of blood vessels and chondroclasts/osteoclasts to digest the hypertrophic matrix and initiate formation of the bone marrow cavity [170, 184, 186]. Chondrocyte proliferation and differentiation continues at the distal ends of the bones in highly organized structures termed the growth plate [148].

The posterior *Hox* genes (*Hox9-13*) function regionally to pattern the limb skeleton along the proximal to distal axis. The mutant phenotypes resulting from paralogous loss-of-function mutations in these genes are well described, however the mechanism of Hox function during early skeletal development and patterning continue to be largely unknown [187]. *Hox11* genes pattern the zeugopod region of the limb and complete loss-of-function mutations of the *Hox11* paralogs results in significant mis-pattering of this region [16, 80, 83]. Early specification of the elements is unaffected in these mutants. Sox9-expressing chondrogenic progenitors condense normally, forming two skeletal anlagen in the zeugopod that express a type II collagen matrix by embryonic